Conformal and Asymptotic Properties of Embedded Genus-g Minimal Surfaces with One End

by

Jacob Bernstein

Submitted to the Department of Mathematics
in partial fulfillment of the requirements for the degree of

Doctor of Philosophy

at the

MASSACHUSETTS INSTITUTE OF TECHNOLOGY

June 2009

Author .....
Department of Mathematics
May 18, 2009

Certified by .....
Tobias H. Colding
Professor of Mathematics
Thesis Supervisor

Accepted by .....
David Jerison
Chairman, Department Committee on Graduate Students

Conformal and Asymptotic Properties of Embedded Genus-g Minimal Surfaces with One End

by

Jacob Bernstein

Submitted to the Department of Mathematics
on May 18, 2009, in partial fulfillment of the
requirements for the degree of
Doctor of Philosophy

Abstract

Using the tools developed by Colding and Minicozzi in their study of the structure of embedded minimal surfaces in $\mathbb{R}^3$ [12, 19–22], we investigate the conformal and asymptotic properties of complete, embedded minimal surfaces of finite genus and one end. We first present a more geometric proof of the uniqueness of the helicoid than the original, due to Meeks and Rosenberg [45]. That is, the only properly embedded and complete minimal disks in $\mathbb{R}^3$ are the plane and the helicoid. We then extend these techniques to show that any complete, embedded minimal surface with one end and finite topology is conformal to a once-punctured compact Riemann surface. This completes the classification of the conformal type of embedded finite topology minimal surfaces in $\mathbb{R}^3$. Moreover, we show that such s surface has Weierstrass data asymptotic to that of the helicoid, and as a consequence is asymptotic to a helicoid (in a Hausdorff sense). As such, we call such surfaces *genus-g helicoids*. In addition, we sharpen results of Colding and Minicozzi on the shapes of embedded minimal disks in $\mathbb{R}^3$, giving a more precise scale on which minimal disks with large curvature are "helicoidal". Finally, we begin to study the finer properties of the structure of genus-g helicoids, in particular showing that the space of genus-one helicoids is compact (after a suitably normalization).

Thesis Supervisor: Tobias H. Colding
Title: Professor of Mathematics

Acknowledgments

I would like to thank my advisor, Tobias Colding, for giving me the problem that was the genesis of this thesis and for giving me support and help in navigating the vagaries of mathematical research. I would also like to thank Bill Minicozzi for his constant enthusiasm and for his always extremely helpful suggestions.

There are many other people at MIT I would like to acknowledge (in no particular order): Richard Melrose for teaching me analysis and for humoring some of my more ill-posed queries; Hans Christianson and Brett Kotschwar for handling most of the rest; Linda Okun and the rest of the math department staff for helping me understand some of MIT's more arcane policies; Chris Kottke being a great office-mate and for our many procrastination driven conversations; Gigliola Staffilani for helping me in my job search; Michael Eichmair for energizing geometric analysis at MIT and for being a great friend; Tom Mrowka and William Lopes for discussing some elementary Morse theory with me, the results of which are in Chapter 6; thanks also to Vedran, YankI, Lu, James and Max for many great mathematical discussions.

Away from MIT, my collaborator Christine Breiner must be mentioned, both as a great conference co-attendee and friend. Special thanks to my fianceé Jessie Howell for putting up with me, even at my most slovenly and unshaven. I couldn't have done it with out you. I would also like to thank my parents. I am especially grateful to my father exposing me to deep mathematics at young age, and thank him for his copy of Kelley's *General Topology*, my first encounter with abstract mathematics.

Finally, I would like to dedicate this thesis to the memory of Juha Heinonen without whom I very likely would have left mathematics. His contribution to my mathematical education cannot be overstated.

Contents

List of Figures

Chapter 1

Introduction

The study of minimal surfaces has a long history, dating to the eighteenth century and the beginnings of the calculus of variations. The theory sits at a fundamental intersection of geometry, analysis and topology and has provided important tools, techniques and insights in all three areas. Moreover, even in its most classical setting, minimal surface theory remains an active area of research. Recall, a minimal surface is a surface that is a stationary point of the area functional; in other words, infinitesimal deformations of the surface do not change its area. A particularly important class of these, and indeed a major motivation for the theory, are surfaces that actually minimize area in a global sense, as these can be taken as a model of the shape of a soap film.

While minimal surfaces can be studied in a large number of different contexts, we will restrict our attention to the classical setting of minimal surfaces in $\mathbb{R}^3$. This is, of course, the context in which the theory was originally developed and remains an area of active research. We will be interested in classifying the complete embedded minimal surfaces in $\mathbb{R}^3$. Before discussing such a classification program further, we first record the three most important such surfaces. We do this both to illustrate that this is a non-trivial question and to have some simple examples on hand. The first, and least interesting, is the plane, the second is the catenoid and the final is the helicoid. The catenoid was discovered by Euler in 1744 and is the surface of revolution of the catenary (see Figure 2-1). The helicoid was discovered by Meusnier in 1776 and looks like a double-spiral staircase (see Figure 2-2). It is the surface swept out by a line moving through space at a constant rate while rotating at a constant rate in the plane perpendicular to the motion.

A reason to classify all complete, embedded, minimal surfaces, is that doing so allows one, in a sense, to understand the structure of all embedded minimal surfaces. Indeed, the local structure of any embedded minimal surface is modeled on one of the complete examples. This is because there exist powerful compactness theories for such surfaces which come from the ellipticity of the minimal surface equation. We emphasize that the assumption that the surfaces are embedded is both extremely natural and also crucial, without it, very pathological complete minimal surfaces can be constructed, and there is very little local geometric structure.

The first step in any such geometric classification program is to first classify the

underlying topologies of the geometric objects. Because we are interested only in surfaces, this is well known and the possible topologies are particularly simple. Nevertheless, at this step we do simplify a bit and restrict our attention only to surfaces of *finite topology*. That is, surfaces diffeomorphic to a compact surface with a finite number of punctures. We point out that there are a great number of examples of surfaces with infinite genus, and so a classification of these surfaces would be very difficult. On the other hand, surfaces with an infinite number of ends are much more rigid. Indeed, Meeks, Perez and Ros in [44] completely classify complete, properly embedded minimal surfaces of genus zero that have an infinite number of ends.

The next step is to understand, to a degree, the conformal structure of the surfaces. Recall, any (oriented) surface in $\mathbb{R}^3$ has a canonical complex structure, induced by the metric. Furthermore, the minimality of the surface is equivalent to the Gauss map being holomorphic with respect to this structure. As such, there is an intimate connection between complex analysis and the properties of minimal surfaces in $\mathbb{R}^3$. The crucial step at this stage is to determine the conformal type of the ends, as this has important global complex analytic, and hence geometric, consequences. Precisely, one must determine whether a neighborhood of the end, which is topologically an annulus, is conformally a punctured disk or conformally an annulus. This is usually accomplished by first gaining some weak understanding of the asymptotic geometry of the end. When this implies that the end is conformally a punctured disk, complex analytic arguments then give much stronger asymptotic geometric information. Indeed, in this last case one shows that the surface is asymptotic to either a plane, half a catenoid or a helicoid. The final step is to understand the finer geometric (and conformal) properties of the surface. This is a difficult and subtle problem and very little is known when the genus is positive (for surfaces with genus zero, much stronger rigidity results can be usually be immediately deduced).

A classic result of Huber, [41], states that oriented surfaces of finite total curvature are parabolic. In other words, if the surface is also complete then it is conformally a punctured compact Riemann surfaces. Osserman, in [53], specializes this to minimal surfaces and shows that when the surface is minimal, in addition to having this simple conformal type, the Gauss map extends holomorphically to the puncture (as does the height differential, see (2.3)). Using this, Osserman proves that the only complete minimal disk of finite total curvature is the plane. The results of Huber and Osserman have been the guiding principle in the study of embedded minimal surfaces with more than one end. This is because a pair of embedded ends can be used as barriers in a Perron method construction. Indeed, using the ends one constructs a much nicer minimal surface between the ends, which can be used to get some asymptotic geometric information about the ends. Ultimately, this allows one to prove that the ends have finite total curvature.

One of the first results implementing this idea was, [33], wherein Hoffman and Meeks show that any complete properly embedded minimal surface with finite topology and two or more ends has at most two of the ends having infinite total curvature. As a consequence, conformally such a surface is a punctured compact Riemann surface with at most two disks removed. This was refined by Meeks and Rosenberg in [48]; they show that such surfaces are necessarily conformal to punctured compact

Riemann surfaces. However, like [33], they can not rule out infinite total curvature for some of the ends. Nevertheless, this classifies the conformal type of all complete, properly embedded minimal surfaces of finite topology and two or more ends. Finally, Collin in [25] showed that in fact any complete, properly embedded minimal surface of finite topology and two or more ends has finite total curvature.

This weak restriction on the asymptotic geometry allows one to say much more. In [50], Lopez and Ros show that the only complete embedded minimal surfaces with finite total curvature and genus zero are the catenoid and plane. Similarly, (though using very different methods) Schoen, in [57], shows that the catenoid is the unique complete minimal surface of finite total curvature and two ends. Note, both of these results pre-date [25] and assumed a priori bounds on the total curvature. In particular, taken together with the work of [25], this completely classifies the space of complete embedded minimal surfaces of finite topology that are in addition either genus zero or which have precisely two ends – in either case the the only non-flat surface is a catenoid.

The helicoid has, by inspection, infinite total curvature, and so the above approach has no hope of working for surfaces with one end. Indeed, until very recently, the only results for minimal surfaces with one end required extremely strong geometric assumptions (see for instance [31] or [37]); the main difficulty was that there were no tools available to analyze (even very weakly) the asymptotic geometry of the end. The big breakthrough came with the highly original and groundbreaking work of Colding and Minicozzi. They abandoned the global approach to the theory and instead, through very deep analysis, were able to directly describe the the interior geometric structure of an embedded minimal disk. It is important to emphasize that their work is local and makes no use of complex analysis (and so in particular generalizes to other ambient 3-manifolds). This theory is developed in the series of papers [19–22] (see [23] for nice expository article). Roughly, speaking they show that any embedded minimal disk of large curvature is modeled (in a weak sense) on the helicoid. As a consequence of this, Colding and Minicozzi give a compactness result for embedded minimal disks that satisfy only a (mild) geometric condition, in particular they impose no area or curvature bounds. That is, they show that any sequence of embedded disks whose boundary goes to infinity has a sub-sequence that either converges smoothly on compact subsets or behaves in a manner analogous to the homothetic blow-down of a helicoid.

Using this compactness theorem, Meeks and Rosenberg in [45], were able to finally gain some geometric information about the end of a general properly embedded minimal disks. Using some subtle complex analytic arguments, this allowed Meeks and Rosenberg to completely classify these surfaces, determining that they must be either a plane or a helicoid. In Chapter 4, we will treat the same subject, but rather then appealing to the compactness theory, we make direct use of the results of Colding and Minicozzi on the geometric structure of embedded minimal disks. This dramatically simplifies the proof as well as giving strong hints as to how to extend to higher genus surfaces. In Chapter 6, we develop this approach and determine the conformal type of once punctured surfaces of finite genus – showing that any such surface is conformal to a punctured compact Riemann surface. This completes (along with [48])

the classification the conformal types of complete, embedded, minimal surfaces of finite topology. As a consequence, we deduce that these surfaces are asymptotically helicoidal and so feel free to refer to them as *genus-g helicoids*. In Chapter 5, we investigate what the uniqueness of the helicoid tells us about the shapes of minimal disks near points of large curvature. Finally, in Chapter 7, we investigate more carefully the finer geometric structure of genus-one helicoids. In particular, we show that the space of genus-one helicoids is compact.

Chapter 2

Background

Minimal surfaces have been extensively studied for centuries and so any attempt to summarize the theory will be woefully incomplete. Nevertheless, we at least attempt to introduce the concepts and theory we will need in the sequel. Thus, we restrict attention to the classical setting of minimal surfaces in $\mathbb{R}^3$. For more details, we refer to the excellent books on the subject, [13, 54], from which the following is drawn.

2.1 Minimal Surface Theory in $\mathbb{R}^3$

2.1.1 Basic theory

For simplicity, we restrict our attention to minimal surfaces in $\mathbb{R}^3$, though many of the basic concepts can be generalized to arbitrary co-dimension surfaces in arbitrary ambient Riemannian manifolds. We point out, however, that minimal surface theory in $\mathbb{R}^3$ admits particularly strong results. One important reason for this is that there is a powerful connection with complex analysis. This connection has proven to be a very important approach to the theory and exists only in $\mathbb{R}^3$; we will make substantial use of it.

Suppose M is a 2-dimensional, connected, orientable manifold (possibly open and with boundary) and let $F : M \to \mathbb{R}^3$ be a smooth immersion. We will denote by Σ the image of M and so Σ is a surface parametrized by M, though we will rarely distinguish between the two. If F is injective, then we say that Σ is *embedded*. We denote by $\mathbf{n}$ a smooth choice of normal to Σ that is a smooth map $\mathbf{n} : M \to \mathbb{S}^2 \subset \mathbb{R}^3$ so $\mathbf{n}(p)$ is orthogonal to Σ at p. Recall, by assumption, M is orientable and so such $\mathbf{n}$ exists. We denote by h_Σ the metric induced on M by the euclidean metric of $\mathbb{R}^3$ and denote by $dvol_\Sigma$ the volume form associated to this metric. We say that Σ is *complete* if h_Σ is a complete metric on M and that F (or Σ) is *proper* if the pre-image of a compact (in the subspace topology induced by $\mathbb{R}^3$) subset of Σ is compact. We will only study surfaces M with "finite" topology, that is:

Definition 2.1.1. We say that M a smooth surface (possibly open and with boundary) has *finite topology* if it is diffeomorphic to a finitely punctured compact surface

$\bar{M}$. Moreover, we say M *has genus* g if $\bar{M}$ has genus g and we say M *has* e *ends* if M is obtained from $\bar{M}$ by removing e points.

Let us define the local area functional as follows: for $K \subset \mathring{M}$ a compact set define $\text{Area}_\Sigma(K) = \int_K dvol_\Sigma$. We say that Σ is minimal if it is a stationary point for the area functional, in other words infinitesimal deformations of Σ do not change the area. Precisely:

Definition 2.1.2. We say that $\Sigma = F(M)$ is *minimal* if, for all K compact in $\mathring{M}$ and $\phi \in C_0^\infty(K)$, the following holds:

$$\left.\frac{d}{dt}\right|_{t=0} \text{Area}_{\Sigma_t}(K) = 0, \tag{2.1}$$

where $F_t : M \to \mathbb{R}^3$ is defined by $F_t(p) = F(p) + t\phi(p)\mathbf{n}(p)$ and $\Sigma_t = F_t(M)$.

For example, any surface which minimizes area relative to its boundary $\gamma = \partial\Sigma$ is minimal. Physically, this surface represents the shape of a soap film spanning a wire given by the curve γ. Note that surfaces that minimizes area in this respect form a much smaller class than those that are merely stationary. They were extensively studied by the physicist Plateau and the problem of determining whether a given curve is bounded by a minimal surface bears his name. We note that there is an incredibly rich theory devoted to answering this question, which we will completely ignore.

Minimality is equivalent to a curvature condition on Σ. Indeed, an integration by parts gives the first variation formula:

$$\left.\frac{d}{dt}\right|_{t=0} \text{Area}_{\Sigma_t}(K) = \int_M H\phi dvol_\Sigma. \tag{2.2}$$

Here, H is the mean curvature of Σ with respect to $\mathbf{n}$, that is, the trace of $D\mathbf{n}$, or equivalently, the sum of the two principle curvatures. Thus, an equivalent characterization of smooth minimal surfaces is as surfaces with mean curvature identically zero. This can also be interpreted to mean that F is a solution to a second order non-linear elliptic system. Indeed, in $\mathbb{R}^3$, the minimality of Σ is equivalent to the harmonicity of the coordinate functions. That is, $x_i \circ F$, the components of F, are harmonic functions on M with respect to the Laplace-Beltrami operator, Δ_Σ, associated to h_Σ.

A simple but extremely important consequence of the maximum principle and the harmonicity of the coordinate functions is the following convex hull property:

Theorem 2.1.3. *Suppose K is a convex subset of $\mathbb{R}^3$ and Σ is minimal with $\partial\Sigma \subset K$ then $\Sigma \subset K$.*

As M is a surface the metric induced on it by F gives M a canonical complex structure, given by rotation by 90°. Thus, M is naturally a Riemann surface. The mean curvature vanishing is then equivalent to the Gauss map $\mathbf{n}$ being (anti-) holomorphic when one views $\mathbb{S}^2$ as $\mathbb{C}P^1$. In particular, the stereographic projection of $\mathbf{n}$,

which we hence forth denote by g, is a meromorphic function on M. In particular, dx_3 is the real part of a holomorphic one form on M, dh, the height differential. Note, the Gauss map is vertical only at the zeros of dh.

Using this data one obtains the Weierstrass representation of Σ, namely for ν a path in M connecting p to p_0:

$$F(p) = \mathrm{Re} \int_\nu \left(\frac{1}{2}\left(g - \frac{1}{g}\right), \frac{i}{2}\left(g + \frac{1}{g}\right), 1 \right) dh + F(p_0). \tag{2.3}$$

Conversely, given a Riemann surface M, a holomorphic one-form dh and a meromorphic function g, that g vanishes or has a pole only at the zeros of dh, then the above representation gives a minimal immersion into $\mathbb{R}^3$ as long as certain compatibility conditions are satisfied. These conditions, known as *period conditions*, must be satisfied for F to be well defined. In other words, the closed forms $\mathrm{Re}\,\frac{1}{2}\left(g - \frac{1}{g}\right)$, $\mathrm{Re}\,\frac{i}{2}\left(g + \frac{1}{g}\right)$ and $\mathrm{Re}\, dh$ must be exact.

A particularly nice class of minimal surfaces are those that are a graph of a function. Suppose $u : \Omega \to \mathbb{R}$ is a C^2 function on Ω an open subset of $\mathbb{R}^2$. The the graph of u, $\Gamma_u = \{(p, u(p) : p \in \Omega\} \subset \mathbb{R}^3$ is minimal if and only if u satisfies the minimal surface equation:

$$\mathrm{div}\left(\frac{\nabla u}{\sqrt{1 + |\nabla u|^2}} \right) = 0. \tag{2.4}$$

Notice, that u is a solution to a quasi-linear elliptic equation and so standard elliptic theory as in [30] can be applied to u. Moreover, it can be shown that Γ_u is actually area-minimizing with respect to $\partial\Gamma_u$. A consequence of this is that solutions of (2.4) are much more rigid than solutions to general second-order elliptic equations. For instance, S. Bernstein shows in [5] that the only entire solution is a plane:

Theorem 2.1.4. *Suppose $u : \mathbb{R}^2 \to \mathbb{R}$ is a solution to (2.4) then u is affine.*

A related result proved by Bers [6]:

Theorem 2.1.5. *Suppose $u : \mathbb{R}^2 \backslash B_1 \to \mathbb{R}$ is a solution to (2.4) then u has an asymptotic tangent plane.*

Finally, we introduce and briefly discuss another important sub-class of minimal surfaces. We say a minimal surface Σ is *stable* if it minimizes area with respect to "nearby surfaces", i.e. the surface is not merely a critical point of area but is a "local minimum". This is made precise by means of the second variation formula. Here Σ_0 is minimal, and ϕ, Σ_t are as in Definition 2.1.2:

$$\left.\frac{d^2}{dt^2}\right|_{t=0} \mathrm{Area}_{\Sigma_t}(K) = \int_M |\nabla\phi|^2 - |A|^2\phi^2 dvol_\Sigma. \tag{2.5}$$

In particular, Σ is stable if and only if this value is always greater than or equal to 0 for any choice of ϕ. As is clear from the above, stable surfaces admit a nice curvature

estimate, called the stability inequality:

$$\int_M |\nabla_\Sigma \phi|^2 dvol_\Sigma \geq \int_M |A|^2 \phi^2 dvol_\Sigma. \tag{2.6}$$

We wish to have an infinitesimal notion of stability. To that end, an integration by parts shows that a surface is stable if and only if the stability operator $L = \Delta_\Sigma + |A|^2$ has no negative eigenvalues. We call a zero eigenfunction of L a *Jacobi field*. If Σ is complete in $\mathbb{R}^3$ then it is a special case of a well known result of Fischer-Colbrie and Schoen [29] that Σ is stable if and only if there is a positive Jacobi field.

Unsurprisingly, stable minimal surfaces are quite a bit more rigid then general minimal surfaces. In particular, a (specialization to $\mathbb{R}^3$ of a) result of Schoen, [56], that will prove of great importance is the following Bernstein-type result for stable minimal surfaces:

Theorem 2.1.6. *Suppose Σ is a complete, stable, minimally immersed surface in $\mathbb{R}^3$, then Σ is a plane.*

2.1.2 Classical and modern constructions

We will now illustrate some important classical and modern examples of embedded and complete minimal surfaces, both to illustrate the rich history of the theory and to provide us a number of examples to refer to. Euler gave the first non-trivial minimal surface, the catenoid, in 1744. It is topologically an annulus and is the surface of revolution of a catenary (see Figure 2-1). In 1776, Meusnier found another example, the helicoid, which is the surface traced out by a line rotating at a constant rate while at the same time being translated parallel to the z-axis (see 2-2). As we will see, along with the trivial complete embedded minimal surface, the plane, these three surfaces can be shown to in some sense characterize the asymptotic geometry of any complete embedded minimal surface. Further complete embedded minimal surfaces, though of infinite topology, were discovered in the nineteenth century, a particularly beautiful family of examples is due to Riemann, who discovered a periodic two parameter family of surfaces with genus zero and and an infinite number of planar ends.

In 1983, Costa gave the first new example of an embedded minimal surface in over a hundred years (see [27]) this was a genus one surface with two catenoidal and one planar ends. Note that, Costa only wrote down the Weierstrass data for the surface and did not rigorously prove it was embedded. This was done by Hoffman and Meeks in [32]. In addition, they extended the construction and found embedded examples of every genus (see [34]). The (unexpected) existence of these surfaces initiated a burst of activity in the field. In 1993, using the Weierstrass representation, Hoffman, Karcher, and Wei in [36] constructed an immersed genus one helicoid. Computer graphics suggested it was embedded, but the existence of an embedded genus one helicoid followed only after Hoffman and Wei proposed a new construction in [38]. They constructed their surface as the limit of a family of screw-motion invariant minimal surfaces with periodic handles and a helicoidal end. Weber, Hoffman, and Wolf confirmed the existence of such a family of surfaces in [59] and ultimately proved

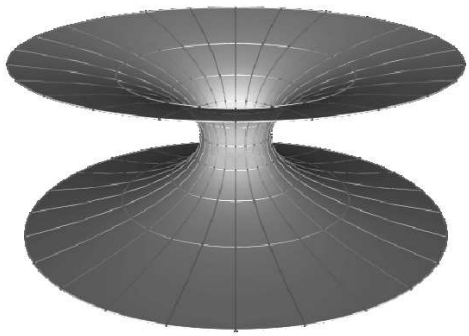

Figure 2-1: The catenoid (Courtesy of Matthias Weber)

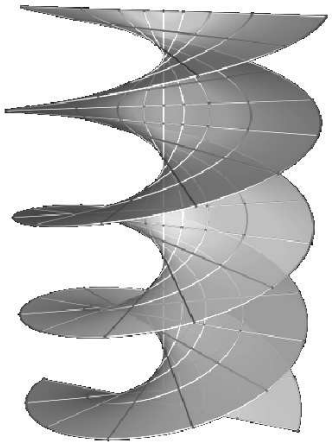

Figure 2-2: The helicoid (Courtesy of Matthias Weber)

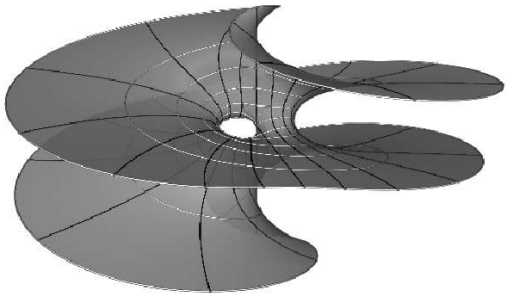

Figure 2-3: A genus one helicoid (Courtesy of Matthias Weber)

their embeddedness in [61]. Hoffman, Weber, and Wolf conjecture that this surface is not only the same surface as the one produced in [36], but is actually the "unique" genus-one helicoid. Recently, Hoffman and White, in [40], used a variational argument to construct an embedded genus-one helicoid, though whether their construction is the same as the surface produced in [61] is unknown.

2.2 Notation

Throughout, unless otherwise stated, Σ will be a complete, non-flat, element of $\mathcal{E}(1,g)$, the space of complete, properly embedded minimal surfaces with one end and finite genus g. We set $\mathcal{E}(1) = \cup_{g\geq 0}\mathcal{E}(1,g)$ be the space of all complete, properly embedded minimal surfaces with one end and finite genus and $\mathcal{E}(1,+) = \cup_{g>0}\mathcal{E}(1,g)$ to be the set of such surfaces with positive genus. We note that a result of Colding and Minicozzi, [24] (see also 3.2.2), allows one to drop "properly" from the definition of $\mathcal{E}(1,g)$. That is, a complete, embedded minimal surface with one end and finite genus is automatically properly embedded. Notice that as Σ has one end and is properly embedded and complete in $\mathbb{R}^3$, there exists an $R > 0$ so that if $\Sigma \in \mathcal{E}(1,+)$ then one of the components $\overline{\Sigma}$ of $\Sigma \cap B_R$ is a compact surface with connected boundary and the same genus as Σ. Thus, $\Sigma\backslash\overline{\Sigma}$ has genus 0 and is a neighborhood of the end of Σ. We will often refer to the *genus* of Σ when we wish not to specify a specific choice of $\overline{\Sigma}$, but rather to indicate some compact and connected subset of Σ of genus g.

Denote by $\Pi : \mathbb{R}^3 \to \mathbb{R}^2$ the projection $\Pi(x_1,x_2,x_3) = (x_1,x_2)$. Let

$$\mathbf{C}_\delta(y) = \left\{x : (x_3-y_3)^2 \leq \delta^2\left((x_1-y_1)^2+(x_2-y_2)^2\right)\right\} \subset \mathbb{R}^3 \tag{2.7}$$

be the complement of a double cone and set $\mathbf{C}_\delta = \mathbf{C}_\delta(0)$. Extrinsic balls (i.e. in $\mathbb{R}^3$) of radius R and centered at x are denoted by $B_R(x)$. For Σ a surface in $\mathbb{R}^3$, if $x \in \Sigma$ then $\mathcal{B}_R(x)$ is the intrinsic ball (in Σ) of radius R. We denote by $\Sigma_{x,R}$ the component of $\Sigma \cap B_R(x)$ containing x. Note that $\mathcal{B}_R(x) \subset \Sigma_{x,R}$ with equality if and only if $\Sigma_{x,R}$ is flat.

We denote a polar rectangle as follows:

$$S^{\theta_1,\theta_2}_{r_1,r_2} = \{(\rho,\theta) \mid r_1 \leq \rho \leq r_2, \theta_1 \leq \theta \leq \theta_2\}\,. \tag{2.8}$$

For a real-valued function, u, defined on a polar domain $\Omega \subset \mathbb{R}^+ \times \mathbb{R}$, define the map $\Phi_u : \Omega \to \mathbb{R}^3$ by $\Phi_u(\rho,\theta) = (\rho\cos\theta, \rho\sin\theta, u(\rho,\theta))$. In particular, if u is defined on $S^{\theta_1,\theta_2}_{r_1,r_2}$, then $\Phi_u(S^{\theta_1,\theta_2}_{r_1,r_2})$ is a multivalued graph over the annulus $D_{r_2}\backslash D_{r_1}$. We define the separation of the graph u by $w(\rho,\theta) = u(\rho,\theta+2\pi) - u(\rho,\theta)$. Thus, $\Gamma_u := \Phi_u(\Omega)$ is the graph of u, and Γ_u is embedded if and only if $w \neq 0$.

The graphs of interest to us throughout this paper will (almost) always be assumed to satisfy the following flatness condition:

$$|\nabla u| + \rho|\text{Hess }_u| + 4\rho\frac{|\nabla w|}{|w|} + \rho^2\frac{|\text{Hess }_w|}{|w|} \leq \epsilon < \frac{1}{2\pi}. \tag{2.9}$$

Note that if w is the separation of a u satisfying (2.4) and (2.9), then w satisfies a uniformly elliptic equation. Thus, if Γ_u is embedded then w has point-wise gradient bounds and a Harnack inequality.

Chapter 3

Colding-Minicozzi Theory

When we introduced minimal surfaces in Chapter 2, we allowed them to be immersed, as, from certain perspectives, this is quite natural. However, as the Weierstrass representation (2.3) shows, it is quite easy to construct many immersed minimal disks and so structural results are correspondingly weak. When one demands that the surfaces are, in addition, embedded, one greatly reduces the possible space of surfaces and extremely powerful structural results can be obtained. This is the point of view that Colding and Minicozzi take in their ground-breaking study of the structure of embedded minimal surfaces in [12, 19–22]. The key principle is that embeddedness is analogous to positivity, i.e. embedded minimal surfaces are analogous to positive solutions of second order elliptic equations. Recall, such positive solutions are necessarily much more rigid than general solutions as, for instance, one has Harnack inequalities.

The foundation of Colding and Minicozzi's work is their description of embedded minimal disks in [19–22], which underpins their more general results in [12]. Their description is as follows: If the curvature is small, then the surface is nearly flat and hence modeled on a plane (i.e. is, essentially, a single-valued graph). On the other hand, suppose $\Sigma \subset \mathbb{R}^3$ is an embedded minimal disk with $\partial\Sigma \subset \partial B_R$ and with large curvature, then it is modeled on a helicoid. That is, in a smaller ball the surface consists of two multivalued graphs that spiral together and that are glued along an "axis" of large curvature. Using this description, they derive very powerful rigidity results and settle several outstanding conjectures. Their applications include: developing a compactness theory for embedded minimal surfaces without area bounds (Theorem 3.2.1); proving the so-called one-sided curvature estimate Theorem 3.1.8, an effective version for embedded disks of the strong half-space theorem; and positively answering the Calabi-Yau conjecture for embedded minimal surfaces of finite topology (see Section 3.2.2). They also extend their work (in [12]) to minimal surfaces of arbitrary finite genus.

In proving their result for disks, Colding and Minicozzi prove a number of quantitative results making the rough dichotomy given above more precise. Our work is heavily based on these results and so we discuss them here in some detail. We state the main theorems of [19–22] and discuss, as much as possible, the ideas that go into of Colding and Minicozzi's proofs.

3.1 Structure of Embedded Minimal Disks

Let us first outline Colding and Minicozzi's argument and then go into more detail below. Suppose Σ is an embedded minimal disk with $\partial\Sigma \subset \partial B_R$ and with large curvature. In order to study Σ, Colding and Minicozzi first locate points $y \in \Sigma$ of "large curvature". By this they mean points which are an almost maximum (in a ball of the appropriate scale) of the curvature. To make this rigorous, for a point $x \in \Sigma$, they fix a scale $s_x > 0$ that is proportional to the inverse of the curvature at x. They call a pair $(y, s) \in \Sigma \cap \mathbb{R}^+$, a "blow-up pair," when y is an almost maximum for curvature in the ball around y of radius $s = s_y$. As an example, think of a point on the axis of a helicoid and the scale s as the distance between the sheets (see Figure 5-2 for an illustration). The points y, so (y, s) is a blow-up pair, are the points of large curvature. We note that standard blow-up arguments imply that, if there is large curvature in a ball, relative to the size of the ball, then there must be be a blow-up pair in the ball.

Let (y, s) be a blow-up pair, near y and on the scale s, the minimality and embeddedness force the surface to spiral like a helicoid. Indeed, Colding and Minicozzi show that Σ contains a small multi-valued graph $\tilde{\Sigma}_1$ near y. Using very delicate arguments that rely on the embeddedness of Σ and the connectedness of $\partial\Sigma$, they are able to show that the initial multi-graph found near y extends almost all the way to the boundary (in Σ) as a multi-graph, Σ_1. Using estimates for such graphs coming from elliptic theory and a barrier construction that relies on Meeks and Yau's results [46, 47] they look between the sheets of Σ_1 and show that there Σ consists of exactly one other multi-graph Σ_2. Using these two sheets, Colding and Minicozzi show that there are regions of large curvature above and below the original sheets and hence blow-up pairs. This allows them to iterate and form a "skeleton" of sheets. By appealing to their "one-sided" curvature estimate (whose proof only relies on being able to find such a "skeleton") they fill in the "skeleton" and obtain the claimed structure for Σ.

3.1.1 Points of large curvature

We begin by stating more precisely what is meant by blow-up pair and then discuss what is meant by the formation of small multi-graph and what quantitative information can be derived about these multi-graphs. We will also very briefly indicate how Colding and Minicozzi prove this.

Colding and Minicozzi have a number of equivalent definitions of what they mean by blow-up pair, but we will use throughout the following definition:

Definition 3.1.1. The pair $(y, s) \in \Sigma \times \mathbb{R}^+$, is a (C) *blow-up pair* if

$$\sup_{\Sigma \cap B_s(y)} |A|^2 \leq 4|A|^2(y) = 4C^2 s^{-2}. \tag{3.1}$$

Here C is a (large) parameter that will be specified by some of the theorems. As mentioned, these points are best understood by looking at a helicoid. For the helicoid,

a point on the axis is a a blow-up point and the scale s is proportional to the scale of the helicoid (i.e. the distance between sheets), in this case, C can be interpreted as this proportionality constant (see also Figure 5-2).

By a standard blow-up argument if there is large curvature in a ball (measured in terms of the scale of the ball) then there exists a blow-up pair in the ball. This is Lemma 5.1 of [20]:

Lemma 3.1.2. *If $0 \in \Sigma \subset B_{r_0}$, $\partial\Sigma \subset \partial B_{r_0}$ and $\sup_{B_{r_0/2}\cap\Sigma} |A|^2 \geq 16C^2 r_0^{-2}$ then there exists a pair (y, r_1) with $y \in \Sigma$ and $r_1 < r_0 - |y|$ so (y, r_1) is a C blow-up pair.*

We then have the following result giving the existence of a small multi-graph near a blow-up pair. This is Theorem 0.4 of [20]:

Theorem 3.1.3. *Given $N, \omega > 1$ and $\epsilon > 0$, there exists $C = C(N, \omega, \epsilon) > 0$ so: Let $0 \in \Sigma \subset B_R \subset \mathbb{R}^3$ be an embedded minimal disk, $\partial\Sigma \subset \partial B_R$. If $(0, r_0)$ is a C blow-up pair for $0 < r_0 < R$, then there exist $\bar{R} < r_0/\omega$ and (after a rotation) an N-valued graph $\Sigma_g \subset \Sigma$ over $D_{\omega\bar{R}} \backslash D_{\bar{R}}$ with gradient $\leq \epsilon$, and $dist_\Sigma(0, \Sigma_g) \leq \bar{R}$.*

To prove Theorem 3.1.3 Colding and Minicozzi first note the following consequence of the Gauss-Bonnet theorem and minimality, which they call the Caccioppoli inequality (Corollary 1.3 of [20]):

$$t^2 \int_{\mathcal{B}_{r_0}-2t} |A|^2 \leq r_0^2 \int_{\mathcal{B}_{r_0}} |A|^2 (1 - r/r_0)^2/2 = \int_0^{r_0} \int_0^r \int_{\mathcal{B}_\rho(x)} |A|^2 \\ = 2(Area(\mathcal{B}_{r_0}) - \pi r_0^2) \leq r_0 \ell(\partial\mathcal{B}_{r_0}) - 2\pi r_0^2. \tag{3.2}$$

That is the area of an intrinsic ball (or equivalently the length of its boundary) controls the total curvature of a fixed sub-ball. There is also a reverse inequality (i.e. where total curvature controls area) which holds for general surfaces and which Colding and Minicozzi call the Poincaré inequality. The Caccioppoli inequality implies that, when a minimal surface has extremely large curvature in a fixed extrinsic ball, it must have large area. The relationship between total curvature and point-wise curvature is based on the results of Choi and Schoen [11]. As a consequence, if the curvature is large then there must be points of the surface that are intrinsically a fixed distance apart, but extrinsically close. The fact that Σ is embedded implies that, by looking near these points, one then has two disjoint minimal disks that are extrinsically very close.

This heuristically suggests that the surfaces are nearly flat. Indeed, if these two disks have an a priori curvature estimate then the disjointness implies they are almost stable and hence one recovers such a flatness result (this is along the lines of [56], i.e. Theorem 2.1.6). It turns out that this is even true without the a priori curvature bounds (though without such curvature bounds this is only known a posteriori and follows from the one-sided curvature bounds 3.1.8). Motivated by this, Colding and Minicozzi, by very careful analysis, prove that away from a set of small area one does have uniform curvature bounds so deduce that away from a set of small area the disk is flat. This allows them to deduce Theorem 3.1.3.

3.1.2 Extending the sheets

Using the initial small multi-graph, Colding and Minicozzi show that it can be extended, as a graph and within the surface Σ, nearly all the way to the boundary of Σ. This result is one of the hardest parts of their argument and the proof relies on understanding the very delicate interplay between the geometry of Σ and elliptic estimates on the multi-graphs.

The main upshot of this analysis is Theorem 0.3 of [19]:

Theorem 3.1.4. *Given $\tau > 0$ there exist $N, \Omega, \epsilon > 0$ so that the following hold: Let $\Sigma \subset B_{R_0} \subset \mathbb{R}^3$ be an embedded minimal disk with $\partial\Sigma \subset B_{R_0}$. $\Omega r_0 < 1 < R_0/\Omega$ and Σ contains a N-valued graph Σ_g over $D_1 \backslash D_{r_0}$ with gradient $\leq \epsilon$ and*

$$\Sigma_g \subset \left\{ x_3^2 \leq \epsilon^2 (x_1^2 + x_2^2) \right\} \tag{3.3}$$

then Σ contains a 2-valued graph Σ_d over $D_{R_0/\Omega} \backslash D_{r_0}$ with gradient $\leq \epsilon$ and $(\Sigma_g)^M \subset \Sigma_d$.

Here $(\Sigma_g)^M$ indicates the "middle" 2-valued sheet of Σ_g. Combining this with the Theorem 3.1.3 one immediately obtains the existence of a multi-graph near a blow-up pair that extend almost all the way to the boundary. Namely, Theorem 0.2 of [20]:

Theorem 3.1.5. *Given $N \in \mathbb{Z}^+, \epsilon > 0$, there exist $C_1, C_2, C_3 > 0$ so: Let $0 \in \Sigma \subset B_R \subset \mathbb{R}^3$ be an embedded minimal disk, $\partial\Sigma \subset \partial B_R$. If $(0, r_0)$ is a C_1 blow-up pair then there exists (after a rotation) an N-valued graph $\Sigma_g \subset \Sigma$ over $D_{R/C_2} \backslash D_{2r_0}$ with gradient $\leq \epsilon$ and $\Sigma \subset \{x_3^2 \leq \epsilon^2 (x_1^2 + x_2^2)\}$. Moreover, the separation of Σ_g over ∂D_{r_0} is bounded below by $C_3 r_0$.*

Note that the lower bound on the initial separation is not explicitly stated in Theorem 0.2 of [20] but is proved in Proposition 4.15 of [20], as it will prove of crucial importance in our applications we include it in the theorem.

3.1.3 Finding large curvature

The preceding two sections show the existence near a blow-up point of a multi-graph, Σ_g, in Σ that extends almost all the way to the boundary. Colding and Minicozzi next show that, "between the sheets" of Σ_g, Σ consists of exactly one other multi-graph. That is, we have that, at least part of, Σ looks like (a few sheets of) a helicoid. Precisely, one has Theorem I.0.10 of [22]:

Theorem 3.1.6. *Suppose $0 \in \Sigma \subset B_{4R}$ is an embedded minimal disk with $\partial\Sigma \subset \partial B_{4R}$ and $\Sigma_1 \subset \{x_3 \leq x_1^2 + x_2^2\} \cap \Sigma$ is an $(N+2)$-valued graph of u_1 over $D_{2R} \backslash D_r$ with $|\nabla u_1| \leq \epsilon$ and $N \geq 6$. There exist $C_0 > 2$ and $\epsilon_0 > 0$ so that if $R \geq C_0 r_1$ and $\epsilon_0 \geq \epsilon$, then $E_1 \cap \Sigma \backslash \Sigma_1$ is an (oppositely oriented) N-valued graph Σ_2.*

Here E_1 is the region between the sheets of Σ_1:

$$\begin{aligned} &\{(r\cos\theta, r\sin\theta, z) : \\ &\qquad 2r_1 < r < R, -2\pi \leq \theta < 0, u_1(r, \theta - N\pi) < z < u_1(r, \theta + (N+2)\pi)\}. \end{aligned} \tag{3.4}$$

The proof of this relies uses Meeks and Yau's solution of the embedded plateau problem for 3-manifolds with mean convex boundary [46, 47]. Colding and Minicozzi apply this result to the region E_1 to construct a barrier, which they use to prove the theorem.

Thus, near a blow-up point there are two multi-graphs that spiral together and extend within Σ almost all the way to the boundary of Σ. This allows Colding and Minicozzi to use the following result, from [21], to deduce that there are regions of large curvature above and below the original blow-up pairs (and hence by Lemma 3.1.2 blow-up points there). They use Corollary III.3.5 of [21]:

Corollary 3.1.7. *Given C_1 there exists C_2 so: Let $0 \in \Sigma \subset B_{2C_2r_0}$ be an embedded minimal disk. Suppose $\Sigma_1, \Sigma_2 \subset \Sigma \cap \{x_3^2 \leq (x_1^2 + x_2^2)\}$ are graphs of u_i satisfying (2.9) on $S^{-2\pi,2\pi}_{r_0,C_2r_0}$, $u_1(r_0, 2\pi) < u_2(r_0, 0) < u_1(r_0, 0)$, and $\nu \subset \partial\Sigma_{0,2r_0}$ a curve from Σ_1 to Σ_2. Let Σ_0 be the component of $\Sigma_{0,C_2r_0} \setminus (\Sigma_1 \cup \Sigma_2 \cup \nu)$ which does not contain Σ_{0,r_0}. Suppose $\partial\Sigma \subset \partial B_{2C_2r_0}$ then*

$$\sup_{x \in \Sigma_0 \setminus B_{4r_0}} |x|^2 |A|^2(x) \geq 4C_1^2. \tag{3.5}$$

If one desired to prove only that there was *one* region of large curvature one would note that $|x|^2|A|^2 \leq C$ in Σ implies that the curvature, of Σ, has a certain growth rate. In this case, Colding and Minicozzi can show that, if C is small enough, this growth rate forces Σ to be a single graph outside of a ball of a certain size, which contradicts the existence of the two multi-graphs. It can be shown that the multi-graphs have faster than quadratic curvature decay (this is similar to Bers' Theorem 2.1.5) and so this region of large curvature is either above or below the multi-graph. To get that there are *two* regions of large curvature, one must use that the two multi-graphs coming from Theorem 3.1.6 are intrinsically close (see for instance the last statement of 3.1.5). Thus, these multi-graphs, together with a "short connecting" curve, ν, separate (a subset of) Σ into two regions, one above the graphs, and one below. Arguing as before, one still shows that both these regions contain large curvature.

Using Corollary 3.1.7, one sees how a "skeleton" of multi-graphs can be iteratively constructed. Notice that, a priori, we have very little control on the structure of this "skeleton," because the new blow-up pairs only lie above and below the original one in a very weak sense.

3.1.4 One-sided curvature estimate

As we have seen, in an embedded minimal disk with large curvature one can find a helicoidal "skeleton" of the surface. Colding and Minicozzi exploit this to show an extremely powerful curvature estimate for embedded disks that are close to, and on one side of, a plane. This one-sided curvature estimate not only significantly restricts the structure of the "skeleton," but also allows one to fill it in, and so recover the structure of nearly the entire disk. In addition, the one-sided curvature estimate is of great importance in its own right; it is, essentially, an effective version, for embedded disks, of the strong half-space theorem. This last theorem, proved by Hoffman and

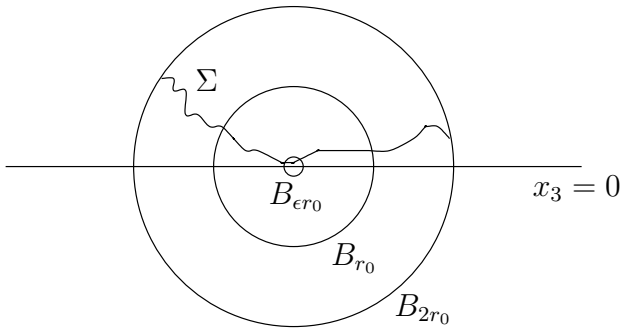

Figure 3-1: The one-sided curvature estimate

Meeks in [35], says that any complete and proper minimal immersion that lies on one side of a plane is necessarily a plane. The effective version says that an embedded disk that lies on one side of a plane, and is close to the plane, has a uniform curvature estimate. Note that rescalings of the catenoid show that the topological restriction is essential. The simplest one-sided curvature estimate is Theorem 0.2 of [22]:

Theorem 3.1.8. *(see Figure 3-1) There exists $\epsilon > 0$, so that if $\Sigma \subset B_{r_0} \cap \{x_3 > 0\} \subset \mathbb{R}^3$ is an embedded minimal disk with $\partial\Sigma \subset B_{2r_0}$, then for all components, Σ', of $B_{r_0} \cap \Sigma$ which intersect $B_{\epsilon r_0}$ we have $\sup_{\Sigma'} |A_\Sigma|^2 \leq r_0^{-2}$*

This result can be extend to the more general situation where one replaces the plane with a general embedded minimal surface. Namely, we have Corollary 0.4 of [22]:

Corollary 3.1.9. *There exist $c > 1$, $\epsilon > 0$ so that the following holds: Let Σ_1 and $\Sigma_2 \subset B_{cr_0} \subset \mathbb{R}^3$ be disjoint embedded minimal surfaces with $\partial\Sigma_i \subset \partial B_{cr_0}$ and $B_{\epsilon r_0} \cap \Sigma_i \neq \emptyset$. If Σ_1 is a disk, then for all components Σ_1' of $B_{r_0} \cap \Sigma_1$ which intersect B_{r_0}:*

$$\sup_{\Sigma'} |A|^2 \leq r_0^{-2}. \tag{3.6}$$

An important corollary of this theorem is the specialization of the above to a minimal disk, Σ, that contains a double-valued graph. In this case, one obtains uniform curvature estimates for Σ outside of a cone whose axis is transverse to the multi-graph. Precisely, one has Corollary I.1.9 of [22]:

Corollary 3.1.10. *(see Figure 3-2) There exists $\delta_0 > 0$ so that the following holds: Let $\Sigma \subset B_{2R}$ be an embedded minimal disk with $\partial\Sigma \subset \partial B_{2R}$. If Σ contains a 2-valued graph $\Sigma_d \subset \{x_3^2 \leq \delta_0^2(x_1^2 + x_2^2\}$ over $D_R \backslash D_{r_0}$ with gradient $\leq \delta_0$, then each component of $B_{R/2} \cap \Sigma \backslash (\mathbf{C}_{\delta_0}(0) \cup B_{2r})$ is a multi-valued graph with gradient ≤ 1*

Remark 3.1.11. In the above $\mathbf{C}_{\delta_0}$ represents the cone with axis the x_3-axis, that is the complement of the set we define in Section 2.2.

This last corollary makes it clear that the blow-up points that lie above and below a given point actually lie outside of $\mathbf{C}_{\delta_0}$ (i.e. within a cone with axis transverse to

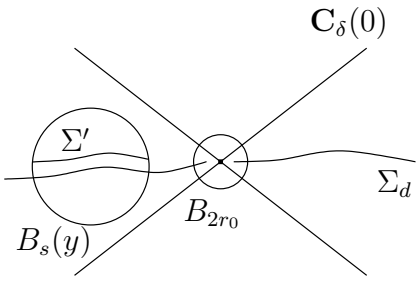

Figure 3-2: The one-sided curvature estimate in a cone

the sheets of the graph) and so are actually a fixed height above and below the given one. This restricts the structure of the "skeleton" considered in the previous section. Moreover, the corollary allows one to fill in the "skeleton" and see that the disk really does have the structure of two multi-graphs that spiral together and are glued along an axis.

The idea of the proof of Theorem 3.1.8 is to suppose one had a minimal disk, Σ, near and on one side of a plane but with very large curvature in $B_1 \cap \Sigma$. If this were true, then there would be a blow-up pair (y_0, s_0) with $y_0 \in B_1 \cap \Sigma$ (and s_0 very small). Thus, two multi-graphs would form near y_0 and so there is another blow-up pair (y_1, s_1) below (y_0, s_0). Continuing in this fashion Σ would eventually be forced to spiral through the plane, yielding a contradiction. There are a number technical difficulties making this argument rigorous. The main problem is due to the weak a priori understanding on what "below" means. By some very careful analysis, Colding and Minicozzi are nevertheless able to resolve these difficulties, and we refer the interested reader to [22] for the details.

A final important consequence of the one-sided curvature estimate is that the axis along which the curves are glued lies in an intersection of cones and so is "Lipschitz". This follows as once one has a single blow-up point, one can use the associated graph that forms, to get curvature bounds outside of a cone (of a uniform angle) with fulcrum at the blow-up point. This forces all other blow-up pairs to lie within this cone.

3.2 Some Applications

The theory developed in [19–22] to study embedded minimal disks and outlined above has had a number of important applications. We introduce here those that are most important to our own work. The first of these topics is the lamination theory of Colding and Minicozzi, which gives a compactness for sequences of embedded disks subject to very mild conditions (in particular without area or curvature bounds). We next discuss Colding and Minicozzi's proof of the Calabi-Yau conjecture for embedded minimal surfaces of finite topology. Finally, we will briefly sketch their extension of the lamination result to sequences admitting more general topologies.

3.2.1 Lamination theory

The ellipticity of the minimal surface equation suggests that one should have nice compactness results for sequences of minimal surfaces. Classically, one does obtain such compactness after assuming uniform area or curvature bounds. In the former case one only has convergence in a weak sense, whereas in the later, the Arzela-Ascoli theorem and Schauder estimates allow one to obtain smooth sub-sequential convergence (though, without area bounds the limit is not necessarily a surface). For sequences of embedded minimal disks, Colding and Minicozzi are able to prove a compactness result that only requires a very mild geometric condition on the boundaries of the disks and in particular does not require area or curvature bounds. Roughly speaking, their structural result implies that either there is a uniform curvature bound a sub-sequence or else a sub-sequence is modeled (locally) on the singular behavior of the homothetic blow-down of the helicoid. This is Theorem 0.1 of [22]:

Theorem 3.2.1. *Let $\Sigma_i \subset B_{R_i} = B_{R_i}(0) \subset \mathbb{R}^3$ be a sequence of embedded minimal disks with $\partial\Sigma_i \subset \partial B_{R_i}$ where $R_i \to \infty$. If $\sup_{B_1 \cap \Sigma_i} |A|^2 \to \infty$ then there exists a sub-sequence, Σ_j, and a Lipschitz curve $\mathcal{S} : \mathbb{R} \to \mathbb{R}^3$ such that after a rotation of $\mathbb{R}^3$:*

1. *$x_3(\mathcal{S}(t)) = t$.*
2. *Each Σ_j consists of exactly two multi-valued graphs away from $\mathcal{S}$ (which spiral together).*
3. *for each $1 > \alpha > 0$ $\Sigma_j \backslash \mathcal{S}$ converges in the C^α-topology to the foliation, $\mathcal{F} = \{x_3 = t\}_t$ of $\mathbb{R}^3$.*
4. *$\sup_{B_r(\mathcal{S}(t)) \cap \Sigma_j} |A|^2 \to \infty$ for all $r > 0, t \in \mathbb{R}$.*

Notice that away from the singular set $\mathcal{S}$, the convergence is classical, whereas at the singular set the curvature must blow-up. Also note that the assumption that $R_i \to \infty$ is essential, as is shown by examples constructed by Colding and Minicozzi in [17] (see also Chapter 5 and in particular Figure 5-2). One would hope to deduce Theorem 3.2.1 directly from the description of embedded disks given in Section 3.1. However, it is not this easy because the description of embedded disks is a local statement, whereas the compactness theorem is global in nature – a point made clear by the examples of [17]. The results needed to bridge this gap can be found in [15].

3.2.2 The Calabi-Yau conjecture

In 1965, Calabi conjectured that there are no bounded complete minimal hypersurface in $\mathbb{R}^n$ (see [8]). If one allows the surface to be immersed, this is false, for example Nadirashvili in [52] constructs a complete minimal immersion lying within the unit ball of $\mathbb{R}^3$. However, when one additionally demands that the surface be embedded (and of finite topology in $\mathbb{R}^3$), Colding and Minicozzi, in [24], show that not only is the surface necessarily unbounded, but that several of Calabi's more ambitious conjectures are true. Indeed, they show that any such surface is actually properly

embedded. Consequently, we may take $\mathcal{E}(1, g)$ to be the set of complete, embedded minimal surfaces of genus g and with one end, as these conditions automatically imply the surface is properly embedded.

The key tool Colding and Minicozzi use is what they call the "chord-arc" bound for embedded minimal disks. This is Theorem 0.5 of [24], which roughly shows that, near a point of large curvature, extrinsic distance controls intrinsic distance:

Theorem 3.2.2. *There exists a constant $C > 0$ so that if $\Sigma \subset \mathbb{R}^3$ is an embedded minimal disk, $\mathcal{B}_{2R} = \mathcal{B}_{2R}(0)$ is an intrinsic ball in $\Sigma \backslash \partial\Sigma$ of radius $2R$, and $\sup_{B_{r_0}} |A|^2 > r_0^{-2}$ where $R > r_0$, then for $x \in \mathcal{B}_R$*

$$C\mathrm{dist}_\Sigma(x, 0) < |x| + r_0. \tag{3.7}$$

This theorem allows one to easily deduce that complete, embedded minimal disks are properly embedded. Namely, either Σ is flat and so is necessarily properly embedded, or outside a sufficiently large intrinsic ball one may apply the chord-arc bounds and get a two-sided comparison between extrinsic and intrinsic distance. The generalization to embedded minimal surfaces of finite topology is not much more difficult.

The chord-arc bounds are themselves an easy consequence (using the one-sided curvature estimate) of the following weak chord-arc bound (Proposition 1.1 of [24]):

Proposition 3.2.3. *There exists $\delta_1 > 0$ so that if $\Sigma \subset \mathbb{R}^3$ is an embedded minimal disk, then for all intrinsic balls $\mathcal{B}_R(x)$ in $\Sigma \backslash \partial\Sigma$ the component $\Sigma_{x,\delta_1 R}$ of $B_{\delta_1 R}(x) \cap \Sigma$ containing x satisfies*

$$\Sigma_{x,\delta_1 R} \subset \mathcal{B}_{R/2}(x). \tag{3.8}$$

This result is proved by Colding and Minicozzi using their structural theory and a blow-up argument, we refer the reader to [24] for more details.

3.2.3 Generalizations to non-trivial topology

In [12], Colding and Minicozzi generalize their lamination theory for minimal disks to a compactness result that allows for more or less arbitrary sequences of minimal surfaces with finite (and uniformly bounded) genus. To do so, they must allow for a more general class of singular models, as is clear from considering a rescaling of the catenoid. In order to prove such a compactness result, they must also develop a structural theory for a more general class of topological types. Surfaces modeled on the neck of a catenoid form an important such class, one that is characterized by having genus zero and disconnected boundary. Another important class, especially for our purposes, are surfaces of finite genus and connected boundary. This second class of surfaces, because they have connected boundary, turn out to be structurally very similar to disks. Indeed, most of the results of [19–22] hold for them (in a suitably form) and with only slight modifications of the proofs.

As we will use results from [12] in Chapters 6 and (even more so) in Chapter 7, we give a bit more details about the theory, though provide only a sketch. The most

general lamination result of [12] is very similar to Theorem 3.2.1 but the lamination $\mathcal{L}$ can no longer be guaranteed to foliate all of $\mathbb{R}^3$ and the singular set $\mathcal{S}$ is in general much more complicated.

More precisely, suppose Σ_i is a sequence of embedded minimal surfaces, with a uniform bound on the genus and $\partial\Sigma_i \subset B_{R_i}$ with $R_i \to \infty$. Colding and Minicozzi show that if the curvature of the sequence blows up at a point $y \in \mathbb{R}^3$ (i.e. if for all $r > 0$, $\sup_i \sup_{B_r(y)\cap\Sigma_i} |A|^2 = \infty$), then after a rotation, a sub-sequence Σ_i converge to the singular lamination $\mathcal{L}\backslash\mathcal{S}$ in the C^α topology ($\alpha \in (0,1)$) and the curvature blows up at all points of $\mathcal{S}$. Here $\mathcal{L} = \{x_3 = t\}_{t\in\mathcal{I}}$, $\{x_3(y) : y \in \mathcal{S}\} = \mathcal{I}$ and $\mathcal{I}$ is a closed subset of $\mathbb{R}^3$ (this is Theorem 0.14 of [12]). Note, if the Σ_i are disks then Theorem 3.2.1 implies that $\mathcal{I} = \mathbb{R}$ and $\mathcal{S}$ is a Lipschitz graph over the x_3-axis (and is in fact is a line).

More generally, the topology of the sequence restricts $\mathcal{I}$ and gives more information about convergence near $\mathcal{S}$ (and structure of $\mathcal{S}$). We distinguish between two types of singular points $y \in \mathcal{S}$. Heuristically, the distinction is between points where the topology of the sequence does not concentrate (i.e. on small scales near the point all the Σ_i are disks) and points where it does (i.e. on small scales near the point all the Σ_i contain necks). This is the exact description if the genus of the surfaces is zero, but must be refined for sequences with positive genus. Following [12], we make this precise for a sequence Σ_i converging to the lamination $\mathcal{L}$ with singular set $\mathcal{S}$:

Definition 3.2.4. We say $y \in \mathcal{S}$ is an element of $\mathcal{S}_{ulsc}$ if there exist both $r > 0$ fixed and a sequence $r_i \to 0$ such that $B_r(y) \cap \Sigma_i$ and $B_{r_i}(y) \cap \Sigma_i$ have the same genus and every component of $B_{r_i}(y) \cap \Sigma_i$ has connected boundary.

Definition 3.2.5. We say $y \in \mathcal{S}$ is an element of $\mathcal{S}_{neck}$ if there exist both $r > 0$ fixed and a sequence $r_i \to 0$ such that $B_r(y) \cap \Sigma_i$ and $B_{r_i}(y) \cap \Sigma_i$ have the same genus and $B_{r_i}(y) \cap \Sigma_i$ has at least one component with disconnected boundary.

If the Σ_i are the homothetic blow-down of helicoid or of a genus-one helicoid, then 0 is a element of $\mathcal{S}_{ulsc}$, whereas if the Σ_i are the homothetic blow-down of a catenoid then 0 is an element of $\mathcal{S}_{neck}$. Colding and Minicozzi show that near a point of $\mathcal{S}_{ulsc}$ this is the model behavior, i.e. locally the sequence looks like the homothetic blow-down of a helicoid. On the other hand, near a point of $\mathcal{S}_{neck}$ the convergence near y is modeled on the homothetic blow-down of a catenoid.

One of the major results of [12], is to give refinements of the general compactness theorem based on more careful analysis of the topology of the sequence. The most powerful of these is the no-mixing theorem (i.e. Theorem 0.4 of [12]), which states that, up to a passing to a sub-sequence, either $\mathcal{S} = \mathcal{S}_{ulsc}$ or $\mathcal{S} = \mathcal{S}_{neck}$. This is particularly, important as ULSC sequences (i.e. sequences where $\mathcal{S} = \mathcal{S}_{ulsc}$) have a great deal of structure. Indeed, in this case Theorem 0.9 of [12] tells us that we (nearly) have the same behavior of Theorem 3.2.1, i.e. $\mathcal{I} = \mathbb{R}$ and $\mathcal{S}$ is either a single line parallel to the x_3-axis or the union of two lines. In the latter case, the global picture is that of the degeneration of the Riemann examples; as this case must be considered in our work in only a handful of places, we defer a more detailed discussion to Section 6.4.2. On the other hand, when $\mathcal{S} = \mathcal{S}_{neck}$ there is in general no additional structure to $\mathcal{S}$ and $\mathcal{I}$ may be a proper subset of $\mathbb{R}$.

Chapter 4

Uniqueness of the Helicoid

In this chapter we discuss the so called "uniqueness of the helicoid," proved by Meeks and Rosenberg (Theorem 0.1 in [45]):

Theorem 4.0.6. *The only elements of $\mathcal{E}(1,0)$ are planes and helicoids.*

Meeks and Rosenberg's proof, which we will outline in Section 4.1, depends crucially on the lamination theory and one-sided curvature estimate of Colding and Minicozzi (see [22]). Their proof also uses quite sophisticated (and subtle) complex analytic arguments. By making more direct use of the results of Colding and Minicozzi on the structure of embedded minimal disks, we present a more geometric and significantly simpler proof. As we will see in Chapter 6, this proof generalizes quite easily to the case of embedded minimal surfaces with finite genus and one end.

4.1 Meeks and Rosenberg's Approach

In [45], Meeks and Rosenberg apply Colding and Minicozzi's lamination theory, Theorem 3.2.1, to show that a non-flat, complete embedded minimal disk, Σ, must be the helicoid (i.e. the helicoid is "unique"). Their approach uses the lamination theory to gain a (weak) understanding of the asymptotic geometry of Σ. Prior to to the work of Colding and Minicozzi, there were no tools available to gain such an understanding of the asymptotic geometry and essentially nothing was known without strong assumptions. With this (weak) information about the end Meeks and Rosenberg then take a classical approach to understanding the surface, in particular they make heavy use of some rather subtle complex analytic arguments.

In order to get at the asymptotic structure of, Σ, a non-flat element of $\mathcal{E}(1,0)$, Meeks and Rosenberg consider the homothetic blow-down of Σ. That is they take a sequence $\lambda_i \searrow 0$ of positive numbers and consider $\lambda_i\Sigma$ a sequence of rescalings of Σ. Such a sequence satisfies the conditions of Colding and Minicozzi's lamination theorem and must (as Σ is non-flat) having curvature blowing up at 0. Thus, it contains a sub-sequence converging to a singular lamination. That is, up to a rotation of $\mathbb{R}^3$, away from some Lipschitz curve, the $\lambda_i\Sigma$ converge to a foliation of flat parallel planes transverse to the x_3-axis. Meeks and Rosenberg argue that this foliation is

independent of the choice of blow-down (i.e. the rotation is independent) and so gives a sort of "tangent cone at infinity" to Σ. Thus, weakly, the surface is asymptotic to a helicoid, which they use to conclude that the Gauss map of Σ omits the north and south poles. Due to their reliance on the lamination theory, this, like many of their arguments, is based on a somewhat involved proof by contradiction. An important (and easily derived) consequence is that, $\nabla_\Sigma x_3 \neq 0$ and so locally x_3 together with it's harmonic conjugate x_3^* give a holomorphic coordinate $z = x_3 + ix_3^*$.

This asymptotic structure, combined with a result on parabolicity of Collin, Kusner, Meeks and Rosenberg [26], is then used to show that z is actually a proper conformal diffeomorphism between Σ and $\mathbb{C}$ and hence the end is conformally a punctured disk. Here a surface with boundary is said to be parabolic if two bounded harmonic functions whose values agree on the boundary are in fact identically equal. For instance, the closed disk with a point removed from the boundary is parabolic whereas the closed disk with an open interval removed from the boundary is not. The result of [26] implies that Σ intersected with half-spaces $\{\pm x_3 \geq h\}$ is parabolic. As parabolic domains can be rather subtle, quite a bit of work goes into deducing that that Σ is conformally equivalent to $\mathbb{C}$ and that z is actually a conformal diffeomorphism between the two spaces.

Finally, Meeks and Rosenberg look at level sets of the log of the stereographic projection of the Gauss map and use a Picard type argument to show that this holomorphic map does not have an essential singularity at ∞ and in fact is linear. Using the Weierstrass representation, they conclude that Σ is the helicoid.

4.2 Outline of the Argument

By using the work of Colding and Minicozzi more directly, we are able to get a much stronger and more explicit description of the asymptotic geometry, which significantly simplifies the argument. Following Colding and Minicozzi (and fundamentally using their work), we show Σ contains a central "axis" of large curvature away from which it consists of two multi-valued graphs spiraling together, one strictly upward, the other downward. Additionally, the "axis" is shown to be nearly orthogonal to the sheets of the graph. Notice this strict spiraling and "orthogonality" of the axis only follows as Σ is complete, and need not hold for general embedded minimal disks.

More precisely we have (see Figure 6-1):

Theorem 4.2.1. *There exist subsets of Σ, $\mathcal{R}_A$ and $\mathcal{R}_S$, with $\Sigma = \mathcal{R}_A \cup \mathcal{R}_S$ such that, after possibly rotating $\mathbb{R}^3$, $\mathcal{R}_S$ can be written as the union of two (oppositely oriented) multivalued graphs u^1 and u^2 with non-vanishing angular derivative. Further, there exists $\epsilon_0 > 0$ such that on $\mathcal{R}_A$, $|\nabla_\Sigma x_3| \geq \epsilon_0$.*

Remark 4.2.2. Here u^i multivalued means that it can be decomposed into N-valued ϵ-sheets (see Definition 4.3.1) with varying center. The angular derivative is then with respect to the obvious polar form on each of these sheets. For simplicity we will assume throughout that both u^i are ∞-valued.

In order to establish this decomposition, we first use the explicit existence of multi-valued graphs to get the strict spiraling in $\mathcal{R}_S$. An application of the proof of Rado's theorem (see [55] or [54]), then gives non-vanishing of $|\nabla_\Sigma x_3|$ on $\mathcal{R}_A$ and, by a Harnack inequality, the uniform lower bound. Crucially,

Proposition 4.2.3. *On Σ, after a rotation of $\mathbb{R}^3$, $\nabla_\Sigma x_3 \neq 0$ and, for all $c \in \mathbb{R}$, $\Sigma \cap \{x_3 = c\}$ consists of exactly one properly embedded smooth curve.*

This implies that $z = x_3 + ix_3^*$ is a holomorphic coordinate on Σ. By looking at the stereographic projection of the Gauss map, g, in $\mathcal{R}_S$ we show that z maps onto $\mathbb{C}$ and so Σ is conformally the plane. This follows from the control on the behavior of g due to strict spiraling. Indeed, away from a neighborhood of $\mathcal{R}_A$, Σ is conformally the union of two closed half-spaces with $\log g = h$ providing the identification. It then follows that h is also a conformal diffeomorphism and hence $h(p) = \lambda z(p)$. The Weierstrass representation (2.3) and embeddedness together imply that Σ is the helicoid.

This Chapter is based on [3].

4.3 Geometric Decomposition

4.3.1 Initial sheets

As we saw in Chapter 3, multivalued minimal graphs are the basic building blocks Colding and Minicozzi use to study the structure of minimal surfaces. We will also make heavy use of the properties of such graphs and so introduce the following notation:

Definition 4.3.1. A multivalued minimal graph Σ_0 is an *N-valued (ϵ-)sheet (centered at 0 on the scale 1)*, if $\Sigma_0 = \Gamma_u$ and u, defined on $S_{1,\infty}^{-\pi N, \pi N}$, satisfies (2.4), (2.9), $\lim_{\rho\to\infty} \nabla u(\rho, 0) = 0$, and $\Sigma_0 \subset \mathbf{C}_\epsilon$.

Using Simons' inequality, Corollary 2.3 of [15] shows that on the one-valued middle sheet of a 2-valued graph satisfying (2.9), the hessian of u has faster than linear decay. Thus, one has a Bers like result on asymptotic tangent planes (see 2.1.5) for such graphs when they are defined over unbounded annuli (see also [14]). In particular, our normalization at ∞ of an ϵ-sheet is well defined. Indeed, the normalization at ∞ gives gradient decay for Γ_u, an ϵ-sheet,

$$|\nabla u| \leq C\epsilon\rho^{-5/12}. \tag{4.1}$$

We now give a condition for the existence of ϵ-sheets. Roughly, all that is required is a point with large curvature relative to nearby points, that is a blow-up pair. Recall,

Definition 4.3.2. The pair (y, s), $y \in \Sigma$, $s > 0$, is a (C) *blow-up pair* if

$$\sup_{\Sigma\cap B_s(y)} |A|^2 \leq 4|A|^2(y) = 4C^2 s^{-2}. \tag{4.2}$$

As we saw in Chapter 3, near a blow-up pair, there is a large multi-valued graph (see Theorem 3.1.3, i.e. Theorem 0.4 of [20]). In particular, after a suitable rotation we obtain an ϵ-sheet. For a more thorough treatment of this in the context of complete disks, see Theorem 4.5.1 in Section 4.5.

Once we have one ϵ-sheet, we can use Colding and Minicozzi's one-sided curvature estimate, Theorem 3.1.8 (i.e. Theorem 0.2 of [22]) to extend the graph (and (2.9)) from an ϵ-sheet to the outside of a wide cone (see Figure 3-2). Recall, there is a uniform curvature bound on embedded minimal disks close to, but on one side of, an embedded minimal surface. Thus, using the initial ϵ-sheet as this "nearby" surface, the embeddedness of Σ implies that, outside of a cone, all components of Σ are graphs. A barrier argument then shows that there are only two such pieces. Namely, by Theorem 3.1.6 (i.e. I.0.10 of [22]), the parts of Σ that lie in between an ϵ-sheet make up a second multi-valued graph. Furthermore, the one-sided curvature estimates gives gradient estimates which, when coupled with elliptic estimates on the multi-valued graphs, reveal that this multi-valued graph actually contains an ϵ-sheet. Thus, around a blow-up point, Σ consists of two ϵ-sheets spiraling together.

We now make the last statement precise. Suppose u is defined on $S^{-\pi N-3\pi,\pi N+3\pi}_{1/2,\infty}$ and Γ_u is embedded. We define E to be the region over $D_\infty \backslash D_1$ between the top and bottom sheets of the concentric subgraph of. That is (see also (3.4)):

$$E = \{(\rho\cos\theta, \rho\sin\theta, t) : \\ 1 \leq \rho \leq \infty, -2\pi \leq \theta < 0, u(\rho, \theta - \pi N) < t < u(\rho, \theta + (N+2)\pi\}. \tag{4.3}$$

Using Theorem 3.1.6 (i.e. Theorem I.0.10 of [22]), Theorem 4.5.1, and the one-sided curvature estimate, we have:

Theorem 4.3.3. *Given $\epsilon > 0$ sufficiently small, there exist $C_1, C_2 > 0$ so: Suppose $(0, s)$ is a C_1 blow-up pair. Then there exist two 4-valued ϵ-sheets $\Sigma_i = \Gamma_{u_i}$ $(i = 1, 2)$ on the scale s which spiral together (i.e. $u_1(s, 0) < u_2(s, 0) < u_1(s, 2\pi)$). Moreover, the separation over ∂D_s of Σ_i is bounded below by $C_2 s$.*

Remark 4.3.4. We refer to Σ_1, Σ_2 as (ϵ-)blow-up sheets *associated with* (y, s).

Proof. Choose $\epsilon_0 > 0$ and N_0 as in Theorem 3.1.6). For $\epsilon < \epsilon_0$ choose N_ϵ, δ_ϵ as in the proof of Theorem 4.5.1. With $N - 6 = \max\{N_\epsilon + 4, N_0\}$ denote by C_1', C_2' the constants given by Theorem 4.5.1. Thus, if $(0, r)$ is a C_1' blow-up pair then there exists an N-valued ϵ-sheet $\Sigma_1' = \Gamma_{u_1'}$ on scale r inside of Σ. Applying Theorem I.0.10 to u_1', we see that $\Sigma \cap E \backslash \Sigma_1'$ is given by the graph of a function u_2' defined on $S^{-\pi N_\epsilon - 4\pi, \pi N_\epsilon + 4\pi}_{2r,\infty}$. In particular, for u_2' on $S^{-4\pi,4\pi}_{2e^{N_\epsilon} r,\infty}$ we have (2.9) as long as we can control $|\nabla u_2'|$. But here we use one-sided curvature (and the ϵ-sheet Σ_1'). Namely, given $\alpha = \min\{\epsilon/2, \delta_\epsilon\}$, one-sided curvature estimates allow us to choose $\delta_0 > 0$ so that in the cone $\mathbf{C}_{\delta_0}$ (and outside a ball) Σ is graphical with gradient less than α. By (4.1), there exists $r_1 > 0$ such that $|\nabla u_1'| \leq \delta_0$ on $S^{-5\pi,5\pi}_{r_1,\infty}$ and this 5-valued graph is contained in $\mathbf{C}_{\delta_0} \backslash B_{r_1}$. Moreover, since five sheets of u_1' are inside of $\mathbf{C}_{\delta_0}$, the four concentric sheets of u_2' are also in that cone. Set $\gamma = \max\left\{2e^{N_\epsilon}, 1\right\}$. Let u_1 and u_2 be given by restricting u_1' and u_2' to $S^{-4\pi,4\pi}_{\gamma r_1,\infty}$ and define $\Sigma_i = \Gamma_{u_i}$.

Set $C_1 = \gamma C_1'$, so if $(0, s)$ is a C_1 blow-up pair then Σ_i will exist on scale s. Integrating (2.9), the lower bound C_2' gives a lower bound on initial separation of Σ_1. We find C_2 by noting that if the initial separation of Σ_2 was too small there would be two sheets between one sheet of Σ_1. □

4.3.2 Blow-up pairs

Since Σ is not a plane, we can always find at least one blow-up pair (y, s). We then use this initial pair to find a sequence of blow-up pairs forming an "axis" of large curvature. The key results we need are Lemma 3.1.2 (i.e Lemma 5.1 of [20]), recall this lemma says that as long as curvature is large enough in some ball we can find a blow-up pair in the ball, and Corollary 3.1.7 (i.e. Corollary III.3.5 of [21]), which guarantees points of large curvature above and below blow-up points. Colding and Minicozzi, in Lemma 2.5 of [24], provide a good overview of this process of decomposing Σ into (what we call) blow-up sheets. The main result is the following:

Theorem 4.3.5. *For $1/2 > \gamma > 0$ and $\epsilon > 0$ both sufficiently small, let C_1 be given by Theorem 4.3.3. Then there exists $C_{in} > 4$ and $\delta > 0$ so: If $(0, s)$ is a C_1 blow-up pair then there exist (y_+, s_+) and (y_-, s_-), C_1 blow-up pairs, with $y_\pm \in \Sigma \cap B_{C_{in}s} \setminus (B_{2s} \cup \mathbf{C}_\delta)$, $x_3(y_+) > 0 > x_3(y_-)$, and $s_\pm \leq \gamma |y_\pm|$.*

Hence, given a blow-up pair, we can iteratively find a sequence of blow-up pairs ordered by height and lying within a cone, with the distance between subsequent pairs bounded by a fixed multiple of their scale.

4.3.3 Asymptotic helicoids

We now wish to show that an ϵ-sheet, Γ_u, strictly spirals for sufficiently large radius. The key result needed to show this is Lemma 14.1 of [18]. This lemma and the gradient decay (4.1) implies that ϵ-sheets can be approximated by a combination of planar, helicoidal, and catenoidal pieces. That is, there is a "Laurent expansion" for the almost holomorphic function $u_x - iu_y$. This result allows us to bound the oscillation on broken circles $C(\rho) := S^{-\pi,\pi}_{\rho,\rho}$ of u_θ, which yields asymptotic lower bounds for u_θ. The precise statement of the lemma is:

Lemma 4.3.6. *Given Γ_u, a 3-valued ϵ-sheet on scale 1, set $f = u_x - iu_y$. Then for $r_1 \geq 1$ and $\zeta = \rho e^{i\theta}$ with $(\rho, \theta) \in S^{-\pi,\pi}_{2r_1,\infty}$*

$$f(\zeta) = c\zeta^{-1} + g(\zeta) \tag{4.4}$$

where $c = c(r_1, u) \in \mathbb{C}$ and $|g(\zeta)| \leq C_0 r_1^{-1/4} |\zeta|^{-1} + C_0 \epsilon r_1^{-1} |w(r_1, -\pi)|$.

The proof is an exercise in integration by parts using the fact that the faster than linear decay on the hessian of an initial sheet gives good decay for Δu. Using this approximation result, we now bound the oscillation:

Lemma 4.3.7. *Suppose Γ_u is a 3-valued ϵ-sheet on scale 1. Then for $\rho \geq 2$, there exists a universal $C > 0$ so:*

$$\operatorname*{osc}_{C(\rho)} u_\theta \leq C\rho^{-1/4} + C\epsilon|w(\rho, -\pi)|. \tag{4.5}$$

Proof. Using Lemma 4.3.6 and the identification $u_\theta(\rho, \theta) = -\operatorname{Im} \zeta f(\zeta)$ for $\zeta = \rho e^{i\theta}$, we compute:

$$\begin{aligned} \operatorname*{osc}_{C(\rho)} u_\theta &= \sup_{|\zeta|=\rho} \operatorname{Im}\ (-c - \zeta g(\zeta)) - \inf_{|\zeta|=\rho} \operatorname{Im}\ (-c - \zeta g(\zeta)) \\ &\leq 2 \sup_{|\zeta|=\rho} |\zeta||g(\zeta)| \ \leq\ 4C_0\rho^{-1/4} + 2C_0\epsilon|w(\rho/2, -\pi)|. \end{aligned}$$

The last inequality comes from Lemma 4.3.6, setting $2r_1 = \rho$. Finally, integrate (2.9) to get the bound $|w|(\rho/2, -\pi) \leq 4|w|(\rho, -\pi)$ and choose C sufficiently large. □

Integrating u_θ on $C(\rho)$ gives $w(\rho, -\pi)$, which yields a lower bound on $\sup_{C(\rho)} u_\theta$ in terms of the separation. The oscillation bound of (4.5) then gives a lower bound for u_θ. Indeed, for ϵ sufficiently small and large ρ, u_θ is positive.

Proposition 4.3.8. *There exists an ϵ_0 so: Suppose Γ_u is a 3-valued ϵ-sheet on scale 1 with $\epsilon < \epsilon_0$ and $w(1, \theta) \geq C_2 > 0$. Then there exists $C_3 = C_3(C_2) \geq 2$, so that on $S^{-\pi,\pi}_{C_3,\infty}$:*

$$u_\theta(\rho, \theta) \geq \frac{C_2}{8\pi}\rho^{-\epsilon}. \tag{4.6}$$

Proof. Since $\int_{-\pi}^{\pi} u_\theta(\rho, \theta)\ d\theta = w(\rho, -\pi)$ we see $w(\rho, -\pi) \leq 2\pi \sup_{C(\rho)} u_\theta$. Using the oscillation bound (4.5) then gives the lower bound:

$$(1 - 2\pi C\epsilon)w(\rho, -\pi) - 2\pi C\rho^{-1/4} \leq 2\pi \inf_{C(\rho)} u_\theta. \tag{4.7}$$

Pick ϵ_0 so that $2\pi C\epsilon_0 \leq 1/2$. Integrating (2.9) yields $w(\rho, \theta) \geq w(1, \theta)\rho^{-\epsilon} \geq C_2\rho^{-\epsilon}$. Thus,

$$\inf_{C(\rho)} u_\theta \geq \frac{C_2}{4\pi}\rho^{-\epsilon} - C\rho^{-1/4}. \tag{4.8}$$

Since $\epsilon < 1/4$, just choose C_3 large. □

4.3.4 Decomposition of Σ

In order to decompose Σ, we use the explicit asymptotic properties found above to show that, away from the "axis," (ultimately $\mathcal{R}_{\mathcal{A}}$) Σ consists of two strictly spiraling graphs. In particular, this implies that all intersections of Σ with planes transverse to the x_3-axis have exactly two ends. The proof of Rado's theorem then gives that $\nabla_\Sigma x_3$ is non-vanishing and so each level set consists of one unbounded smooth curve.

A curvature estimate and a Harnack inequality then give the lower bound on $|\nabla_\Sigma x_3|$ near the axis. To prove Theorem 4.2.1 we first construct $\mathcal{R}_S$.

Lemma 4.3.9. *There exist constants C_1, R_1 and a sequence (y_i, s_i) of C_1 blow-up pairs of Σ so that: $x_3(y_i) < x_3(y_{i+1})$ and for $i \geq 0$, $y_{i+1} \in B_{R_1 s_i}(y_i)$ while for $i < 0$, $y_{i-1} \in B_{R_1 s_i}(y_i)$. Moreover, if $\tilde{\mathcal{R}}_A$ is the connected component of $\bigcup_i B_{R_1 s_i}(y_i) \cap \Sigma$ containing y_0 and $\mathcal{R}_S = \Sigma \backslash \tilde{\mathcal{R}}_A$, then $\mathcal{R}_S$ has exactly two unbounded components, which are (oppositely oriented) multivalued graphs u^1 and u^2 with $u^i_\theta \neq 0$. In particular, $\nabla_\Sigma x_3 \neq 0$ on the two graphs.*

Proof. Fix $\epsilon < \epsilon_0$ where ϵ_0 is given by Proposition 4.3.8. Using this ϵ, from Theorem 4.3.3 we obtain the blow-up constant C_1 and denote by C_2 the lower bound on initial separation. Suppose $0 \in \Sigma$ and that $(0, 1)$ is a C_1 blow-up pair. From Theorem 4.3.5 there exists a constant C_{in} so that there are C_1 blow-up pairs (y_+, s_+) and (y_-, s_-) with $x_3(y_-) < 0 < x_3(y_+)$ and $y_\pm \in B_{C_{in}}$. Note by Proposition 4.5.3 that there is a fixed upper bound N on the number of sheets between the blow-up sheets associated to $(y_\pm, s_\pm)$ and the sheets Σ^0_i $(i = 1, 2)$ associated to $(0, 1)$.

As a consequence of Theorem 4.5.2, there exists an R so that all the N sheets above and the N sheets below Σ^0_i are ϵ-sheets centered on the x_3-axis on scale R. Call these pairs of 1-valued sheets Σ^j_i with $-N \leq j \leq N$. Integrating (2.9), we obtain from C_2 and N a value, C_2', so that for all Σ^j_i, the separation over ∂D_R is bounded below by C_2'. Non-vanishing of the right hand side of (4.6) is scaling invariant, so there exists a C_3 such that: on each Σ^j_i, outside of a cylinder centered on the x_3-axis of radius RC_3, $u^i_\theta \neq 0$. The chord-arc bounds of [24] (i.e. Theorem 3.2.2) then allow us to pick R_1 large enough so the component of $B_{R_1} \cap \Sigma$ containing 0 contains this cylinder, the points y_+, y_- and meets each Σ^j_i. Finally, we note that all the statements in the theorem are invariant under rescaling. Hence, we may use Theorem 4.3.5 to construct a sequence of C_1 blow-up pairs (y_i, s_i) satisfying the necessary conditions. □

The placement of the blow-up pairs and the strict spiraling gives:

Lemma 4.3.10. *For all h, there exist $\alpha, \rho_0 > 0$ so that for all $\rho > \rho_0$ the set $\Sigma \cap \{x_3 = c\} \cap \{x_1^2 + x_2^2 = \rho^2\}$ consists of exactly two points for $|c - h| \leq \alpha$.*

Proof. First note, for ρ_0 large, the intersection is never empty by the maximum principle and because Σ is proper. Without loss of generality we may assume $h = 0$ with $0 \in Z^0 = \Sigma \cap \{x_3 = 0\}$ and $|A|^2(0) \neq 0$. Let R_1 and the set of blow-up pairs be given by Lemma 4.3.9. There then exists ρ_0 so for $2\rho > \rho_0$, $\{x_1^2 + x_2^2 = \rho^2\} \cap Z^0$ lies in the set $\mathcal{R}_S$. If no such ρ_0 existed then, since the blow-up pairs lie outside a cone, there would exist $\delta > 0$ and a subset of the blow-up pairs (y_i, s_i) so $0 \in B_{\delta R_1 s_i}(y_i)$. However, Lemma 2.26 of [24] (see also Lemma 6.4.4), with $K_1 = \delta R_1$, would then imply $|A|^2(0) \leq K_2 s_i^{-2}$, or $|A|^2(0) = 0$, a contradiction. Now, for some small α and $\rho > \rho_0$, $Z^c \cap \{x_1^2 + x_2^2 = \rho^2\}$ lies in $\mathcal{R}_S$ for all $|c| < \alpha$, and so $\{x_1^2 + x_2^2 = \rho^2\} \cap \{-\alpha < x_3 < \alpha\} \cap \Sigma$ consists of the union of the graphs of u^1 and u^2 over the circle ∂D_ρ, both of which are monotone increasing in height. □

As x_3 is harmonic on Σ, Proposition 4.2.3 is an immediate consequence of the previous result and Rado's Theorem. Recall, Rado's theorem [55] implies that any minimal surface whose boundary is a graph over the boundary of a convex domain is a graph over that domain. The proof of Rado's theorem reduces to showing that a non-constant harmonic function on a closed disk has an interior critical point if and only if the level curve of the function through that point meets the boundary in at least 4 points, which is exactly what we use. We now show Theorem 4.2.1:

Proof. By Lemma 4.3.9 it remains only to construct $\mathcal{R}_A$ and to show that $|\nabla_\Sigma x_3|$ is bounded below on it. Suppose that $(0,1)$ is a blow-up pair. By the chord-arc bounds of [24], there exists γ large enough so that the intrinsic ball of radius γR_1 contains $\Sigma \cap B_{R_1}$. Lemma 2.26 of [24] implies that curvature is bounded in $B_{2\gamma R_1} \cap \Sigma$ uniformly by K. The function $v = -2\log|\nabla_\Sigma x_3| \geq 0$ is well defined and smooth by Proposition 4.2.3 and standard computations give $\Delta_\Sigma v = |A|^2$. Then, since $|\nabla_\Sigma x_3| = 1$ somewhere in the component of $B_1(0) \cap \Sigma$ containing 0, we can apply a Harnack inequality (see Theorems 9.20 and 9.22 in [30]) to obtain an upper bound for v on the intrinsic ball of radius γR_1 that depends only on K. Consequently, there is a lower bound ϵ_0 on $|\nabla_\Sigma x_3|$ in $\Sigma \cap B_{R_1}$. Since this bound is scaling invariant, the same bound holds around any blow-up pair. Finally, any bounded component, Ω, of $\mathcal{R}_S$ has boundary in $\tilde{\mathcal{R}}_A$ and so, since v is subharmonic, $|\nabla_\Sigma x_3| \geq \epsilon_0$ on Ω. We take $\mathcal{R}_A$ to be the union of all such Ω with $\tilde{\mathcal{R}}_A$ and so by shrinking $\mathcal{R}_S$ obtain Theorem 4.2.1. □

4.4 Conformal Structure of a Complete Embedded Minimal Disk

4.4.1 Conformal structure

Since $\nabla_\Sigma x_3$ is non-vanishing and the level sets of x_3 in Σ consist of a single curve, the map $z = x_3 + ix_3^* : \Sigma \to \mathbb{C}$ is a global holomorphic coordinate (here x_3^* is the harmonic conjugate of x_3). Additionally, $\nabla_\Sigma x_3 \neq 0$ implies that the normal of Σ avoids $(0,0,\pm 1)$. Thus, the stereographic projection of the Gauss map, denoted by g, is a holomorphic map $g : \Sigma \to \mathbb{C}\setminus\{0\}$. By monodromy, there exists a holomorphic map $h = h_1 + ih_2 : \Sigma \to \mathbb{C}$ so that $g = e^h$. We will use h to show that z is actually a conformal diffeomorphism between Σ and $\mathbb{C}$. As the same is then true for h, embeddedness and the Weierstrass representation imply Σ is the helicoid.

4.4.2 Conformal mapping properties of the Gauss map

We note the following relation between $\nabla_\Sigma x_3$, g and h which comes from (2.3):

$$|\nabla_\Sigma x_3| = 2\frac{|g|}{1+|g|^2} \leq 2e^{-|h_1|}. \tag{4.9}$$

An immediate consequence of (4.9) and the decomposition of Theorem 4.2.1 is that there exists $\gamma_0 > 0$ so on $\mathcal{R}_A$, $|h_1(z)| \leq \gamma_0$. This imposes strong rigidity on h:

Proposition 4.4.1. *Let $\Omega_\pm = \{x \in \Sigma : \pm h_1(x) \geq 2\gamma_0\}$ then h is a proper conformal diffeomorphism from $\Omega_\pm$ onto the closed half-spaces $\{z : \pm \mathrm{Re}\, z \geq 2\gamma_0\}$.*

Proof. Let $\gamma > \gamma_0$ be a regular value of h_1. Such γ exists by Sard's theorem and indeed form a dense subset of (γ_0, ∞). We first claim that the smooth submanifold $Z = h_1^{-1}(\gamma)$ has a finite number of components. Note that Z is non-empty by (4.1) and (4.9). By construction, Z is a subset of $\mathcal{R}_S$ and, up to choosing an orientation, Z lies in the graph of u^1, which we will henceforth denote as u. Let us parametrize one of the components of Z by $\phi(t)$, non-compact by the maximum principle, and write $\phi(t) = \Phi_u(\rho(t), \theta(t))$. Note, $h_2(\phi(t))$ is monotone in t by the Cauchy-Riemann equations and because $\nabla_\Sigma h_1(\phi(t)) \neq 0$.

At the point $\Phi_u(\rho, \theta)$ we compute:

$$g(\rho, \theta) = -\frac{1}{\sqrt{1 + |\nabla u|^2} - 1} \left(u_\rho(\rho, \theta) + i \frac{u_\theta(\rho, \theta)}{\rho} \right) e^{i\theta}. \tag{4.10}$$

Since $u_\theta(\rho(t), \theta(t)) > 0$, there exists a function $\tilde{\theta}(t)$ with $\pi < \tilde{\theta}(t) < 2\pi$ such that

$$|\nabla u|(\rho(t), \theta(t)) e^{i\tilde{\theta}(t)} = -u_\rho(\rho(t), \theta(t)) - i \frac{u_\theta(\rho(t), \theta(t))}{\rho(t)}. \tag{4.11}$$

Thus, $h_2(\phi(t)) = \theta(t) + \tilde{\theta}(t)$.

We now claim that, up to replacing $\phi(t)$ by $\phi(-t)$, $\lim_{t \to \pm\infty} h_2(\phi(t)) = \pm\infty$. With out loss of generality we need only rule out the possibility that $\lim_{t \to \infty} h_2(\phi(t)) = R < \infty$. Suppose this occurred, then by the monotonicity of h_2, $h_2(\phi(t)) < R$. The formula for $h_2(\phi(t))$ implies that, for t large, $\phi(t)$ lies in one sheet. The decay estimates (4.1) together with (4.9) imply $\rho(t)$ cannot became arbitrarily large and so the positive end of ϕ lies in a compact set. Thus, there is a sequence of points $p_j = \phi(t_j)$, with t_j monotonically increasing to ∞, so $p_j \to p_\infty \in \Sigma$. By the continuity of h_1, $p_\infty \in Z$, and since $h_2(p_j)$ is monotone increasing with supremum R, $h_2(p_\infty) = R$, and so p_∞ is not in ϕ. However, $p_\infty \in Z$ implies $\nabla_\Sigma h(p_\infty) \neq 0$ and so h restricted to a small neighborhood of p_∞ is a diffeomorphism onto its image, contradicting ϕ coming arbitrarily close to p_∞.

Thus, the formula for $h_2(\phi(t))$ and the bound on $\tilde{\theta}$ show that $\theta(t)$ must extend from $-\infty$ to ∞. We now conclude that there are at most a finite number of components of Z. Namely, since $\theta(t)$ runs from $-\infty$ to ∞ we see that every component of Z must meet the curve $\eta(\rho) = \Phi_u(\rho, 0) \in \mathcal{R}_S$. Again, the gradient decay of (4.1) says that the set of intersections of Z with η lies in a compact set, and so consists of a finite number of points. Now, suppose there was more than one component of Z. Looking at the intersection of Z with η, we order these components innermost to outermost; parametrize the innermost curve by $\phi_1(t)$ and the outermost by $\phi_2(t)$. Pick τ a regular value for h_2, and parametrize the component of $h_2^{-1}(\tau)$ that meets ϕ_1 by $\sigma(t)$, writing $\sigma(t) = \Phi_u(\rho(t), \theta(t))$ in $\mathcal{R}_S$. From the formula for h_2, $|\theta(t) - \tau| \leq 2\pi$. Again, $\sigma(t)$ cannot have an end in a compact set, so $\rho(t) \to \infty$. Hence, σ must also intersect ϕ_2 contradicting the monotonicity of h_1 on σ.

Hence, when $\gamma > \gamma_0$ is a regular value of h_1, $h_1^{-1}(\gamma)$ is a single smooth curve.

We claim this implies that all $\gamma > \gamma_0$ are regular values. Suppose $\gamma' > \gamma_0$ were a critical value of h_1. Then, as h_1 is harmonic, the proof of Rado's theorem implies for $\gamma > \gamma_0$, a regular value of h_1 near γ', $h_1^{-1}(\gamma)$ would have at least two components. Thus, $h : \Omega_+ \to \{z : \mathrm{Re}\, z \geq 2\gamma_0\}$ is a conformal diffeomorphism that maps boundaries onto boundaries, immediately implying that h is also proper on Ω_+, and similarly for Ω_-. □

By looking at z, which already has well understood behavior away from ∞, we see that Σ is conformal to $\mathbb{C}$ with z providing an identification.

Proposition 4.4.2. *The map $h \circ z^{-1} : \mathbb{C} \to \mathbb{C}$ is linear.*

Proof. We first show that z is a conformal diffeomorphism between Σ and $\mathbb{C}$ – i.e. z is onto. This will follow if we show x_3^* goes from $-\infty$ to ∞ on the level sets of x_3. The key fact is: each level set of x_3 has one end in Ω_+ and the other in Ω_-. This is an immediate consequence of the radial gradient decay on level sets of x_3 forced by the one-sided curvature estimate. Thus, x_3 runs from $-\infty$ to ∞ along the curve $\partial\Omega_+$ and so $z(\partial\Omega_+)$ splits $\mathbb{C}$ into two components with only one, V, meeting $z(\Omega_+) = U$. After conformally straightening the boundary of V (using the Riemann mapping theorem) and precomposing with $h|_{\Omega_+}^{-1}$ we obtain a map from a closed half-space *into* a closed half-space with the boundary mapped *into* the boundary. We claim that this map is necessarily *onto*, that is U equals $\bar{V}$. Suppose it was not onto, then a Schwarz reflection would give a holomorphic map from $\mathbb{C}$ into a simply connected proper subset of $\mathbb{C}$. Because the latter is conformally a disk, Liouville's theorem would imply this map was constant, a contradiction. As a consequence, if $p \to \infty$ in Ω_+ then $z(p) \to \infty$, with the same true in Ω_-. Thus, along each level set of x_3, $|x_3^*(p)| \to \infty$ and so z is onto. Then, by the level set analysis in the proof of 4.4.1 and Picard's theorem, $h \circ z^{-1}$ is a polynomial and is indeed linear. □

4.4.3 Uniqueness

After a translation in $\mathbb{R}^3$ and a re-basing of x_3^*, $h(z) = \alpha z$ for some $\alpha \in \mathbb{C}$. As dz is the height differential, the Weierstrass representation (2.3) gives:

$$x_1(it) = |\alpha|^{-2} \left(\alpha_2 \sinh(\alpha_2 t) \sin(\alpha_1 t) - \alpha_1 \cosh(\alpha_2 t) \cos(\alpha_1 t)\right)$$

and

$$x_2(it) = |\alpha|^{-2} \left(\alpha_2 \sinh(\alpha_2 t) \cos(\alpha_1 t) + \alpha_1 \cosh(\alpha_2 t) \sin(\alpha_1 t)\right),$$

where $\alpha = \alpha_1 + i\alpha_2$. By inspection, this curve is only embedded when $\alpha_1 = 0$, i.e. if $\alpha = i\alpha_2$. The factor α_2 corresponds to a homothetic rescaling and so Σ is the helicoid.

4.5 Addendum

In the interest of clarity, we specialize some of Colding and Minicozzi's work to complete disks. As these results are mostly technical points we collect them here in order not to interrupt the flow of the argument.

4.5.1 Blow-up sheets

To show that near a blow-up pair there is a single N-valued ϵ-sheet, one needs two results of Colding and Minicozzi. First, from [20], is the existence, near a blow-up point, of N-valued graphs that extend almost to the boundary. Then, by [19], since a large number of sheets gives (2.9), after a suitable rotation one has an ϵ-sheet.

Theorem 4.5.1. *Given $\epsilon > 0$, $N \in \mathbb{Z}^+$, there exist $C_1, C_2 > 0$ so: Suppose that $(0, s)$ is a C_1 blow-up pair of Σ. Then there exists (after a rotation of $\mathbb{R}^3$) an N-valued ϵ-sheet $\Sigma_0 = \Gamma_{u_0}$ on the scale s. Moreover, the separation over ∂D_s of Σ_0 is bounded below by $C_2 s$.*

Proof. Proposition II.2.12 of [19] and standard elliptic estimates give an $N_\epsilon \in \mathbb{Z}^+$ and $\delta_\epsilon > 0$ so that if u satisfies (2.4) on $S^{-\pi N_\epsilon, \pi N_\epsilon}_{e^{-N_\epsilon}, \infty}$ and $\Gamma_u \subset \mathbf{C}_{\delta_\epsilon}$, then on $S^{0,2\pi}_{1,\infty}$ we have all the terms of (2.9) bounded (by $\epsilon/2$) except $|\nabla u|$. Setting $\tau = \min\left\{\frac{\epsilon}{4}, \frac{\delta_\epsilon}{2}\right\}$ and $N_0 = N + N_\epsilon + 2$, apply Corollary 4.14 from [20] to obtain C. That is, if $(0, t)$ is a C blow-up pair, then the corollary gives an N_0-valued graph u defined on $S^{-\pi N_0, \pi N_0}_{t,\infty}$ with $\Gamma_u \subset \mathbf{C}_\tau \cap \Sigma$ and $|\nabla u| \leq \tau$. Hence by above (and a rescaling) we see that u satisfies (2.9) on $S^{-\pi N, \pi N}_{e^{N_\epsilon} t, \infty}$. At this point we do not a priori know that $\lim_{\rho \to \infty} \nabla u(\rho, 0) = 0$. However, there is an asymptotic tangent plane. Thus after a small rotation to make this parallel to the x_1-x_2 plane (and a small adjustment to τ and t), we may assume the limit is zero.

Proposition 4.15 of [20] gives a $\beta > 0$ so that $w(t, \theta) \geq \beta t$. Integrating (2.9), we obtain from this a C_2 so that $w(e^{N_\epsilon} t, \theta) \geq C_2 e^{N_\epsilon} t$. Finally, if we set $C_1 = C e^{N_\epsilon}$ then $(0, s)$ being a C_1 blow-up pair implies that $(0, e^{-N_\epsilon} s)$ is a C blow-up pair. This gives the result. □

Once we have a single sheet, we can immediately apply the one-sided curvature estimate to obtain a graphical region inside of a cone which, moreover, satisfies (2.9) in a smaller cone. Results along these lines can by found in [15] and [21]. We will need:

Theorem 4.5.2. *Suppose Σ contains a 4-valued ϵ-sheet Σ_0 on the scale 1 with ϵ sufficiently small. Then there exist $R \geq 1$, $\delta > 0$ depending only on ϵ such that the component of $\Sigma \cap (\mathbf{C}_\delta \backslash B_R)$ that contains the 3-valued middle sheet on scale R of Σ_0 can be expressed as the multivalued graph of a function, u, which satisfies* (2.9).

4.5.2 Geometry near a blow-up pair

The existence of a blow-up pair imposes strong control on nearby geometry. The chord-arc bound and Lemma 2.26 of [24] are examples. We also have:

Proposition 4.5.3. *Given K, there is an N so that: If (y_1, s_1) and (y_2, s_2) are C blow-up pairs of Σ with $y_2 \in B_{K s_1}(y_1)$, then the number of sheets between the associated blow-up sheets is at most N.*

Proof. We note that for a large, universal constant C' the area of $B_{C'Ks_1}(y_1) \cap \Sigma$ gives a bound on N, so it is enough to uniformly bound this area. The chord-arc bounds of [24] give a uniform constant γ depending only on C' so that $B_{C'Ks_1}(y_1) \cap \Sigma$ is contained in $\mathcal{B}_{\gamma Ks_1}(y_1)$ the intrinsic ball in Σ of radius γKs_1. Furthermore, Lemma 2.26 of [24] gives a uniform bound on the curvature of Σ in $\mathcal{B}_{\gamma Ks_1}(y_1)$ and hence a uniform bound on the area of $\mathcal{B}_{\gamma Ks_1}(y_1)$ by the Poincaré inequality of [20]. Since $B_{C'Ks_1}(y_1) \cap \Sigma \subset \mathcal{B}_{\gamma Ks_1}(y_1)$ it also has uniformly bounded area. □

Chapter 5

Structure Near a Blow-up Pair

As has been discussed in Chapter 3, Colding and Minicozzi give a complete, but essentially qualitative, description of the structure of an embedded minimal disk in $\mathbb{R}^3$. Recall they, roughly speaking, show that any such surface is either modeled on a plane (i.e. is nearly graphical) or is modeled on a helicoid (i.e. is two multi-valued graphs glued together along an axis). In the latter case, the distortion may be quite large. For instance, in [51], Meeks and Weber "bend" the helicoid; that is, they construct minimal surfaces where the axis is an arbitrary $C^{1,1}$ curve (see Figure 5-1). A more serious example of distortion is given by Colding and Minicozzi in [17]. There they construct a sequence of minimal disks modeled on the helicoid, where the ratio between the scales (a measure of the tightness of the spiraling of the multi-graphs) at nearby points of the axis becomes arbitrarily large (see Figure 5-2).

Nevertheless, when viewed on the appropriate scale ,there is very little distortion. Indeed, by combining Colding and Minicozzi's compactness result for sequences of disks and the uniqueness of the helicoid of Chapter 4, we give a more quantitative and sharper description of embedded minimal disks near the points of large curvature. That is, we look near a blow-up pair (y, s) in an embedded minimal disk and show that on the scale s the disk is Lipschitz close to a helicoid (i.e. there is very little distortion on this scale). Moreover, using the surfaces of [17] we show that the scale that we find for which the surface is near a helicoid must be nearly optimal.

We note that the material appearing in this chapter is drawn from [3] and [2].

5.1 Lipschitz Approximation

We wish to show that, on the correct scale, the qualitative description of an embedded minimal disk of large curvature given by Colding and Minicozzi can be made quantitative. That is, near a point of large curvature, the surface looks, in a Lipschitz sense, like a piece of the helicoid. Note that Lipschitz could be replaced by C^k (with some constants being suitably adjusted), but the geometric structure is already captured on the Lipschitz level and the description is simplest in this form.

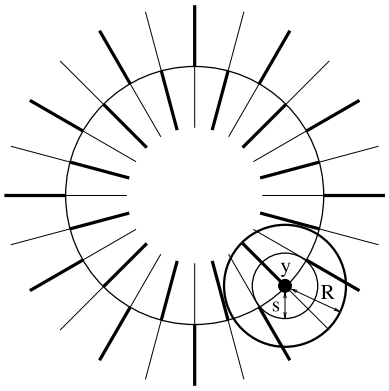

Figure 5-1: A cross section of one of Meeks and Weber's examples, with the axis as a circle. We indicate a subset which is a disk. Here R is the outer scale of said disk and s the blow-up scale.

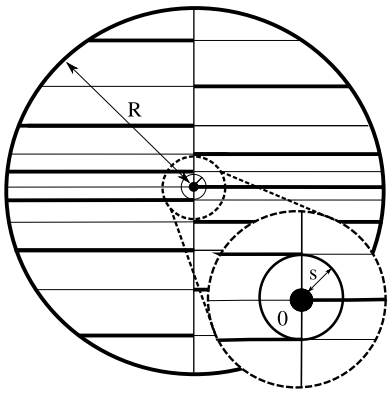

Figure 5-2: A cross section of one of Colding and Minicozzi's examples. We indicate the two important scales: $R = 1$ the outer scale and s the blow-up scale. (Here $(0, s)$ is a blow-up pair.)

Theorem 5.1.1. *Given $\epsilon, R > 0$ there exists $R' \geq R$ so: Suppose $0 \in \Sigma'$ is an embedded minimal disk with $\Sigma' \subset B_{R's}(0)$, $\partial\Sigma' \subset \partial B_{R's}(0)$, and $(0, s)$ a blow-up pair (see 3.1.1). Then there exists Ω, a subset of a helicoid, so that Σ, the component of $\Sigma' \cap B_{Rs}$ containing 0, is bi-Lipschitz with Ω, and the Lipschitz constant is in $(1-\epsilon, 1+\epsilon)$.*

Before proving the theorem, we need the following simple lemma. First, consider two surfaces $\Sigma_1, \Sigma_2 \subset \mathbb{R}^3$, so that Σ_2 is the graph of ν over Σ_1. Then the map $\phi : \Sigma_1 \to \Sigma_2$ defined as $\phi(x) = x + \nu(x)\mathbf{n}(x)$ is smooth. Moreover, if ν is small, in a C^1 sense, then ϕ is an "almost isometry".

Lemma 5.1.2. *Let Σ_2 be the graph of ν over Σ_1, with $\Sigma_1 \subset B_R$, $\partial\Sigma_1 \subset \partial B_R$ and $|A_{\Sigma_1}| \leq 1$. Then, for ϵ sufficiently small, $|\nu| + |\nabla_{\Sigma_1}\nu| \leq \epsilon$ implies ϕ is a diffeomorphism with $1 - \epsilon \leq ||d\phi|| \leq 1 + \epsilon$.*

Proof. For ϵ sufficiently small (depending on Σ_1), ϕ is injective by the tubular neighborhood theorem. Viewing the tangent spaces of the Σ_i as subspaces of $\mathbb{R}^3$, for orthonormal vectors $e_1, e_2 \in T_p\Sigma_1$ we compute:

$$d\phi_p(e_i) = e_i + \langle \nabla_{\Sigma_1}\nu(p), e_i\rangle \mathbf{n}(p) + \nu(p) D\mathbf{n}_p(e_i). \tag{5.1}$$

The last two terms are together controlled by ϵ. Hence, $1 - \epsilon < |D\phi_p(e_i)| < 1 + \epsilon$. □

Proof. (of Theorem 5.1.1) By rescaling we may assume that $s = 1$. We proceed by contradiction. Suppose no such R' existed for fixed ϵ, R. That is, there exists a sequence of counter-examples; embedded minimal disk Σ_i' with $\Sigma_i' \subset B_{R_i}$, $\partial\Sigma_i' \subset \partial B_{R_i}$, $(0,1)$ a C blow-up pair of each Σ_i' and $R \leq R_i \to \infty$, but Σ_i, the component of $B_R \cap \Sigma_i'$ containing zero, is not close to a helicoid.

By definition, $|A_{\Sigma_i'}(0)|^2 = C > 0$ for all Σ_i' and so the lamination theory of Colding and Minicozzi (i.e. Theorem 3.2.1) implies that a sub-sequence of the Σ_i' converge smoothly, and with multiplicity one, to Σ_∞, a complete embedded minimal disk. Namely, in any ball centered at 0 the curvature of Σ_i is uniformly bounded by Lemma 2.26 of [24]. Furthermore, the chord-arc bounds of [24] give uniform area bounds and so by standard compactness arguments one has smooth convergence (possibly with multiplicity) to Σ_∞. If the multiplicity of the convergence is greater than 1, then one can construct a positive solution to the Jacobi equation (see Appendix B of [12]). That implies Σ_∞ is stable, and thus a plane by Schoen's extension of the Bernstein theorem [56]. This would contradict the non-vanishing curvature at 0. As Corollary 0.7 of [24] gives properness of Σ_∞, Theorem 4.0.6 implies Σ_∞ is a helicoid. We may, by rescaling, assume Σ_∞ has curvature 1 along the axis.

For any fixed R' a sub-sequence of $\Sigma_i' \cap B_{R'}$ converges to $\Sigma_\infty \cap B_{R'}$ in the smooth topology. And so, for any ϵ, with i sufficiently large, we find a smooth ν_i defined on a subset of Σ_∞ so that $|\nu_i| + |\nabla_{\Sigma_\infty}\nu_i| < \epsilon$ and the graph of ν_i is $\Sigma_i' \cap B_{R'}$. Choosing R' large enough to ensure minimizing geodesics between points in Σ_i lie in $\Sigma_i' \cap B_{R'}$ (using the chord-arc bounds of [24]), Lemma 5.1.2 gives the desired contradiction. □

5.2 Scale of the Approximation

We now wish to study the sharpness the Lipschitz approximation given by Theorem 5.1.1. In particular, we are interested in whether such a result can hold on a scale larger than the blow-up scale. To try and make this more precise, let $0 \in \Sigma$ be an embedded minimal disk with $\partial\Sigma \subset \partial B_R = \partial B_R(0)$ and $(0, s)$ is a blow-up pair. There are then two important scales; R the outer scale and s the blow-up scale. Colding and Minicozzi's description of Σ holds on the outer scale R, i.e. they give a value $0 < \Omega < 1$ so that the component of $\Sigma \cap B_{\Omega R}$ containing 0 consists of two multi-valued graphs glued together. On the other hand, Theorem 5.1.1 shows that on the scale of s (provided R/s is large), Σ is bi-Lipschitz to a piece of a helicoid with Lipschitz constant near 1. Using the surfaces constructed in [17] we show that such a result cannot hold on the outer scale and indeed fails to hold on certain smaller scales:

Theorem 5.2.1. *Given $1 > \Omega, \epsilon > 0$ and $1/2 > \gamma \geq 0$ there exists an embedded minimal disk $0 \in \Sigma$ with $\partial\Sigma \subset \partial B_R$ and $(0, s)$ a blow-up pair so: the component of $B_{\Omega R^{1-\gamma} s^{\gamma}} \cap \Sigma$ containing 0 is not bi-Lipschitz to a piece of a helicoid with Lipschitz constant in $((1+\epsilon)^{-1}, 1+\epsilon)$.*

Remark 5.2.2. At the time of writing, the surfaces of [17] were the most "distorted" helicoids known. However, recently much worse surfaces have been constructed in [49] (based on the constructions of [17] and [28]). It is possible that, using the surfaces of [49], the blow-up scale can be shown to be the optimal scale.

Recall that as an application of their work on the structure of disks, Colding and Minicozzi proved a compactness result for sequences of embedded minimal disks $0 \in \Sigma_i \subset \mathbb{R}^3$ as long as $\partial\Sigma_i \subset \partial B_{R_i}$ and $R_i \to \infty$, i.e. Theorem 3.2.1. In particular, they show there are only two options. Either such a sequence contains a sub-sequence converging smoothly on compact sets to a complete embedded minimal disk or, if the curvature is unbounded on some compact subset of $\mathbb{R}^3$, the convergence is (in a certain sense, see [22] for details) to a singular minimal lamination of parallel planes. The surfaces constructed by Colding and Minicozzi in [17] show that the condition that the boundaries of the surface go to infinity is essential, i.e this compactness result is global in nature. In a similar vein, the result depends very strongly on the ambient geometry of the three-manifold. In particular, in the proof of their compactness result, Colding and Minicozzi rely heavily on a flux argument (the details of which are in [15]). That is, they use that the coordinate functions of $\mathbb{R}^3$ restrict to harmonic functions on minimal $\Sigma \subset \mathbb{R}^3$, a fact that generalizes only to certain other highly symmetric three-manifolds. An example showing the necessity of this type of condition can be found in [9].

One of the most important problems in this area is determining when a Colding and Minicozzi type of compactness result (or indeed any compactness result) extends to surfaces embedded in more general three-manifolds. Understanding precisely the best scale for which the Lipschitz approximation holds (for which Theorem 5.2.1 gives an upper bound) may be an important tool to establish removable singularities theorems for minimal laminations in arbitrary Riemannian manifolds. In turn, such results could prove key to proving more general compactness theorems.

To produce our example, we first recall the surfaces constructed in [17]:

Theorem 5.2.3. *(Theorem 1 of [17]) There is a sequence of compact embedded minimal disks $0 \in \Sigma_i \subset B_1 \subset \mathbb{R}^3$ with $\partial\Sigma_i \subset \partial B_1$ containing the vertical segment $\{(0,0,t) : |t| \leq 1\} \subset \Sigma_i$ such that the following conditions are satisfied:*

1. $\lim_{i\to\infty} |A_{\Sigma_i}|^2(0) \to \infty$
2. $\sup_{\Sigma_i} |A_{\Sigma_i}|^2 \leq 4|A_{\Sigma_i}|^2(0) = 8a_i^{-4}$ *for a sequence* $a_i \to 0$
3. $\sup_i \sup_{\Sigma_i \setminus B_\delta} |A_{\Sigma_i}|^2 < K\delta^{-4}$ *for all* $1 > \delta > 0$ *and* K *a universal constant.*
4. $\Sigma_i \setminus \{x_3 - axis\} = \Sigma_{1,i} \cup \Sigma_{2,i}$ *for multi-valued graphs* $\Sigma_{1,i}$ *and* $\Sigma_{2,i}$.

Remark 5.2.4. (2) and (3) are slightly sharper than what is stated in Theorem 1 of [17], but follow easily. (2) follows from the Weierstrass data (see Equation (2.3) of [17]). This also gives (3) near the axis, whereas away from the axis use (4) and Heinz's curvature estimates.

Next introduce some notation. For a surface Σ (with a smooth metric) we define the (*intrinsic*) *density ratio* at a point p as: $\theta_s(p,\Sigma) = (\pi s^2)^{-1}\text{Area}(\mathcal{B}_s^\Sigma(p))$. When Σ is immersed in $\mathbb{R}^3$ and has the induced metric, $\theta_s(p,\Sigma) \leq \Theta_s(p,\Sigma) = (\pi s^2)^{-1}\text{Area}(B_s(p) \cap \Sigma)$, the usual (extrinsic) density ratio. Importantly, the intrinsic density ratio is well-behaved under bi-Lipschitz maps. Indeed, if $f : \Sigma \to \Sigma'$ is injective and with $\alpha^{-1} < \text{Lip}\, f < \alpha$ (where $\text{Lip}\, f$ is the Lipschitz constant of f), then:

$$\alpha^{-4}\theta_{\alpha^{-1}s}(p,\Sigma) \leq \theta_s(f(p),\Sigma') \leq \alpha^4\theta_{\alpha s}(p,\Sigma). \tag{5.2}$$

This follows from the inclusion, $\mathcal{B}^\Sigma_{\alpha^{-1}s}(f^{-1}(p)) \subset f^{-1}(\mathcal{B}^{\Sigma'}_s(p))$ and the behavior of area under Lipschitz maps, $\text{Area}(f^{-1}(\mathcal{B}^{\Sigma'}_s(p)) \leq (\text{Lip}\, f^{-1})^2\text{Area}(\mathcal{B}^{\Sigma'}_s(p))$.

Note that by standard area estimates for minimal graphs, if $\Sigma \cap B_s(p)$ is a minimal graph then $\theta_s(p,\Sigma) \leq 2$. In contrast, for a point near the axis of a helicoid, for large s the density ratio is large. Thus, in a helicoid the density ratio for a fixed, large s measures, in a rough sense, the distance to the axis. More generally, this holds near blow-up pairs of embedded minimal disks:

Lemma 5.2.5. *Given $D > 0$ there exists $R > 1$ so: If $0 \in \Sigma \subset B_{2Rs}$ is an embedded minimal disk with $\partial\Sigma \subset \partial B_{2Rs}$ and $(0,s)$ a blow-up pair then $\theta_{Rs}(0,\Sigma) \geq D$.*

Proof. We proceed by contradiction, that is suppose there were a $D > 0$ and embedded minimal disks $0 \in \Sigma_i$ with $\partial\Sigma_i \subset \partial B_{2R_is}$ with $R_i \to \infty$ and $(0,s)$ a blow-up pair so that $\theta_{R_is}(0,\Sigma_i) \leq D$. The chord-arc bounds of [24] imply there is a $1 > \gamma > 0$ so $\mathcal{B}^{\Sigma_i}_{R_is}(0) \supset \Sigma_i \cap B_{\gamma R_is}$. Hence, the intrinsic density ratio bounds the extrinsic density ratio, i.e. $D \geq \theta_{R_is}(p,\Sigma_i) \geq \gamma^2\Theta_{\gamma R_is}(p,\Sigma_i)$. Then, by a result of Schoen and Simon [58] there is a constant $K = K(D\gamma^{-2})$, so $|A_{\Sigma_i}|^2(0) \leq K(\gamma R_i s)^{-2}$. For R_i large this contradicts that $(0,s)$ is a blow-up pair for all Σ_i. □

In order to show the existence of the surface Σ of Theorem 5.2.1, we exploit the fact that two points on a helicoid that are equally far from the axis must have the same

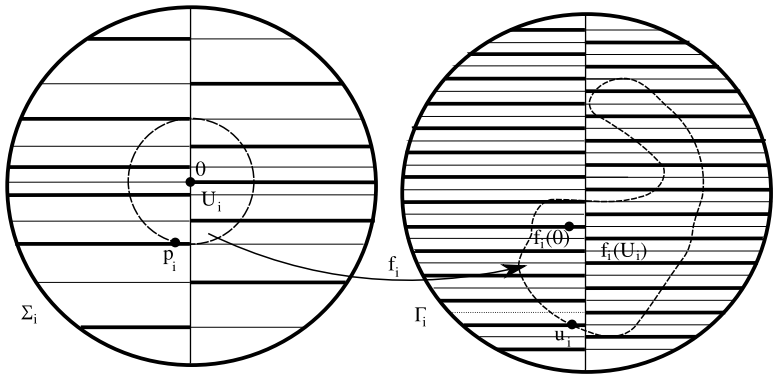

Figure 5-3: The points p_i and u_i. Note that the density ratio of u_i is much larger than the density ratio of p_i.

density ratio (which can be most easily seen by noting that the helicoid is invariant under screw-motions and rotations by 180° degrees around the axis). Assuming the existence of a Lipschitz map between Σ and a helicoid, we get a contradiction by comparing the densities for two appropriately chosen points that map to points equally far from the axis of the helicoid.

Proof. (of Theorem 5.2.1) Fix $1 > \Omega, \epsilon > 0$ and $1/2 > \gamma \geq 0$ and set $\alpha = 1 + \epsilon$. Let Σ_i be the surfaces of Theorem 5.2.3; we claim for i large, Σ_i will be the desired example. Suppose this was not the case. Setting $s_i = Ca_i^2/\sqrt{2}$, where a_i is as in (2) and C is the blow-up constant,one has $(0, s_i)$ is a blow-up pair in Σ_i, since $\sup_{\Sigma_i \cap B_{s_i}} |A_{\Sigma_i}|^2 \leq 8a_i^{-4} = 4C^2 s_i^{-2} = 4|A_{\Sigma_i}|^2(0)$, moreover, $s_i \to 0$. Hence, with $R_i = \Omega s_i^{\gamma} < 1$, the component of $B_{R_i} \cap \Sigma_i$ containing 0, Σ_i', is bi-Lipschitz to a piece of a helicoid with Lipschitz constant in (α^{-1}, α). That is, there are subsets Γ_i of helicoids and diffeomorphisms $f_i : \Sigma_i' \to \Gamma_i$ with Lip $f_i \in (\alpha^{-1}, \alpha)$.

We now begin the density comparison. First, Lemma 5.2.5 implies there is a constant $r > 0$ so for i large $\theta_{rs_i}(0, \Sigma_i') \geq 4\alpha^8$ and thus by (5.2) $\theta_{\alpha r s_i}(f_i(0), \Gamma_i) \geq 4\alpha^4$. We proceed to find a point with small density on Σ_i that maps to a point on Γ_i equally far from the axis as $f_i(0)$ (which has large density).

Let U_i be the (interior) of the component of $B_{1/2R_i} \cap \Sigma_i$ containing 0. Note for i large enough, as $s_i/R_i \to 0$, the distance between ∂U_i and $\partial {\Sigma_i}'$ is greater than $4\alpha^2 r s_i$. Similarly, for $p \in \partial U_i$ for i large, $p' \in \mathcal{B}^{\Sigma_i'}_{4\alpha^2 r s_i}(p)$ implies $|p'| \geq \frac{1}{4} R_i$. Hence, property (3) gives that $|A_{\Sigma_i'}|^2(p') \leq K' s_i^{-4\gamma}$. Thus, for i sufficiently large $\mathcal{B}_{\alpha^2 r s_i}(p)$ is a graph and so $\theta_{\alpha^2 r s_i}(p, \Sigma_i') \leq 2$. Pick $u_i \in \partial f(U_i)$ at the same distance to the axis as $f_i(0)$ and so the density ratio is the same at both points (see Figure 5-3). As $f_i(U_i)$ is an open subset of Γ_i containing $f_i(0)$, $p_i = f_i^{-1}(u_i) \in \partial U_i$. Notice that $\theta_{\alpha r s_i}(u_i, \Gamma_i) = \theta_{\alpha r s_i}(f_i(0), \Gamma_i) \geq 4\alpha^4$ so $2\alpha^4 \geq \alpha^4 \theta_{\alpha^2 r s_i}(p_i, \Sigma_i') \geq 4\alpha^4$.

□

Chapter 6

Genus-g Helicoids

We now apply the techniques of Chapter 4 to study non-simply connected, complete, embedded minimal surfaces with finite topology and one end. Recall, the space $\mathcal{E}(1,+)$ of such surfaces is non-trivial; the embedded genus one helicoid, $\mathcal{H}$ (see figure 2-3), constructed in [61] by Hoffman, Weber, and Wolf is an element of $\mathcal{E}(1,+)$ that, moreover, has the property of being asymptotically helicoidal (see also [60] for a good exposition).

In [39], Hoffman and White proved rigidity results for immersed minimal genus one surfaces with one end that, in addition, contain, and are symmetric with respect to, the x_1 and x_3-axes. In particular, they show the surface is conformally a punctured torus with end asymptotic to a helicoid. In this chapter, we show that any $\Sigma \in \mathcal{E}(1,+)$ is conformally a once punctured, compact Riemann surface, with Weierstrass data that has helicoid-like behavior at the puncture. Precisely,

Theorem 6.0.6. *$\Sigma \in \mathcal{E}(1,+)$ is conformally a punctured, compact Riemann surface. Moreover, the height differential, dh, extends meromorphically over the puncture with a double pole, as does the meromorphic one form $\frac{dg}{g}$.*

In [45], Meeks and Rosenberg discuss how one might be able to show something similar to Theorem 6.0.6 for surfaces in $\mathcal{E}(1)$ and the implications this has to the possible conformal structure of complete embedded minimal surfaces in $\mathbb{R}^3$. They do this without going into the details or addressing the difficulties, but indicate how such a statement might be proved using the ideas and techniques of their paper. That is, they anticipated a proof using their derivation of the uniqueness of the helicoid from the lamination result of Colding and Minicozzi [22].

Theorem 6.0.6 completes the understanding of the conformal type of complete, embedded minimal surfaces of finite topology. In [48], Meeks and Rosenberg prove conformality results for properly embedded minimal surfaces of finite topology which have two or more ends. Using their work, Corollary 0.13 of [24], and Theorem 6.0.6, we have the following:

Corollary 6.0.7. *Every complete, embedded minimal surface of finite topology in $\mathbb{R}^3$ is conformal to a compact Riemann surface with a finite number of punctures.*

As Σ is embedded, Theorem 6.0.6 has the following corollary:

Corollary 6.0.8. *For $\Sigma \in \mathcal{E}(1,+)$, there exists an $\alpha \in \mathbb{R}$ so $\frac{dg}{g} - i\alpha dh$ has holomorphic extension to the puncture, with a zero at the puncture. Equivalently, after possibly translating parallel to the x_3-axis, in an appropriately chosen neighborhood of the puncture, Γ, $g(p) = \exp(i\alpha z(p) + F(p))$ where $F : \Gamma \to \mathbb{C}$ extends holomorphically over the puncture with a zero there and $z = x_3 + ix_3^*$ is a holomorphic coordinate on Γ. (Here x_3^* is the harmonic conjugate of x_3 and is well defined in Γ.)*

Indeed, this allows us to apply a result of Hauswirth, Perez and Romon [31]:

Corollary 6.0.9. *If $\Sigma \in \mathcal{E}(1)$ is non-flat, then Σ is C^0-asymptotic to some helicoid.*

The work in this chapter is drawn from [4].

6.1 Outline of the Proof

Let $\Sigma \in \mathcal{E}(1,+)$, because Σ is properly embedded and has finite genus and one end the topology of Σ is concentrated in a ball in $\mathbb{R}^3$. Thus, the maximum principle implies that all components of the intersection of Σ with a ball disjoint from the genus are disks. Hence, outside of a large ball, one may use the local results of [19–22] about embedded minimal disks. In Chapter 4, the trivial topology of Σ allows one to deduce global geometric structure immediately from these local results. For $\Sigma \in \mathcal{E}(1,+)$, the presence of non-zero genus complicates matters. Nevertheless, the global structure will follow from the far reaching description of embedded minimal surfaces given by Colding and Minicozzi in [12]. In particular, as Σ has one end, globally it looks like a helicoid (see Section 3.2.3 and Section 6.4.2). Following the argument presented in Chapter 4, we first prove a sharper description of the global structure (in Section 6.2.4); indeed, one may generalize the decomposition of Theorem 4.2.1 to $\Sigma \in \mathcal{E}(1,+)$ as:

Theorem 6.1.1. *There exist $\epsilon_0 > 0$ and $\mathcal{R}_A$, $\mathcal{R}_S$, and $\mathcal{R}_G$, disjoint subsets of Σ, such that $\Sigma = \mathcal{R}_A \cup \mathcal{R}_S \cup \mathcal{R}_G$. The set $\mathcal{R}_G$ is compact, connected, has connected boundary and $\Sigma \backslash \mathcal{R}_G$ has genus 0. $\mathcal{R}_S$ can be written as the union of two (oppositely oriented) multi-valued graphs u^1 and u^2 with $u^i_\theta \neq 0$. Finally, (after a rotation of $\mathbb{R}^3$) $|\nabla_\Sigma x_3| \geq \epsilon_0$ in $\mathcal{R}_A$. (See Figure 6-1)*

Remark 6.1.2. Here u^i multi-valued means that it can be decomposed into N-valued ϵ-sheets (see Definition 4.3.1) with varying center. The angular derivative, $(u_i)_\theta$, is then with respect to the obvious polar form on each of these sheets. For simplicity we will assume throughout that both u^i are ∞-valued.

As an important step in establishing the decomposition theorem, notice that the minimal annulus $\Gamma = \Sigma \backslash \mathcal{R}_G$ has exactly the same weak asymptotic properties as an embedded non-flat minimal disk. Thus, as in Chapter 4, strict spiraling in $\mathcal{R}_S$ and a lower bound for $|\nabla_\Sigma x_3|$ on $\mathcal{R}_A$ together give (for appropriately chosen $\mathcal{R}_G$):

Proposition 6.1.3. *In Γ, $\nabla_\Sigma x_3 \neq 0$ and, for all $c \in \mathbb{R}$, $\Gamma \cap \{x_3 = c\}$ consists of either one smooth, properly embedded curve or two smooth, properly embedded curves each with one endpoint on $\partial\Gamma$.*

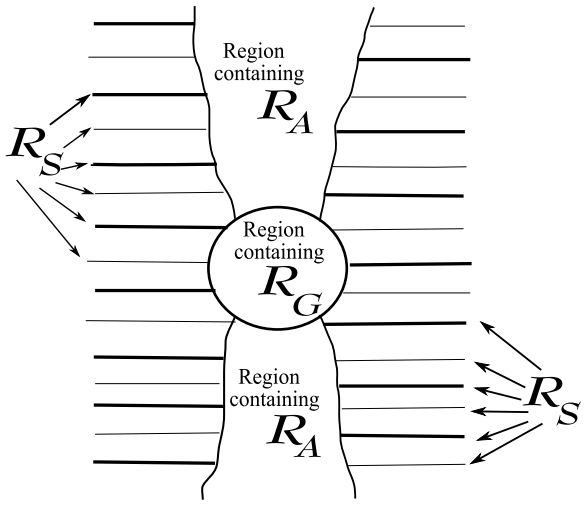

Figure 6-1: A rough sketch of the decomposition of Σ given by Theorem 6.1.1.

The decomposition allows us to argue as in Chapter 4, though the non-trivial topology again adds some technical difficulties. By Stokes' Theorem, x_3^* (the harmonic conjugate of x_3) exists on Γ and thus there is a well defined holomorphic map $z : \Gamma \to \mathbb{C}$ given by $z = x_3 + ix_3^*$. Proposition 6.1.3 implies that z is a holomorphic coordinate on Γ. We claim that z is actually a proper map and so Γ is conformally a punctured disk. Following Chapter 4, this can be shown by studying the Gauss map. On Γ, the stereographic projection of the Gauss map, g, is a holomorphic map that avoids the origin. Moreover, the minimality of Σ and the strict spiraling in $\mathcal{R}_S$ imply that the winding number of g around the inner boundary of Γ is zero. Hence, by monodromy there exists a holomorphic map $f : \Gamma \to \mathbb{C}$ with $g = e^f$. Then, as in Chapter 4, the strict spiraling in $\mathcal{R}_S$ imposes strong control on f which is sufficient to show that z is proper. Further, once we establish Γ is conformally a punctured disk, the properties of the level sets of f imply that it extends meromorphically over the puncture with a simple pole. This gives Theorem 6.0.6 and ultimately Corollaries 6.0.8 and 6.0.9.

6.2 Geometric Decomposition

In the next four subsections, we develop the tools needed to prove the structural results of Theorem 6.1.1 and Proposition 6.1.3. Many of these are extensions of those developed for the simply connected case, which can be found in Section 4.3 of Chapter 4. We prove Theorem 6.1.1 and Proposition 6.1.3 at the conclusion of Section 6.2.4.

6.2.1 Structural results

To obtain the decomposition of Theorem 6.1.1 we will need two important structural results which generalize results for disks from [19] and [20] (it should be noted that many of the proofs of these results did not require that the surface be a disk but only that the boundary be connected, a fact used in [12]). The first is the existence

of an N-valued graph starting near the genus and extending as a graph all the way out. The second result is similar but for a blow-up pair far from the genus. Namely, for such a pair a multi-valued graph forms on the scale of the pair and extends as a graph all the way out. It may be helpful to compare with the comparable results for disks, i.e. Theorem 0.3 of [19] (see Theorem 3.3) and Theorem 0.4 of [20] (see Theorem 3.1.3).

Note that variants of the propositions are used in [12], specifically in the proof of the compactness result, i.e. Theorem 0.9 for finite genus surfaces, though they are not made explicit there. For the sake of completeness we provide proofs (in Section 6.4.2) of these propositions using Theorem 0.9 of [12]. Note that while both propositions require a rotation of $\mathbb{R}^3$, they are the same rotation. This is because both propositions actually come from the global geometric structure of Σ.

Proposition 6.2.1. *Given $\epsilon > 0$ and $N \in \mathbb{Z}^+$ there exists an $R > 0$ so that: After a rotation of $\mathbb{R}^3$ there exists an N-valued graph $\Sigma_g \subset \Sigma$ over the annulus $D_\infty \backslash D_R \subset \{x_3 = 0\}$, with gradient bounded by ϵ and in $\mathbf{C}_\epsilon$.*

Proposition 6.2.2. *Given $\epsilon > 0$ sufficiently small and $N \in \mathbb{Z}^+$ there exist $C_1, C_2 > 0$ and $R > 0$ so: After a rotation of $\mathbb{R}^3$, if (y, s) is a C_1 blow-up pair in Σ and $|y| \geq R$ then there exists an N-valued graph Σ_g over the annulus $D_\infty \backslash D_s(\Pi(y)) \subset \{x_3 = 0\}$ with gradient bounded by ϵ and in the cone $\mathbf{C}_\epsilon(y)$, and with initial separation bounded below by $C_2 s$. Finally,* $\mathrm{dist}_\Sigma(\Sigma_g, y) \leq 2s$.

6.2.2 Blow-up sheets

In order to get the strict spiraling in the decomposition of Theorem 6.1.1 we need to check that the multi-valued graphs that make up most of Σ can be consistently normalized. To that end, we recall that for blow-up pairs far enough from the genus one obtains a nearby ϵ-sheet (i.e. we have a normalized multi-valued graph). Indeed, the proof of Theorem 4.5.1 of Chapter 4 applies without change to blow-up pairs satisfying the conditions of Proposition 6.2.2. We claim that in between this sheet, Σ consists of exactly one other ϵ-sheet. For the definition and basic properties of these ϵ-sheets see Section 4.3.1.

Theorem 6.2.3. *Given $\epsilon > 0$ sufficiently small there exist $C_1, C_2 > 0$ and $R > 1$ so: Suppose (y, s) is a C_1 blow-up pair, with $|y| > R$. Then there exist two 4-valued ϵ-sheets $\Sigma_i = \Gamma_{u_i}$ $(i = 1, 2)$ on the scale s centered at y which spiral together (i.e. $u_1(s, 0) < u_2(s, 0) < u_1(s, 2\pi)$). Moreover, the separation over $\partial D_s(\Pi(y))$ of Σ_i is bounded below by $C_2 s$.*

Remark 6.2.4. We refer to Σ_1, Σ_2 as (ϵ-)blow-up sheets *associated with* (y, s).

Proof. We fix a $\delta > 0$ and note that Lemma 6.4.2 gives a $R > 1$ so that if $|y| > R$ then $y \notin \mathbf{C}_\delta$ and using this δ and ϵ we pick $\delta_0 < \epsilon$ as in Corollary 6.4.3 (and increase R if needed). Then, Theorem 4.5.1 and Proposition 6.2.2 together give one δ_0-sheet, Σ_1, forming near (y, s) for appropriately chosen C_1 (and possibly after again increasing

R). Now as long as the part of Σ between the sheets of Σ_1 make up a second minimal graph, the proof of Theorem 6.2.3 applies (and provides the correct C_2).

Recall (4.3), which gives the region, E, in $\mathbb{R}^3$ between the sheets of Σ_1. Theorem I.0.10 of [22] implies that near the blow-up pair the part of Σ between Σ_1 is a graph Σ_2^{in}; i.e. if R_0 is chosen so $B_{4R_0}(y)$ is disjoint from the genus then $B_{R_0}(y) \cap E \cap \Sigma \backslash \Sigma_1 = \Sigma_2^{in}$. To ensure Σ_{in}^2 is non-empty, we increase R so that $|y| \geq 8s$ (which we may do by Corollary 6.4.5). On the other hand, Appendix D of that same paper guarantees that, outside of a very large ball centered at the genus, the part of Σ between Σ_1 is a graph, Σ_2^{out}. That is, for $R_1 \geq |y|$ large, $E \cap \Sigma \backslash (B_{R_1} \cup \Sigma_1) = \Sigma_2^{out}$. Now by one-sided curvature estimates (which Corollary 6.4.3 allows us to use), all the components of $E \backslash \Sigma_1$ are graphs and so it suffices to show that Σ_2^{in} and Σ_2^{out} are subsets of the same component. Suppose not. Then, as Σ_2^{in} is a graph and Σ is complete, Σ_2^{in} must extend inside E beyond B_{R_1}. But this contradicts Appendix D of [22] by giving two components of $\Sigma \backslash \Sigma_1$ in $E \cap \Sigma \backslash B_{R_1}$. □

6.2.3 Blow-Up pairs

While the properties of ϵ-sheets give the strictly spiraling region of Σ, to understand the region where these sheets fit together (i.e. the axis), we need a handle on the distribution of the blow-up pairs of Σ. In the case of trivial topology, non-flatness gives one blow-up pair (y_0, s_0), which in turn yields associated blow-up sheets. Then by Corollary 3.1.7 (i.e. III.3.5 of [21]), the blow-up sheets give the existence of nearby blow-up pairs $(y_{\pm 1}, s_{\pm 1})$ above and below (see Theorem 4.3.5 or Lemma 2.5 of [24]). Iterating, one constructs a sequence of blow-up pairs that give the axis $\mathcal{R}_A$.

Crucially, for the extension of the argument to surfaces in $\mathcal{E}(1, +)$, the result of [21] is local; it depends only on the topology being trivial in a large ball relative to the scale s_0. Thus, the above construction holds in Σ as long as one deals with two issues. First, establish the existence of two initial blow-up pairs far from the genus, one above and the other below, with small scale relative to the distance to the genus. Second, show that the iterative process produces blow-up pairs which continue to have small scale (again relative to the distance to the genus).

We claim that the further a blow-up pair is from the genus, the smaller the ratio between the scale and the distance to the genus; hence both issues can be addressed simultaneously. This is an immediate consequence (see Corollary 6.4.5) of the control on curvature around blow-up pairs as given by Proposition 6.4.4 (an extension of Lemma 2.26 of [24] to Σ). Thus, given an initial blow-up pair far enough above the genus, we can iteratively produce higher and higher blow-up pairs that satisfy the appropriate scale condition, with the same true starting below the genus and going down. Here we establish the existence of a chain of blow-up pairs which will be critical to our decomposition theorem:

Lemma 6.2.5. *Given $\epsilon > 0$ sufficiently small, there exist constants $C_1, C_{in} > 0$ and a sequence $(\tilde{y}_i, \tilde{s}_i)$ of C_1 blow-up pairs of Σ such that: the sheets associated to $(\tilde{y}_i, \tilde{s}_i)$ are ϵ-sheets on scale $\tilde{s}_i$ centered at $\tilde{y}_i$ and $x_3(\tilde{y}_i) < x_3(\tilde{y}_{i+1})$ for $i \geq 1$, $\tilde{y}_{i+1} \in B_{C_{in}\tilde{s}_i}(\tilde{y}_i)$ while for $i \leq -1$, $\tilde{y}_{i-1} \in B_{C_{in}\tilde{s}_i}(\tilde{y}_i)$.*

Proof. Without loss of generality, we work above the genus (i.e. for $x_3 > 1$ and $i \geq 1$), as the argument below the genus is identical. Use ϵ to choose C_1, C_2 and R as in Theorem 6.2.3. By Corollary 3.1.7 there are constants $C_{out} > C_{in} > 0$ such that, for a C_1 blow-up pair (y, s) with $|y| \geq R$, as long as the component of $B_{C_{out}s}(y) \cap \Sigma$ containing y is a disk, we can find blow-up pairs above and below (y, s) and inside $B_{C_{in}s}(y)$. We will also need to make use of the one-sided curvature estimate near the sheets associated to (y, s). This can be ensured by increasing R appropriately as indicated by Corollary 6.4.3. Corollary 6.4.5 and Proposition 6.4.1 ensure a value $h_1 \geq R$, depending on C_{out} so for $|y| \geq h_1$ this condition is satisfied. Thus, it suffices to find an initial blow-up pair $(\tilde{y}_1, \tilde{s}_1)$ with $|\tilde{y}_1| \geq h_1$, as repeated application of Corollary 3.1.7 will give the sequence $(\tilde{y}_i, \tilde{s}_i)$. Notice that by our choice of R we may apply the one-sided curvature estimate and so conclude that y_{i+1} lies within a cone centered at y_i, in particular this implies that $x_3(y_{i+1}) \geq x_3(y_i)$ and thus $|y_i| \geq R$ and so the iteration is justified.

Proposition 6.2.1 and Appendix D of [22] together guarantee the existence of two $\tilde{N}$-valued graphs spiraling together over an unbounded annulus (with inner radius $\overline{R}$). Then, for large enough $\tilde{N}$, the proof of Theorem 4.3.5 gives two N-valued ϵ-sheets around the genus, Σ_1, Σ_2, on some scale $\tilde{R}$ and in the cone $\mathbf{C}_\epsilon$. Theorem III.3.1 of [21] with $r_0 \geq \max\{1, \tilde{R}, h_1\}$ then implies there is large curvature above and below the genus. Hence, by a standard blow-up argument (i.e. Lemma 3.1.2) one gets the desired C_1 blow-up pair $(\tilde{y}_1, \tilde{s}_1)$ above the genus with $|\tilde{y}_1| > 2r_0 \geq h_1$. □

6.2.4 Decomposing Σ

The decomposition of Σ now proceeds as in Chapter 4, with Proposition 4.3.8 giving strict spiraling far enough out in the ϵ-sheets of Σ. After specifying the region of strict spiraling, $\mathcal{R}_S$, the remainder of Σ will be split into the genus, $\mathcal{R}_G$, and the axis, $\mathcal{R}_A$. The strict spiraling, the fact that away from the genus convex sets meet Σ in disks (see Lemma 6.4.1) and the proof of Rado's theorem (see [55]) will then give $\nabla_\Sigma x_3 \neq 0$ in $\mathcal{R}_A$. Then a Harnack inequality will allow us to bound $|\nabla_\Sigma x_3|$ from below there.

Lemma 6.2.6. *There exist constants C_1, R_0, R_1 and a sequence (y_i, s_i) $(i \neq 0)$ of C_1 blow-up pairs of Σ so that: $x_3(y_i) < x_3(y_{i+1})$ and for $i \geq 1$, $y_{i+1} \in B_{R_1 s_i}(y_i)$ while for $i \leq -1$, $y_{i-1} \in B_{R_1 s_i}(y_i)$. Moreover, if $\tilde{\mathcal{R}}_A = \tilde{\mathcal{R}}_A^+ \cup \tilde{\mathcal{R}}_A^-$ where $\tilde{\mathcal{R}}_A^\pm$ is $\bigcup_{\pm i > 0} \Sigma_{R_1 s_i, y_i}$ (and $\Sigma_{R_1 s_i, y_i}$ is the component of $B_{R_1 s_i}(y_i) \cap \Sigma$ containing y_i), then $\mathcal{R}_S = \Sigma \setminus \left(\tilde{\mathcal{R}}_A \cup B_{R_0}\right)$ has exactly two unbounded components which can be written as the union of two multi-valued graphs u^1 and u^2, with $u^i_\theta \neq 0$.*

Proof. We wish to argue as in Lemma 4.3.9 and to do so we must ensure that we may use the chord-arc bounds of [24] and the one-sided curvature estimates of [22] near the pairs (y_i, s_i). As these are both essentially local results it will suffice to work far from the genus.

Fix $\epsilon < \epsilon_0$ where ϵ_0 is given by Proposition 4.3.8 which will be important for the strict spiraling. Next pick $\delta > 0$ and apply Corollary 6.4.3 to obtain a $\delta_0 < \epsilon$ and

$\tilde{R} > 1$. Now using δ_0 in place of ϵ let $(\tilde{y}_i, \tilde{s}_i)$ be the sequence constructed in Lemma 6.2.5. Let us now determine how to choose the (y_i, s_i).

First of all, as long as $y_i \notin \mathbf{C}_\delta \cup B_{\tilde{R}}$ we may use the one-sided curvature estimate in $\mathbf{C}_{\delta_0}(y_i)$. Notice by Lemma 6.4.2 we may increase $\tilde{R}$ and require only that $y_i \notin B_{\tilde{R}}$. Now recall that the chord-arc bounds give a constant $C_{arc} > 0$ so for any $\gamma > 1$, if the component of $B_{2C_{arc}\gamma s_i}(y_i) \cap \Sigma$ containing y_i is a disk, then the intrinsic ball of radius $C_{arc}\gamma s_i$ centered at y_i contains $B_{\gamma s_i}(y_i) \cap \Sigma$. On (y_i, s_i), we want a uniform bound, N, on the number of sheets between the blow-up sheets associated to the pairs (y_i, s_i) and (y_{i+1}, s_{i+1}). This is equivalent to a uniform area bound which in turn follows from the chord-arc bounds described above and curvature bounds of Proposition 6.4.4 (for details see Proposition 4.5.3). To correctly apply this argument, one must be sufficiently far from the genus; i.e. for a fixed constant C_{bnd}, the component of $B_{C_{bnd}s_i}(y_i) \cap \Sigma$ containing y_i must be a disk. To that end, pick $h_2 \geq 0$ by using Corollary 6.4.5 with $\alpha^{-1} \geq \max\left\{C_{bnd}, 2R_1, \tilde{R}\right\}$ where R_1 is to be chosen later. We then pick the sequence (y_i, s_i) from $(\tilde{y}_i, \tilde{s}_i)$ by requiring $x_3(y_i) \geq h_2$ (and then relabeling). Notice that the way we choose the (y_i, s_i) ensures that N is independent of our ultimate choice of R_1.

We now determine R_1. By choice of (y_i, s_i), the one-sided curvature bounds hold and so there is an R_2 such that in $\mathbf{C}_{\delta_0}(y_1)$ all of the (at most) N sheets between the blow-up sheets associated to (y_1, s_1) and (y_2, s_2) are δ_0-sheets on scale $R_2 s_1$ centered on the line ℓ which goes through y_1 and is parallel to the x_3-axis (see Theorem 4.5.2). Label these pairs of δ_0-sheets Σ_k^j, $k = 1, 2$ and $1 \leq j \leq N$. Proceeding now as in the second paragraph of the proof of Lemma 4.3.9, we use N, C_2 and (2.9) to get $\tilde{C}_2$ so $\tilde{C}_2 s_1$ is a lower bound on the separation of each Σ_k^j over the circle $\partial D_{R_2 s_1}(\Pi(y_1)) \subset \{x_3 = 0\}$. Proposition 4.3.8 gives a C_3, depending on $\tilde{C}_2$, such that outside of a cylinder centered at ℓ of radius $R_2 C_3 s_1$, all the Σ_k^j strictly spiral. Choose $\tilde{R}_1$, depending only on C_{in}, N, δ_0, C_3 and R_2, so $B_{\tilde{R}_1 s_1}(y_1)$ contains this cylinder, the point y_2 and meets each Σ_k^j. Then if $R_1 = C_{arc}\tilde{R}_1$ the preceding is also true of the component of $B_{R_1 s_1}(y_1) \cap \Sigma$ containing y_1. By the scaling invariance of strict spiraling and the uniformity of the choices, the same is true for each (y_i, s_i).

Finally, by properness, there exists a finite number, M, of ϵ-sheets between the blow-up sheets associated to $(y_{\pm 1}, s_{\pm 1})$. Pick R_0 large enough so that outside of the ball of radius R_0 the M sheets between the blow-up sheets associated to (y_1, s_1) and (y_{-1}, s_{-1}) strictly spiral. Such an R_0 exists by Proposition 6.2.1 and the above argument. □

Proof. (Proposition 6.1.3) By properness there exists an $R_0' \geq R_0$ so that the component of $B_{R_0'} \cap \Sigma$ containing the genus, $\overline{\Sigma}$, contains $B_{R_0} \cap \Sigma$. We take $\mathcal{R}_G$ to be this component and note that $\partial\mathcal{R}_G$ is connected by Proposition 6.4.1. The strict spiraling in $\mathcal{R}_S$ and the proof of Rado's theorem gives Proposition 6.1.3 (See Section 4.3.4). □

Proof. (Theorem 6.1.1) By using Lemma 6.2.6 the proof of Theorem 4.2.1 in Chapter 4 then gives Theorem 6.1.1. Indeed, we have already constructed $\mathcal{R}_S$ and $\mathcal{R}_G$ in the proofs of Lemma 6.2.6 and Proposition 6.1.3. If we set $\mathcal{R}_A = \Sigma \setminus (\mathcal{R}_S \cup \mathcal{R}_G)$ then we may verify the properties of $\mathcal{R}_A$ exactly as in the proof of Theorem 4.2.1. We may

need to decrease ϵ_0 in the statement of the theorem so $\min_{\partial\mathcal{R}_G} |\nabla_\Sigma x_3| \geq \epsilon_0$, but $\partial\mathcal{R}_G$ is compact so this introduces no new problems. □

6.3 Conformal Structure of the end

In this section we prove Theorem 6.0.6 and Corollary 6.0.8 by analysis nearly identical to that in Section 4.4. To do so, we first show that $\Gamma = \Sigma\backslash\mathcal{R}_G$ is conformally a punctured disk and, indeed, the map $z = x_3 + ix_3^* : \Gamma \to \mathbb{C}$ is a proper, holomorphic coordinate (here x_3^* is the harmonic conjugate of x_3). Note that by Proposition 6.1.3, as long as z is well defined, it is injective and a conformal diffeomorphism. Thus, it suffices to check that z is well defined and that it is proper; i.e. if $p \to \infty$ in Γ then $z(p) \to \infty$.

Proposition 6.3.1. *x_3^* is well defined on Γ.*

Proof. As Σ is minimal, ${}^*dx_3$, the conjugate differential to dx_3, exists on Σ and is closed and harmonic. We wish to show it is exact on Γ. To do so, it suffices to show that for every closed, embedded curve ν in Γ, we have $\int_\nu {}^*dx_3 = 0$. By Proposition 6.4.1, $\Sigma\backslash\nu$ has two components, only one of which is bounded. The bounded component, together with ν, is a manifold with (connected) boundary, and on this manifold ${}^*dx_3$ is a closed form. Hence, the result follows immediately from Stokes' theorem. □

6.3.1 Winding number of the Gauss map

We wish to argue as in Section 4.4, and to do so we must first check that there is a well defined notion of $\log g$ in Γ. In other words, there exists $f : \Gamma \to \mathbb{C}$ such that $g = e^f$ on Γ, where g is the stereographic projection of the Gauss map of Σ. For such an f to exist, the winding number of g from Γ to $\mathbb{C}\backslash\{0\}$ must be zero. Since g is meromorphic in Σ and has no poles or zeros in Γ, this is equivalent to showing that g has an equal number of poles and zeros.

Proposition 6.3.2. *Counting multiplicity, g has an equal number of poles and zeros.*

Proof. The zeros and poles of g occur only at the critical points of x_3. In particular, by Proposition 6.1.3, there exist h and R so that all the zeros and poles are found in the cylinder:

$$C_{h,R} = \left\{|x_3| \leq h, x_1^2 + x_2^2 \leq R^2\right\} \cap \Sigma. \tag{6.1}$$

Moreover, for R and h sufficiently large, $\gamma = \partial C_{h,R}$ is the union of four smooth curves, two at the top and bottom, γ_t and γ_b, and two disjoint helix like curves $\gamma_1, \gamma_2 \subset \mathcal{R}_S$. Hence, for $c \in (-h, h)$, $\{x_3 = c\}$ meets $\partial C_{h,R}$ in exactly two points. Additionally, as γ_1 and γ_2 are compact, there is a constant $\alpha > 0$ so $|\frac{d}{dt} x_3(\gamma_i(t))| > \alpha$, $i = 1, 2$.

Let us first suppose that g has only simple zeros and poles and these occur at distinct values of x_3, thus, the Weierstrass representation implies that the critical

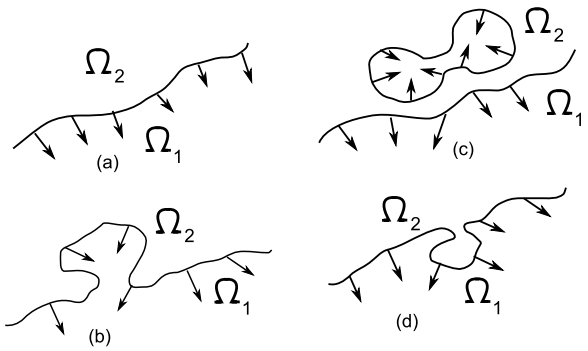

Figure 6-2: Level curve examples in Proposition 6.3.2. (a) Initial orientation chosen at height $x_3 = h$. (b) A curve pinching off from Ω_1. (c) Two curves pinching from one. (d) A curve pinching off from Ω_2.

points of x_3 are non-degenerate. We now investigate the level sets $\{x_3 = c\}$. By the strict spiraling of γ_i $(i = 1, 2)$, at the regular values these level sets consist of an interval with end points in γ_i $(i = 1, 2)$ and the union of a finite number of closed curves. Moreover, by the minimality of $C_{h,R}$, the non-smooth components of the level sets at critical values will consist of either two closed curves meeting in a single point or the interval and a closed curve meeting in a single point. As a consequence of this $\{|x_3| \leq h, x_1^2 + x_2^2 \leq R^2\} \setminus C_{h,R}$ has exactly two connected components Ω_1 and Ω_2. Orient $C_{h,R}$ by demanding that the normal point into Ω_1. Notice that it is well defined to say if a closed curve appearing in $\{x_3 = c\} \cap C_{h,R}$ surrounds Ω_1 or Ω_2.

The restrictions imposed on g and minimality of $C_{h,R}$ imply that at any critical level, as one goes downward, either a single closed curve is "created" or is "destroyed". (See Figure 6-2.) Moreover, when such a curve is created it makes sense to say whether it surrounds Ω_1 or Ω_2 and this is preserved as one goes downward. Now suppose a closed curve is created and that it surrounds Ω_1; then it is not hard to see that at the critical point the normal must point upwards. Similarly, if a closed curve surrounding Ω_1 is destroyed then the normal at the critical point is downward pointing. For, closed curves surrounding Ω_2 the opposite is true; i.e. when a closed curve is created then at the critical point the normal points downward. Thus, since the level sets at h and $-h$ are intervals, one sees that the normal points up as much as it points down. That is, g has as many zeros as poles.

We now drop the restrictions on the poles and zeros of g. Beyond these assumptions the argument above used only that $C_{h,R}$ was minimal and that the boundary curves γ_i $(i = 1, 2)$ meet the level curves of x_3 in precisely one point. It is not hard to check that these last two conditions are preserved by small rotations around lines in the x_1-x_2 plane. We claim that such rotations also ensure that the Gauss map of the new surface must have simple poles or zeros and these are on distinct level sets. To that end we let $C_{h,R}^{\epsilon}$ be the rotation of $C_{h,R}$ by ϵ degrees around a fixed line ℓ in the x_1-x_2 plane and through the origin (note we do not rotate the ambient $\mathbb{R}^3$). Denote by Φ_ϵ the induced isometric isomorphism between the sets.

The strict spiraling of γ_1, γ_2 implies there exists an $\epsilon_0 > 0$, depending on α and R

and a constant $K > 0$, depending on R so: for all $0 < \epsilon < \epsilon_0$, if $c \in (-h + K\epsilon, h - K\epsilon)$ then $\{x_3 = c\} \cap C^\epsilon_{h,R}$ meets $\partial C^\epsilon_{h,R}$ in two points. Moreover, by a suitable choice of ℓ the critical points will be on distinct level sets. Denote by g_ϵ the stereographic projection of the Gauss map of $C^\epsilon_{h,R}$. We now use the fact that g is meromorphic on Σ (and thus the zeros and poles of g are isolated) and that g_ϵ is obtained from g by a Möbius transform. Indeed, these two facts imply that (after shrinking ϵ_0) for $\epsilon \in (0, \epsilon_0)$, g_ϵ has only simple zeros and poles on $C^\epsilon_{h,R}$ and by our choice of ℓ these are on distinct levels of x_3. By further shrinking ϵ_0 one can ensure that all of the critical values occur in the range $(-h + K\epsilon, h - K\epsilon)$. Thus, the level sets in $C^\epsilon_{h,R}$ of x_3 for $c \in (-h + K\epsilon, h - K\epsilon)$ consist of an interval with endpoints in $\partial C^\epsilon_{h,R}$, one in each γ_i for $i = 1, 2$, and the union of a finite number of closed curves.

Our original argument then immediately implies that g_ϵ has as many zeros as poles. Thus, $\int_{\partial C_{h,R}} \Phi^*_\epsilon \frac{dg_\epsilon}{g_\epsilon} = \int_{\partial C^\epsilon_{h,R}} \frac{dg_\epsilon}{g_\epsilon} = 0$ for $\epsilon < \epsilon_0$. Hence, as $\Phi^*_\epsilon \frac{dg_\epsilon}{g_\epsilon}$ is continuous in ϵ, $\int_{\partial C_{h,R}} \frac{dg}{g} = 0$. □

Corollary 6.3.3. *A holomorphic function $f : \Gamma \to \mathbb{C}$ exists so $e^f = g$ on Γ.*

6.3.2 Conformal structure of the end

The strict spiraling in $\mathcal{R}_S$ was used in Chapter 4 to show that the map $f = f_1 + if_2$ was, away from a neighborhood of $\mathcal{R}_A$, a proper conformal diffeomorphism onto the union of two disjoint closed half-spaces. Since every level set of x_3 has an end in each of these sets, properness of z was then a consequence of Schwarz reflection and the Liouville theorem. The same is true when there is non-zero genus:

Proposition 6.3.4. *There exists a $\gamma_0 > 0$ so: with $\Omega_\pm = \{x \in \Gamma : \pm f_1(x) \geq \gamma_0\}$, f is a proper conformal diffeomorphism from $\Omega_\pm$ onto $\{z : \pm \mathrm{Re}\, z \geq \gamma_0\}$.*

Proof. Pick γ_0 as in Proposition 6.3.4 (where γ_0 depends only on the ϵ_0 of Theorem 6.1.1), as long as $f_1^{-1}(\gamma_0) \cap \partial\Gamma = \emptyset$ the proof for the simply connected case carries over unchanged. Note, the proof only depends on having a lower bound for γ_0 and so we may increase, if necessary, so that $\gamma_0 > \max_{\partial \mathcal{R}_G} |f_1|$. □

6.3.3 The proofs of Theorem 6.0.6 and Corollary 6.0.8

Proof. (Theorem 6.0.6) Coupled with the above results, the proof of Proposition 4.4.2 then gives that $z \to \pm\infty$ along each level set of x_3; that is $z : \Gamma \to \mathbb{C}$ is a proper holomorphic coordinate. Thus, $z(\Gamma)$ contains $\mathbb{C}$ with a closed disk removed; in particular, Γ is conformally a punctured disk. Then, since $f_1^{-1}(\gamma_0) \cap \Gamma$ is a single smooth curve, f has a simple pole at the puncture. Similarly, by Proposition 6.1.3, z has a simple pole at the puncture. In Γ, the height differential $dh = dz$ and $\frac{dg}{g} = df$. □

Embeddedness and the Weierstrass representation, (2.3), then imply Corollary 6.0.8:

Proof. Theorem 6.0.6 gives that, in Γ, $f(p) = \alpha z(p) + \beta + F(p)$ where $\alpha, \beta \in \mathbb{C}$ and $F : \Gamma \to \mathbb{C}$ is holomorphic and has holomorphic extension to the puncture (and has a zero there). By translating Σ parallel to the x_3-axis and re-basing x_3^* we may assume $\beta = 0$. By Proposition 6.1.3, $\{x_3 = 0\} \cap \Gamma$ can be written as the union of two smooth proper curves, $\sigma^{\pm}$, each with one end in $\partial\Gamma$, and parametrized so $x_3^*(\sigma^{\pm}(t)) = t$ for $\pm t > T$; here $T > 0$ is large enough that $\sigma^{\pm}(t) \subset \mathcal{R}_S$. Let us denote by $\rho^{\pm}(t)$ and $\theta^{\pm}(t)$ the polar coordinates of $\sigma^{\pm}(t)$. Notice that as we are in Γ, $\operatorname{Im} f(\sigma^{\pm}(t)) = (\operatorname{Re}\alpha)t + \operatorname{Im} F(\sigma^{\pm}(t))$. By the strict spiraling in $\mathcal{R}_S$, there are integers $N^{\pm}$ so $|\theta^{\pm}(t) - \operatorname{Im} f(\sigma^{\pm}(t))| < \pi N^{\pm}$ (see the proof of Proposition 6.3.4). Thus, since $F(\sigma^{\pm}(t)) \to 0$ as $|t| \to \infty$, if $\operatorname{Re}\alpha \neq 0$ then $\theta^{\pm}(t)$ is unbounded as $|t|$ increases. That is, σ^+ and σ^- spiral infinitely and in opposite directions. Moreover, the strict spiraling also gives that $\rho^{\pm}(t)$ is strictly increasing in $|t|$. To see this note that since $\rho'(t)u_\rho(\rho(t), \theta(t)) + \theta'(t)u_\theta(\rho(t), \theta(t)) = 0$ along $\sigma^{\pm}(t)$ and $u_\theta \neq 0$, $\rho'(t)$ can only vanish when $\theta'(t)$ does. But, our choice of parametrization rules out the simultaneous vanishing of these two derivatives. This contradicts embeddedness, as such curves must eventually intersect. This last fact is most easily seen by looking at the universal cover of the annulus $\{\max\{\rho^{\pm}(\pm T_0)\} \leq \rho \leq \min\{\rho^{\pm}(\pm(T_0 + T_1)\}\}$ where $T_0, T_1 > T > 0$ are chosen so $|\theta^{\pm}(\pm(T_0 + T_1)) - \theta^{\pm}(\pm T_0)| \geq 4\pi$ and the annulus is non-empty. In particular, by appropriately lifting σ_+ and σ_-, the intersection is immediate. Therefore, $\operatorname{Re}\alpha = 0$. □

6.4 Addendum

6.4.1 Topological structure of Σ

An elementary, but crucial, consequence of the maximum principle is that each component of the intersection of a minimal disk with a closed ball is a disk. Similarly, each component of the intersection of a genus k surface with a ball has genus at most k (see Appendix C of [22] and Section I of [21]). For Σ with one end and finite genus, we obtain a bit more:

Proposition 6.4.1. *Suppose $\Sigma \in \mathcal{E}(1)$ and $\overline{\Sigma} \subset \Sigma \cap B_1$ is connected and has the same genus as Σ. Then, $\Sigma \backslash \overline{\Sigma}$ is an annulus. Moreover, for any convex set C with non-empty interior, if $C \cap B_1 = \emptyset$, then each component of $C \cap \Sigma$ is a disk. Alternatively, if $B_1 \subset C$ then all the components of $C \cap \Sigma$ not containing $\overline{\Sigma}$ are disks.*

Proof. That $\Sigma \backslash \overline{\Sigma}$ is an annulus is a purely topological consequence of Σ having one end. Namely, if $\partial\overline{\Sigma}$ had more than one connected component, the genus of Σ would be strictly greater than the genus of $\overline{\Sigma}$.

If C and B_1 are disjoint then, as they are convex, there exists a plane P so that P meets Σ transversely and so that P separates B_1 and C. Since $\Sigma \backslash \overline{\Sigma}$ is an annulus and $P \cap \overline{\Sigma} = \emptyset$, the convex hull property implies that $P \cap \Sigma$ consists only of unbounded smooth proper curves. Thus, exactly one of the components of $\Sigma \backslash (P \cap \Sigma)$ is not a disk. As C is disjoint from the non-disk component we have the desired result. On the other hand, if C is convex and contains B_1, denote by C' the component of $C \cap \Sigma$

containing $\overline{\Sigma}$. Suppose there was a component of $C \cap \Sigma$ not equal to C' that was not a disk, then there would be a subset of Σ with boundary in $\bar{C}$ but interior disjoint from C, violating the convex hull property. □

6.4.2 Proofs of Proposition 6.2.1 and 6.2.2

We note that Theorem 6.1.1 is a sharpening, for $\Sigma \in \mathcal{E}(1)$, of a much more general description of the shapes of minimal surfaces given by Colding and Minicozzi in [12]. More precisely, in that paper they show, for a large class of embedded minimal surfaces in $\mathbb{R}^3$, how the geometric structure of a surface is determined by its topological properties. In particular, as Σ has finite topology and one end, their work shows that it roughly looks like a helicoid. That is, away from a compact set containing the genus, Σ is made up of two infinite-valued graphs that spiral together and are glued along an axis. While we do not make direct use of this description, it is needed in order to derive the structural results of Section 6.2.1 from the compactness theory of [12]. Thus, we briefly sketch a proof, we also refer the reader to Section 3.2.3.

First, Theorem 6.4.1 implies that the sequences $\lambda_i\Sigma$, $\lambda_i \to 0$, of homothetic scalings of Σ are all uniformly locally simply connected (ULSC); i.e. there is no concentration of topology other than the genus shrinking to a point (see (1.1) of [12] for the rigorous definition). Theorem 0.9 of [12] (particularly its extension to finite genus ULSC surfaces) gives a compactness result for such sequences. Namely, any ULSC sequence of fixed, finite genus surfaces, with boundaries going to ∞ and curvature blowing up in a compact set, has a sub-sequence converging to a foliation, $\mathcal{L}$, of flat parallel planes with at most two singular lines (where the curvature blows up), $\mathcal{S}_1, \mathcal{S}_2$ orthogonal to the leaves of the foliation. Up to a rotation of $\mathbb{R}^3$ we have $\mathcal{L} = \{x_3 = t\}_{t\in\mathbb{R}}$ and so $\mathcal{S}_i$ are parallel to the x_3-axis. Away from the singular lines the convergence is in the sense of graphs, in the C^α topology on compact sets for any $0 < \alpha < 1$. Moreover, as explained in property (C_{ulsc}) of Theorem 0.9 (see also Proposition 1.5 of [12]), in a small ball centered at a point of the singular set the convergence is (away from the singular set) as a double spiral staircase.

We note that in our case, i.e. $\lambda_i\Sigma, \lambda_i \to 0$, there is only one singular line and indeed since $\overline{\Sigma} \subset B_1$ has non-zero curvature this singular line is the x_3-axis. To see this, we use a further description of the convergence given by property (C_{ulsc}), namely, when there are two singular lines, the double spirals that form around each singular line are glued so that graphs going around both singular lines close up. To be precise, consider bounded, non-simply connected subsets of $\mathbb{R}^3 \setminus (\mathcal{S}_1 \cup \mathcal{S}_2)$ that contain no closed curves homotopic (in $\mathbb{R}^3 \setminus (\mathcal{S}_1 \cup \mathcal{S}_2)$) to a curve around only $\mathcal{S}_i$. That is, consider bounded regions that go only around both singular lines. In these regions, the convergence is as a single valued graph. If this were true of the convergence of $\lambda_i\Sigma$, then one could intersect $\lambda_i\Sigma$ with a ball B_R with R chosen large enough to intersect both singular lines (and contain the genus). Then at least one component of this intersection for i very large would have 3 boundary components which contradicts Proposition 6.4.1. Thus, the local picture near $\mathcal{S}_1$ of a double spiral staircase extends outward and Σ has the claimed structure.

The geometric nature of the proof of Theorem 0.9 of [12] implies that $\lambda_i\Sigma$ always

converges to the same lamination independent of the choice of λ_i. We now use the nature of this convergence to deduce gradient bounds in a cone. This and further application of the compactness theory will then give Propositions 6.2.1 and 6.2.2.

Lemma 6.4.2. *For any $\epsilon > 0, \delta > 0$ there exists an $R > 1$ so every component of $(\mathbf{C}_\delta \backslash B_R) \cap \Sigma$ is a graph over $\{x_3 = 0\}$ with gradient less than ϵ.*

Proof. We proceed by contradiction. Suppose there exists a sequence $\{R_i\}$ with $R_i \to \infty$ and points $p_i \in (\mathbf{C}_\delta \backslash B_{R_i}) \cap \Sigma$ such that the component of $B_{\gamma|p_i|}(p_i) \cap \Sigma$ containing p_i, Ω_i, is not a graph over $\{x_3 = 0\}$ with gradient less than ϵ. Here γ depends on δ and will be specified later. Now, consider the sequence of rescalings $\frac{1}{|p_i|}\Sigma$, which by possibly passing to a sub-sequence converges to $\mathcal{L}$. Passing to another sub-sequence, $\frac{1}{|p_i|}p_i$ converges to a point $p_\infty \in \mathbf{C}_\delta \cap B_1$. Let $\tilde{\Omega}_i = \frac{1}{|p_i|}\Omega_i$. Proposition 1.5 of [12] guarantees that if $B_\gamma(p_\infty) \cap \mathcal{S} = \emptyset$ then the $\tilde{\Omega}_i$ converge to $\tilde{\Omega}_\infty \subset \{x_3 = x_3(p_\infty)\}$ as graphs. As $\mathcal{S}$ is the sole singular set, we may choose γ sufficiently small, depending only on δ, to make this happen. Thus, for sufficiently large j, $\tilde{\Omega}_j$ is a graph over $\{x_3 = 0\}$ with gradient bounded by ϵ, giving the desired contradiction. □

Proof. (Proposition 6.2.1) Choose R from Lemma 6.4.2 with $\delta = \epsilon$. Note, control on the gradient bounds the separation between sheets. Thus, increasing R, if necessary, guarantees N sheets of a graph inside $\mathbf{C}_\epsilon$. □

Proof. (Proof of Proposition 6.2.2) Note that as long as $|y|$ is sufficiently large, Theorem 0.6 of [20] gives an $\Omega < 1/2$ (as well as C_1 and C_2) so that, since the component of $B_{\frac{1}{2}|y|}(y) \cap \Sigma$ containing y is a disk, there exists a N-valued graph Σ_0 over the annulus, $A = D_{\Omega|y|} \backslash D_{s/2}(y) \subset P$ with gradient bounded by $\epsilon/2$, initial separation greater than $C_2 s$ and $\text{dist}_\Sigma(\Sigma_0, y) \leq 2s$. Here P is in principle an arbitrary plane in $\mathbb{R}^3$.

We claim that Lemma 6.4.2 implies a subset, Σ_0', of Σ_0 is a N-valued graph over the annulus $A' = D_{\Omega|y|/2} \backslash D_s(\Pi(y)) \subset \{x_3 = 0\}$ with gradient bounded by ϵ, which further implies Σ_0' can be extended as desired. To that end we note that for $\delta > 1/(4\Omega)$, if $y \notin \mathbf{C}_\delta$ then A (and thus, by possibly increasing δ, Σ_0) meets $\mathbf{C}_\delta$. Lemma 6.4.2 allows us to choose an $R_0 > 0$ so that every component of $\Sigma \cap (\mathbf{C}_\delta \backslash B_{R_0})$ is a multi-valued graph over $\{x_3 = 0\}$ with gradient bounded by $\epsilon/4$. Thus if we take $R > 2R_0$ then there is a point of Σ_0 in $\mathbf{C}_\delta \backslash B_{R_0}$; therefore, for the gradient estimates at the point to be consistent, P must be close enough to $\{x_3 = 0\}$ so that we may choose $\Sigma_0' \subset \Sigma_0$ so it is a multi-valued graph over A'. Furthermore, the part of Σ_0' over the outer boundary of A' is necessarily inside of $\mathbf{C}_\delta \backslash B_{R_0}$ and so Lemma 6.4.2 allows us to extend it as desired. □

6.4.3 One-sided curvature in Σ

In several places we make use of the one-sided curvature estimate of [22]. Recall, this result gives a curvature estimate for a minimal disk that is close to and on one side of a plane. As a sequence of rescaled catenoids shows, it is crucial that the surface be a disk. In our situation, Proposition 6.4.1 allows the use of the one-sided curvature estimate far from the genus. For convenience we record the statement we will need and indicate how it follows from [22]:

Corollary 6.4.3. *Given $\epsilon, \delta > 0$ there exist $\delta_0 > 0$ and $R > 1$ such that, if there exists a 2-valued δ_0-sheet on scale s centered at y where $y \notin \mathbf{C}_\delta \cup B_R$, then all the components of $\Sigma \cap (\mathbf{C}_{\delta_0} \backslash B_{2s}(y))$ are multi-valued graphs with gradient $\leq \epsilon$.*

Proof. The result follows immediately from the proof of Corollary I.1.9 of [22] (see Corollary 3.1.10) as long as one notes that the proof of I.1.9 depends only on each component of $\Sigma \cap \mathbf{C}_{K\delta_0} \backslash B_s(y)$ being a disk for K some large (universal) constant. We refer the reader to Figure 3-2. Thus, by Proposition 6.4.1, we need only check that for a suitable choice of R and upper bound δ_0' for δ_0 (both R and δ_0' depending only on δ), $y \notin \mathbf{C}_\delta \cup B_R$ implies $\mathbf{C}_{K\delta_0'}(y)$ is disjoint from B_1 (i.e. from the genus).

Now suppose $x \in \mathbf{C}_{K\delta_0'}(y)$ and think of x and y as vectors. By choosing δ_0' sufficiently small (depending on δ) we have that $|\langle x - y, y\rangle| < (1-\gamma)|y||x-y|$ (that is the angle between $x - y$ and y is bounded away from 0°); note $1 > \gamma > 0$ depends only on δ. But then $|x|^2 = |x - y + y|^2 \geq |x-y|^2 + 2\langle x - y, y\rangle + |y|^2 \geq \gamma |y|^2$. Hence, picking $R^2 > \frac{1}{\gamma}$ suffices. □

6.4.4 Geometric Bounds near blow-up pairs

We record the following extension of Lemma 2.26 of [24] to surfaces with non-trivial topology. The proof is identical to that of Lemma 2.26 as long as one replaces Colding and Minicozzi's compactness result for minimal disks, i.e. Theorem 0.1 of [22], with the more general Theorem 0.6 of [12]:

Proposition 6.4.4. *Given K_1, g there exists a constant K_2 such that: if $\Sigma \subset \mathbb{R}^3$ is an embedded minimal surface of genus g, $\Sigma \subset B_{K_2 s}(y)$ and $\partial\Sigma \subset \partial B_{K_2 s}(y)$ and (y, s) is a blow-up pair, then we get the curvature bound:*

$$\sup_{B_{K_1 s}(y) \cap \Sigma} |A|^2 \leq K_2 s^{-2}. \tag{6.2}$$

An immediate corollary is that, for blow-up pairs far from the genus, the scale is small relative to the distance to the genus.

Corollary 6.4.5. *Given $\alpha, C_1 > 0$ there exists an R such that for (y, s), a C_1 blow-up pair of Σ with $|y| \geq R$ then $s < \alpha |y|$.*

Proof. Recall we have normalized Σ so $\sup_{B_1 \cap \Sigma} |A|^2 \geq 1$. Now suppose the result did not hold. Then there exists a sequence (y_j, s_j) of C_1 blow-up pairs with $|y_j| \geq j$ and $s_j \geq \alpha |y_j|$. Set $K_1 = 2/\alpha$. By Proposition 6.4.4 there exists K_2 such that $\sup_{B_{K_1 s_j}(y_j) \cap \Sigma} |A|^2 \leq K_2 s_j^{-2}$. Since $B_1 \subset B_{K_1 s_j}(y_j)$, $\sup_{B_1 \cap \Sigma} |A|^2 \leq K_2 s_j^{-2}$. But $s_j \geq \alpha |y_j| \geq \alpha j$, thus for j sufficiently large one obtains a contradiction. □

Chapter 7

The Space of Genus-g Helicoids

The goal of this chapter is to investigate how one might further restrict the space genus-g helicoids, i.e. more fully understand the finer geometric structure of elements of $\mathcal{E}(1, g)$. We do so by showing, after a suitable normalization, a certain compactness result for these spaces. Unfortunately, this result can not rule out the "loss" of genus and so does not give much new geometric information for $g > 1$. However, we have the following strong compactness result for genus-one surfaces:

Theorem 7.0.6. *Let $\Sigma_i \in \mathcal{E}(1, 1)$ and suppose that all the Σ_i are asymptotic to H, a fixed helicoid. Then, a sub-sequence of the Σ_i converge uniformly in C^∞ on compact subsets of $\mathbb{R}^3$ to $\Sigma_\infty \in \mathcal{E}(1, 1) \cup \{H\}$ with Σ_∞ asymptotic to (or equaling) H.*

To prove this result, we must develop a more general compactness theory. Indeed, we prove some results that specialize and extend the compactness theory of Colding and Minicozzi developed in [12]. Specifically, suppose Σ_i is a sequence of minimal surfaces with finite genus and connected boundary. Then if $\partial\Sigma_i \subset \partial B_{R_i}$, $R_i \to \infty$, and one has an appropriate normalization, then a sub-sequence converges smoothly on compact subsets of $\mathbb{R}^3$ to an embedded finite (and positive) genus minimal surface with one end, i.e. an element of $\mathcal{E}(1, +)$ which (as we have seen in Chapter 6) is a genus-g helicoid. Obviously, some normalization is required to obtain smooth convergence; as is clear by looking at the rescalings of a genus-one helicoid. We consider two different normalizations – one intrinsic and one extrinsic. Intrinsically, we normalize by demanding that the injectivity radius is everywhere bounded below by 1 and that $0 \in \Sigma_i$ has injectivity radius uniformly bounded above – a very natural condition from the point of view of metric geometry. We also introduce a slightly more technical extrinsic normalization – we defer a precise definition of it to Section 7.3. Roughly speaking, in the extrinsic case, we normalize so that near 0 one has a handle of Σ of a fixed extrinsic "size". Ultimately, we show that the two normalizations are equivalent. While the definition of the extrinsic normalization is more technical, it is very natural from the point of view of Colding and Minicozzi theory and likely easier to verify in application.

Without any assumptions on the scale of the topology, the bound on the genus and the fact that $R_i \to \infty$ is enough to apply the compactness theory of Colding and Minicozzi [12] (see Section 3.2.3). That is, either a sub-sequence converges smoothly

on compact subsets of $\mathbb{R}^3$ to a complete surface or a sub-sequence converges to a singular lamination in a manner analogous to the homothetic blow-down of a helicoid. Thus, the main thrust of this chapter will be to show that uniform control on the scale of the genus rules out the singular convergence.

Let us define $\mathcal{E}(e, g, R)$ to be the set of smooth, connected, properly embedded minimal surfaces, $\Sigma \subset \mathbb{R}^3$, so that Σ has genus g and $\partial\Sigma \subset \partial B_R(0)$ is smooth, compact and has e components. Additionally, let $\mathcal{E}(e, g, \infty) = \mathcal{E}(e, g)$ be the set of complete embedded minimal surfaces with e ends and genus g. Note, that for $e = 1$ this agrees with our previous definitions. We then have the following compactness results:

Theorem 7.0.7. *Suppose $\Sigma_i \in \mathcal{E}(1, g, R_i)$ ($g \geq 1$) with $0 \in \Sigma_i$, $\text{inj}_{\Sigma_i} \geq 1$, $\text{inj}_{\Sigma_i}(0) \leq \Delta_0$ and $R_i/r_+(\Sigma_i) \to \infty$. Then a sub-sequence of the Σ_i converges uniformly in C^∞ on compact subsets of $\mathbb{R}^3$ with multiplicity 1 to a surface $\Sigma_\infty \in \cup_{l=1}^{g} \mathcal{E}(1, l)$.*

Theorem 7.0.8. *Suppose $\Sigma_i \in \mathcal{E}(1, g, R_i)$ ($g \geq 1$) with $r_-(\Sigma_i) = 1$, $r_-(\Sigma_i, 0) \leq C$, and $R_i/r_+(\Sigma_i) \to \infty$. Then a sub-sequence of the Σ_i converges uniformly in C^∞ on compact subsets of $\mathbb{R}^3$ with multiplicity 1 to a surface $\Sigma_\infty \in \cup_{l=1}^{g} \mathcal{E}(1, l)$ and $r_-(\Sigma_\infty, 0) \leq C$.*

The above theorems are, respectively, our compactness result for intrinsically normalized sequences and for extrinsically normalized sequences. The technical definitions in the statements are thoroughly explained in Section 7.3, in particular see Definitions 7.3.1, 7.3.3 and 7.3.4.

Recall, that Corollary 6.0.9 of Chapter 6, tells us that any element of $\mathcal{E}(1, g)$ is asymptotic to a helicoid. It is natural to investigate whether there is a connection between the scale of the asymptotic helicoid (a global quantity) and the scale of the genus (an essentially local quantity). When $g = 1$ such a connection can be established, as trivially $r_-(\Sigma) = r_+(\Sigma)$, and so Theorem 7.0.8 is particularly strong. Indeed, one has Theorem 7.0.6, that is, compactness in the space $\mathcal{E}(1, 1)$, as long as the asymptotic helicoid is fixed. In particular, for surfaces with genus one, there is a uniform relationship between the scale of the asymptotic helicoid and the scale of the genus. Note that Theorem 7.0.6 is a generalization of a result of Hoffman and White in [40], there they prove such a compactness result after imposing strong symmetry assumptions.

Finally, Theorem 7.0.8 allows one to give an effective geometric description of minimal surfaces with genus one and connected boundary, comparable to the description of the shape of embedded minimal disks near a point of large curvature given by Theorem 5.1.1:

Theorem 7.0.9. *Given $\epsilon > 0$ and $R \geq 1$ there exists an $R' = R'(\epsilon, R) \geq R$ so that if $\Sigma \in \mathcal{E}(1, 1, R')$ with $r_-(\Sigma) = 1$ and the genus of Σ is centered at 0, then the component of $B_R(0) \cap \Sigma$ containing the genus is bi-Lipschitz with a subset of an element of $\mathcal{E}(1, 1)$ and the Lipschitz constant is in $(1 - \epsilon, 1 + \epsilon)$.*

This chapter will appear in [1].

7.1 Outline of Argument

The proofs of Theorems 7.0.7 and 7.0.8 rely on Colding and Minicozzi's fundamental study of the structure of embedded minimal surfaces in $\mathbb{R}^3$. In particular, we make use of three important consequences of their work: the one-sided curvature estimates (see Section 3.1.4); the chord-arc bounds for minimal disks (see Section 3.2.2); and, most importantly, their lamination theory for finite genus surfaces (see Section 3.2.3). As our work depends most critically on this last result, we refer the reader to the discussion of it in Section 3.2.3.

To prove 7.0.7, we first prove a compactness result for a larger class of surfaces. The price we pay is that we no longer have as much information about the topology of the limiting surfaces. This result is of some interest in it's own right and should be compared to very similar results obtained by Meeks, Perez and Ros, [42, 43]:

Theorem 7.1.1. *Let $\Sigma_i \in \mathcal{E}(e, g, R_i)$ $(e, g \geq 1)$ be such that $0 \in \Sigma_i$, $\text{inj}_{\Sigma_i} \geq 1$, $\text{inj}_{\Sigma_i}(0) \leq \Delta_0$ and $R_i \to \infty$ then a sub-sequence of the Σ_i converge smoothly on compact subsets of $\mathbb{R}^3$ and with multiplicity one to a non-simply connected minimal surface in $\cup_{1\leq k\leq e+g, 0\leq l\leq g}\mathcal{E}(k, l)$.*

We will use the lamination theory of [12] to show Theorem 7.1.1. Note, the uniform lower bound on the injectivity radius and the weak chord-arc bounds imply that there is a uniform extrinsic scale on which the surfaces are simply connected. This allows for the local application of the work of Colding and Minicozzi for disks [19–22]. In particular, the sequence of Σ_i is ULSC (see Definition 3.2.4).

The uniform upper bound on the injectivity radius at 0 implies the existence of a closed geodesic, in each Σ_i, close to 0 and which have uniformly bounded length. Using these closed geodesics and the lamination theorem, we show uniform curvature bounds on compact subsets of $\mathbb{R}^3$ for the sequence. Indeed, suppose one had a sequence that did not have uniform curvature bounds. Then a sub-sequence would converge to a singular lamination as in Section 3.2.3. The nature of the convergence implies that any sequence of closed geodesics in the surfaces, which have uniform upper bounds on their lengths and that that don't run off to ∞, must converge (in a Hausdorff sense) to a subset of the singular axis. This is finally ruled out by noting that the uniform scale on which the surfaces are simply connected, allows us to use the one-sided curvature estimate and the weak chord-arc bound to obtain a contradiction. The uniform curvature bounds and Schauder estimates allow us to appeal to the Arzela-Ascoli theorem and which together give the convergence.

As an immediate consequence, we deduce that, for sequences in $\mathcal{E}(1, g, R_i)$, as long as the genus stays inside a fixed uniform ball and does not shrink off, then one has convergence to an element of $\mathcal{E}(1, g)$. Indeed, with such uniform control, the no-mixing theorem of [12] implies that there is a uniform lower bound on the injectivity radius and so Theorem 7.1.1 applies; that the genus remains in a fixed compact space implies that the limit surface must belong to $\mathcal{E}(1, g)$. Using this result, the intrinsically normalized compactness result, i.e. Theorem 7.0.7, proved in Section 7.3, is proved by induction on the genus. When the genus is one, the inner and outer scales coincide. Furthermore, in this case, it is not hard to relate the extrinsic and

intrinsic normalizations and so Theorem 7.0.7 follows immediately from the arguments described above. For larger genus, if one does not have uniform control on the outer scale, then passing to a sub-sequence gives $r_+(\Sigma_i) \to \infty$. In this case the no-mixing theorem of Colding and Minicozzi implies the existence of $r_i < r_+(\Sigma_i)$ with $r_i \to \infty$ such that there is a component Σ_i' of $B_{r_i} \cap \Sigma_i$ so $\Sigma_i' \in \mathcal{E}(1, g', r_i)$ where $0 < g' < g$ and the Σ_i' satisfy the conditions of Theorem 7.0.7. Thus, the induction hypothesis and fact that Σ_i' eventually agrees with Σ_i on any compact subset of $\mathbb{R}^3$ together prove the theorem. Theorem 7.0.7 allows one to relate the intrinsic and extrinsic normalizations for arbitrary genus. Theorem 7.0.8 is then a simple consequence of this.

In order to prove our main compactness result, i.e. Theorem 7.0.6, which we prove in Section 7.4.1, we couple Theorem 7.0.8 with the fact that the surfaces are asymptotic to helicoids (see Chapter 6). The connection between the convergence on compact subsets of $\mathbb{R}^3$ and the asymptotic behavior at the end is made using certain path integrals of the holomorphic Weierstrass data.

7.2 Weak Compactness

We will prove Theorem 7.1.1 by using the lamination theory of Colding and Minicozzi. The key fact is that the weak chord-arc bounds of [24] (see Proposition 3.2.3) allow us to show that our sequence Σ_i is ULSC. That is, there is a small, but uniform, *extrinsic* scale on which the sequence is simply connected (the uniform lower bounds for the injectivity radius provide such a uniform *intrinsic* scale). Thus, the lamination theory of [12] will imply that either there are uniform curvature bounds on a sub-sequence, or, on a sub-sequence, one has one of two possible singular convergence models. A simple topological argument will rule out one of these possibilities and so imply that the sequence behaves like the blow-down of a helicoid (i.e. like Theorem 3.2.1). This will be shown to contradict the origin having an upper bound on its injectivity radius, which proves the desired curvature bounds. One can then appeal to the Arzela-Ascoli theorem.

7.2.1 Technical lemmas

In order to prove these bounds, we will need four technical lemmas. We first note the following simple topological consequence of the maximum principle:

Proposition 7.2.1. *Let $\Sigma \in \mathcal{E}(e, g, R)$ and suppose $B_r(x) \subset B_R(0)$ and $\partial B_r(x)$ meets Σ transversely, then, for any component Σ_0 of $\Sigma \cap B_r(x)$, $\partial\Sigma_0$ has at most $g+e$ components.*

Proof. Let Σ_i, $1 \leq i \leq n$ be the components of $\Sigma \backslash \Sigma_0$, note for $0 \leq i \leq n$, the Σ_i are smooth compact surfaces with boundary. Thus, $\partial\Sigma_i$ is a finite collection of circles and so the Euler characteristic satisfies $\chi(\Sigma) = \sum_{i=0}^n \chi(\Sigma_i)$. By the classification of surfaces one has $\chi(\Sigma) = 2-2g-e$ and $\chi(\Sigma_i) = 2-2g_i-e_i$ where g_i is the genus of Σ_i and e_i number of components of $\partial\Sigma_i$. Note that, $\sum_{i=0}^n g_i \leq g$ and $\sum_{i=1}^n e_i = e_0 + e$. Thus, we compute that $e_0 = n + g - \sum_{i=0}^n g_i$. The maximum principle implies that $n \leq e$ (as any Σ_i, for $i \geq 1$, must meet ∂B_R). Thus, $e_0 \leq e + g$. □

Next we note it is impossible to minimally embed an (intrinsically) long and thin cylinder in $\mathbb{R}^3$ (compare with [16] and Lemma 4.2 of [24]):

Lemma 7.2.2. *Let Γ be an embedded minimal annuli with $\partial\Gamma = \gamma_1 \cup \gamma_2$ where the γ_i are smooth and satisfy $\int_{\gamma_i} |k_g| \leq C_1$ and $\ell(\gamma_i) \leq C_2$, i.e. the curves have bounded total geodesic curvature (in Γ) and bounded length. Then, there exists a $C_3 = C_3(C_1, C_2)$ so that $\text{dist}_\Gamma(\gamma_1, \gamma_2) \leq C_3$.*

Proof. We proceed by contradiction. That is, assume one had a sequence of Γ^i satisfying the hypotheses of the theorem but so that $\text{dist}_{\Gamma^i}(\gamma_1^i, \gamma_2^i) \to \infty$. We claim that, for i sufficiently large, there exist disjoint embedded closed curves σ_1^i and σ_2^i in Γ^i so that the σ_j^i $(j = 1, 2)$ are homotopic to γ_l^i $(l = 1, 2)$ and one component of $\Gamma^i \backslash (\sigma_1^i \cup \sigma_2^i)$ has positive total curvature. As Γ^i is minimal, this is impossible, yielding the desired contradiction.

In order to verify the claim, we note that it is enough (by the Gauss-Bonnet theorem) to find σ_1^i, σ_2^i so that the total geodesic curvature (in Γ^i) of the σ_j^i $(j = 1, 2)$ has appropriate sign. In other words, if we order things so σ_1^i lies between γ_1^i and σ_2^i then we want the total geodesic curvature of σ_1^i to be negative with respect to the normal (in Γ_i) to σ_1^i that points toward γ_1^i and similarly we want the total curvature of σ_2^i to be negative with respect to the normal pointing toward γ_2^i.

Now suppose we translate so $\gamma_1^i \subset B_{C_2}(0)$. The Gauss-Bonnet theorem and the estimates on the total curvature of γ_j^i (for $j = 1, 2$) imply that $\int_{\Gamma^i} |A|^2 \leq 4\pi C_1$. We may thus pass to a sub-sequence of the Γ_i and appeal to the intrinsic version of the estimates of Choi and Schoen [11]. Hence, there is an $R_0 > 0$ with $R_0 = R_0(C_1, C_2)$ so that for any $R > R_0$ there is an $i_0 = i_0(R)$ so if $i > i_0$ and $\text{dist}_{\Gamma^i}(x, \gamma_1^i) \in (R_0, R)$ then $|A|^2(x) \leq 1$. Thus, one has uniform curvature estimates on compact sets sufficiently far from γ_1^i and so may pass to a limit and appeal to Arzela-Ascoli to see that on compact subsets of $\mathbb{R}^3 \backslash B_{2C_2+2R_0}(0)$ the Γ^i converge to an embedded minimal surface Γ^∞. Since each Γ^i has uniformly bounded total curvature this is also true of Γ^∞. By [57], Γ^∞ must be asymptotic to a plane or half a catenoid. Note that for a catenoid or plane (normalized to be symmetric with respect to the origin) by intersecting with the boundary of a very large (extrinsic) ball one obtains a curve (in the catenoid or plane) with total curvature less then $-\pi$ (with respect to the normal pointing inside the ball). As a consequence, for i sufficiently large one can find σ_1^i as desired. The exact same argument, with Γ^i translated so γ_2^i lies in $B_{C_2}(0)$, allows one to construct σ_2^i. □

We will also need a certain sort of "stability" result for minimizing geodesics in flat surfaces:

Lemma 7.2.3. *Let $\Sigma \subset B_2(0)$ be an embedded disk with $\partial\Sigma \subset \partial B_2(0)$. Suppose there exists $u : D_{3/2}(0) \to \mathbb{R}$ so the graph $\big\{(x, u(x)) : x \in D_{3/2}(0)\big\} = \Sigma^0 \subset \Sigma$. Then for any $\delta > 0$ there is an $\epsilon > 0$ so: if $||u||_{C^2} \leq \epsilon$ and $p_\pm \in \partial B_1(0) \cap \Sigma^0$ are such that $\gamma \subset \Sigma^0$, the minimizing geodesic in Σ^0 connecting $p_\pm$, has $\gamma \cap B_\epsilon(0) \neq \emptyset$ then there is a line $0 \in L$ so that the Hausdorff distance between γ and $L \cap D_1(0)$ is less than δ. As a consequence $\ell(\gamma) \geq 2 - 2\delta$.*

Proof. Fix $\delta > 0$ and suppose this result was not true. That is, one has a sequence of Σ_i and u_i with $u_i \to 0$ in C^2 and points $p^i_\pm$ connected by minimizing geodesic $\gamma_i \subset \Sigma^0$ that meet $B_{\epsilon_i}(0)$ where $\epsilon_i \to 0$, but the conclusion of the lemma does not hold.

We first note that for i sufficiently large the control on $|\nabla u_i|$ implies that for any points $a, b \in \Sigma^0_i$, $\mathrm{dist}_{\mathbb{R}^3}(a,b) \geq \frac{1}{2}\mathrm{dist}_{\Sigma^0_i}(a,b)$. Thus, as the condition imposed on γ_i implies that $\mathrm{dist}_{\Sigma_i}(p^i_+, p^i_-) \geq 1$, it follows that $\mathrm{dist}_{\mathbb{R}^3}(p^i_+, p^i_-) \geq 1/2$. Hence, by passing to a sub-sequence we may assume that $u_i \to 0$ and that $p^i_\pm \to p^\infty_\pm \in \partial D_1(0)$ and the distance between p^∞_+ and p^∞_- is bounded below by $1/2$ (and in particular the points don't coincide). Now, let L be the line connecting $p^\infty_\pm$.

We claim that $0 \in L$. If this was not the case then $\ell(L \cap D_1(0)) = 2 - 4\alpha$ for some $\alpha > 0$. Let L_i be the graph (of u_i) over $L \cap D_1(0)$, so L_i is a segment that is a subset of Σ_i. By the convergence it is clear that one may find an i_0 so that for $i \geq i_0$, $\mathrm{dist}_{\Sigma_i}(p^i_\pm, L_i) < \alpha$ and $\ell(L_i) < \ell(L \cap D_1(0)) + \alpha$. Thus, for $i \geq i_0$, one has $\mathrm{dist}_{\Sigma_i}(p^i_-, p^i_+) < 2 - \alpha$. On the other hand, the hypotheses imply that there is a $p^i \in \gamma_i$ with $p^i \to 0$. In particular, by increasing i_0 if needed, one has for $i \geq i_0$, $\mathrm{dist}_{\Sigma_i}(p^i_\pm, p^i) \geq \mathrm{dist}_{\mathbb{R}^3}(p^i_\pm, p^i) \geq 1 - \alpha/2$. But then $\mathrm{dist}_{\Sigma_i}(p^i_-, p^i_+) \geq 2 - \alpha$.

Arguing similarly, we see that $L \cap D_1(0)$ must be Hausdorff close to γ_i, when i is sufficiently large, yielding the desired contradiction. Finally, we note that the length estimate follows as the two segments are Hausdorff close. □

We make the following definition:

Definition 7.2.4. Suppose $\gamma \subset \mathbb{R}^3$ is a smooth, immersed closed curve parametrized by $f : \mathbb{S}^1 \to \gamma$. For a fixed compact subset K of $\mathbb{R}^3$ we say $\gamma' \subset \gamma$ is an *arc of γ in K (through p)* if $\gamma' = f(I')$ where I' is a connected component of $f^{-1}(K \cap \mathbb{S}^1)$ (and $p \in \gamma'$).

Remark 7.2.5. If γ is embedded then an arc in K is just a component of $\gamma \cap K$.

Our final technical lemma shows that, for a sequence of Σ_i converging to a minimal lamination with nice singular set, any closed geodesics in the Σ_i, that are of uniformly bounded length and that do not run off to infinity, must collapse to the singular set.

Lemma 7.2.6. *Fix $\Delta, C > 0$. Suppose $\Sigma_i \in \mathcal{E}(e, g, R_i)$, $R_i \to \infty$, the Σ_i converge to the singular lamination $\mathcal{L}$ with singular set $\mathcal{S} = \mathcal{S}_{ulsc}$ in the sense of Colding and Minicozzi [12], and that $\mathcal{S}$ is the x_3-axis. Then, given $\epsilon > 0$ there exists an i_0 so that for $i \geq i_0$, if γ_i is a closed geodesic in Σ_i, with $\ell(\gamma_i) \leq 2\Delta$ and $\gamma_i \subset B_{C\Delta}$, then $\gamma_i \subset T_\epsilon(\mathcal{S})$, the extrinsic ϵ-tubular neighborhood of $\mathcal{S}$.*

Proof. Suppose the lemma was not true; then there exists a sub-sequence of the Σ_i so that γ_i intersects $K_\epsilon = \overline{B}_{C\Delta}(0) \backslash T_\epsilon(\mathcal{S})$. As a consequence, there are points $p_i \in \gamma_i \cap K_\epsilon$ that (after possible passing to a further sub-sequence) converge to some point $p_\infty \in K_\epsilon$. The convergence of [12] implies that for sufficiently large i (so R_i is large), $B_{\epsilon/2}(p_\infty) \cap \Sigma_i$ converges smoothly to $B_{\epsilon/2}(p_\infty) \cap \{x_3 = t\}_t$ in the sense of graphs. Let γ_i' be an arc of γ_i in $B_{\epsilon/2}(p_\infty)$ through p_i; then γ_i' is a geodesic segment with boundary points $q_i^\pm$ lying in the boundary of $B_{\epsilon/2}(p_\infty)$. Finally, let us choose Γ_i to be the component of $B_{\epsilon/2}(p_\infty) \cap \Sigma_i$ that contains p_i.

For a given $\delta > 0$, there exists i sufficiently large such that Γ_i, γ_i' satisfy the hypotheses of Lemma 7.2.3 (up to a rescaling). Notice that for large i, Γ_i is very flat and in particular is geodesically convex and hence γ_i' is the minimizing geodesic connecting $q_i^{\pm}$. Hence, if L_i is the line given by the lemma, γ_i' lies in the δ-tubular neighborhood of $L_i \cap D_{\epsilon/4}$. By passing to a sub-sequence, the γ_i' converge to a segment of a line L in $\{x_3 = x_3(p_\infty)\}$ that goes through p_∞.

We next show this is impossible. Clearly at least one of the rays of L starting at p_∞, L^+, does not meet $\mathcal{S}$. Thus, there is an $\epsilon/4 > \epsilon_0 > 0$ so one can cover L^+ by balls of radius ϵ_0 that are disjoint from $\mathcal{S}$. Now, let p_∞^1 be the point of intersection of $B_{\epsilon_0/2}(p_\infty)$ with L^+ and inductively define p_∞^{k+1} to be the point of intersection of $B_{\epsilon_0/2}(p_\infty^k)$ with L^+ that is further from p_∞ than p_∞^k. Let $\gamma_{i,1}'$ be an arc of γ_i' in $B_{\epsilon_0/2}(p_\infty^1)$ (note, for i sufficiently large, the convergence, the fact that $B_{\epsilon_0/2}(p_\infty^1) \subset B_{\epsilon/4}(p_\infty)$, and $R_i \to \infty$ together imply this is non-empty). Moreover, one then has that $\gamma_{i,1}'$ converge to $L \cap B_{\epsilon_0/2}(p_\infty^1)$. This comes from applying Lemma 7.2.3, given the fact that an end-point of γ_i' (and thus a point of $\gamma_{i,1}'$) converges to p_∞^1. Now let $\gamma_{i,2}'$ be an arc in $B_{\epsilon_0/2}(p_\infty^2)$ through a point of $\gamma_{i,1}'$ (by increasing i if needed we may ensure this is non-trivial). By Lemma 7.2.3 and the fact that the $\gamma_{i,1}'$ converge to $L \cap B_{\epsilon_0/2}(p_\infty^1)$, the $\gamma_{i,2}'$ converge to $L \cap B_{\epsilon_0/2}(p_\infty^2)$. Now, fixing some large j_0, we may proceed inductively and define $\gamma_{i,j}'$ (for $j \leq j_0$) to be the arc of γ_i in $B_{\epsilon_0/2}(p_\infty^j)$ through a point of $\gamma_{i,j-1}'$. Again, we may have to choose i large enough (depending on j_0) so everything is non-trivial. Note also that, by an inductive argument, we obtain that $\gamma_{i,j}'$ converge to $L \cap B_{\epsilon/2}(p_\infty^j)$ as $i \to \infty$.

Notice by construction that for $|l - j| \geq 2$, $\gamma_{i,j}' \cap \gamma_{i,l}' = \emptyset$. Moreover, by the convergence result, for i sufficiently large, $\ell(\gamma_{i,j}') \geq \epsilon_0/2$. Choose j_0 large enough so $\epsilon_0 j_0 \geq 10\Delta$. This contradicts the upper bound for the length of γ_i, thus proving the lemma. □

7.2.2 Proof of Theorem 7.1.1

We apply the preceding lemmas in order to show uniform curvature bounds:

Lemma 7.2.7. *Let $\Sigma_i \in \mathcal{E}(e, g, R_i)$ be such that $0 \in \Sigma_i$, $\text{inj}_{\Sigma_i} \geq 1$, $\text{inj}_{\Sigma_i}(0) \leq C$ and $R_i \to \infty$ then a sub-sequence of the Σ_i satisfy*

$$\sup_i \sup_{K \cap \Sigma_i} |A|^2 < \infty. \tag{7.1}$$

Proof. If this was not the case then by the lamination theorem of [12] a sub-sequence of the Σ_i would converge to a singular lamination $\mathcal{L}$. For any $x \in \Sigma_i$ with $|x| \leq R_i/2$, the injectivity radius lower bound and the weak chord-arc bounds of [24] imply that there is a $\delta_1 > 0$ so $B_{\delta_1}(x) \cap \Sigma$ is a subset of the intrinsic ball of radius $1/2$ centered at x. Fixing x, as long as i is large enough so $|x| \leq R_i/2$, this implies that every component of $B_{\delta_1}(x) \cap \Sigma_i$ is a disk. Thus, the sequence of Σ_i is ULSC and so the structure of the singular set of $\mathcal{L}$ is $\mathcal{S} = \mathcal{S}_{ulsc}$. Hence, after rotating if needed, $\mathcal{L} = \{x_3 = t\}_{t \in \mathbb{R}}$ and $\mathcal{S}$ is parallel to the x_3-axis and consists of either one or two lines. If there were two lines then pick R_0 large enough so that $B_{R_0/2}(0)$ meets both

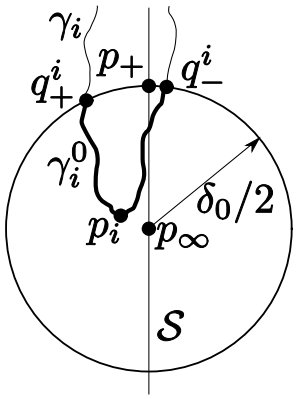

Figure 7-1: The points of interest in the proof of Lemma 7.2.7.

of them. By the nature of the convergence in this case (modeled on the degeneration of the Riemann examples see [12] or Section 6.4.2), for any $f > 0$ there is an i_0 so for $i \geq i_0$, at least one component of $B_{R_0} \cap \Sigma_i$ has boundary consisting of more than f connected components. This contradicts Proposition 7.2.1 and so does not occur.

We next rule out any singular behavior. To that end, we note that the injectivity bound at 0 and the non-positive curvature of Σ_i imply the existence of $0 \in \gamma_i' \subset \Sigma_i$, a geodesic lasso with singular point 0 and $\ell(\gamma_i') \leq 2\Delta_0$ (recall a geodesic lasso is a closed continuous curve that is geodesic away from one point). For the existence of such lassos γ_i' we refer to Proposition 2.12 of [10]. Note that the length bound implies $\gamma_i' \subset B_{3\Delta_0}(0)$. The fact that Σ_i has non-positive curvature implies that γ_i' is not null-homotopic. We may minimize the homotopy class of γ_i' to obtain a closed geodesic γ_i, note that Lemma 7.2.2 allows us to do this without worry even though Σ_i has boundary. Indeed, either γ_i' intersects γ_i and so $\gamma_i \subset B_{6\Delta_0}$ or as $\ell(\gamma_i) \leq \ell(\gamma_i')$ we may apply Lemma 7.2.2 (after smoothing out γ_i' a bit). In the latter case, $\text{dist}_{\Sigma_i}(\gamma_i', \gamma_i) \leq (C-3)D_0$ for some large (but uniform) C and so may take $\gamma_i \subset B_{C\Delta_0}(0)$.

Now for $\epsilon > 0$, let $T_\epsilon(\mathcal{S})$ be the extrinsic ϵ-tubular neighborhood of $\mathcal{S}$. Lemma 7.2.6 then implies there is an i_ϵ so that for all $i \geq i_\epsilon$, $\gamma_i \subset T_\epsilon(\mathcal{S})$. For each i, fix $p_i \in \gamma_i$ so that $x_3(p_i) = \min\{x_3(p) : p \in \gamma_i\}$ i.e. the lowest point of γ_i. Then a subsequence of the p_i converge to p_∞ and, by the above, $p_\infty \in \mathcal{S}$. Let p_+ be the point of intersection of $\partial B_{\delta_0/2}(p_\infty) \cap \mathcal{S}$, chosen so $x_3(p_+) > x_3(p_\infty)$. Pick i_0 large enough so for $i \geq i_0$, $|p_\infty - p_i| \leq \delta_0/4$. The choice of δ_0 implies that γ_i is not contained in $B_{\delta_0/2}(p_\infty)$; but for $i \geq i_0$, γ_i meets this ball. Let γ_i^0 be an arc of γ_i in $B_{\delta_0/2}(p_\infty)$ through p_i. Note that γ_i^0 has boundary on $\partial B_{\delta_0/2}(p_\infty)$. Denote these two boundary points by q_i^+ and q_i^- (See Figure 7.2.2). Notice that for $i \geq i_0$, $\delta_0/3$ gives a uniform lower bound on the intrinsic distance between q_i^+ and q_i^-. To see this we first note that for $i \geq i_0$ the length of γ_i^0 is bounded below by $\delta_0/3$, as the extrinsic distance between $q_i^\pm$ and p_i is bounded below by $\delta_0/4$. On the other hand, by the lower bound on the injectivity radius, either the intrinsic distance between q_i^- and q_i^+ is greater than $1/2$ or both lie in a geodesically convex region and γ_i^0 must be the unique minimizing geodesic connecting them.

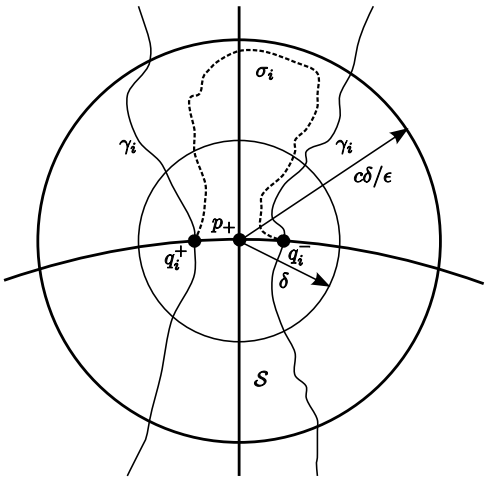

Figure 7-2: Illustrating the consequence of the one sided curvature estimates

Now by Lemma 7.2.6, for any $\delta > 0$, there is an $i_\delta \geq i_0$ so for $i \geq i_\delta$, $q_i^\pm \in B_\delta(p_+)$. By the one-sided curvature estimate of [22] (see in particular Corollary 3.1.9), there exist $c > 1$ and $1 > \epsilon > 0$ so that if Σ_1, Σ_2 are disjoint embedded disks in B_{cR} with $\partial\Sigma_i \subset \partial B_{cR}$ and $B_{\epsilon R} \cap \Sigma_i \neq \emptyset$, then for all components Σ_1' of $B_R \cap \Sigma_1$ that intersect $B_{\epsilon R}$, $\sup_{\Sigma_1'} |A|^2 \leq R^{-2}$. Thus, as long as $\frac{\epsilon}{2c}\delta_0 > \delta > 0$, because $\lim_{i\to\infty} \sup_{\Sigma_i \cap B_\delta(p_+)} |A|^2 \to \infty$, there is an $i_\delta' \geq i_\delta$ so for $i \geq i_\delta'$ there is only one component of $B_{c\delta/\epsilon}(p_+) \cap \Sigma_i$ that meets $B_\delta(p_+)$. As a consequence, for $\frac{\epsilon}{c}\delta_0 > \delta > 0$ and $i \geq i_\delta'$, there is a σ_i in $B_{c\delta/\epsilon}(p_+) \cap \Sigma_i$ that connects $q_i^\pm$ (see Figure 7-2).

Now, choose δ small enough so that $(\frac{c}{\epsilon}+1)\delta < \delta_0$. Then, for $i \geq i_\delta'$, $q_i^- \in B_{2\delta}(q_i^+) \subset B_{\frac{c}{\epsilon}\delta+\delta}(q_i^+)$, and thus the component Σ_i^δ of $B_{\frac{c}{\epsilon}\delta+\delta}(q_i^+) \cap \Sigma_i$ that contains q_i^+ is a disk and, by the above analysis, $q_i^- \in \Sigma_i^\delta$. Let $1 > \delta_1 > 0$ be given by the weak chord arc bounds (see Proposition 3.2.3) and decrease δ, if necessary, so $(\frac{c}{\epsilon}+1)\delta < \frac{1}{2}\delta_0\delta_1$. Then, the intrinsic ball of radius $2(\frac{c}{\epsilon}+1)\delta\delta_1^{-1}$ centered at q_i^+ is a disk, and hence the weak chord arc bounds imply that Σ_i^δ is a subset of the intrinsic ball of radius $(\frac{c}{\epsilon}+1)\delta\delta_1^{-1}$ centered at q_i^+. Thus, there exists a uniform constant $C = (\frac{c}{\epsilon}+1)\delta_1^{-1}$ so that $\text{dist}_{\Sigma_i}(q_i^+, q_i^-) < C\delta$ as long as $i > i_\delta'$. But for δ sufficiently small, this contradicts the uniform lower bound on the distance between q_i^+ and q_i^-, proving the lemma. □

Corollary 7.2.8. *Suppose* $0 \in \Sigma_i \in \mathcal{E}(e, g, R_i)$ *are such that* $\text{inj}_{\Sigma_i} \geq 1$, $\text{inj}_{\Sigma_i}(0) \leq \Delta_0$ *and* $R_i \to \infty$. *Then, a sub-sequence of the* Σ_i *converges uniformly in* C^∞ *on compact subsets of* $\mathbb{R}^3$ *and with multiplicity 1 to a non-simply connected surface* $\Sigma_\infty \in \mathcal{E}(e', g', \infty)$ *where* $e' \leq e + g, g' \leq g$.

Proof. By Lemma 7.2.7, the curvature of the Σ_i is uniformly bounded on any compact subset of $\mathbb{R}^3$. However, we do not, a priori, have uniform area bounds, and so some care must be taken in discussing convergence. In particular, the Arzela-Ascoli theorem and Schauder estimates, only imply that a sub-sequence of the Σ_i converge smoothly on compact subsets of $\mathbb{R}^3$ to some complete, embedded (by the maximum principle) minimal, smooth *lamination*, $\mathcal{L}_\infty$.

We first claim that $\mathcal{L}_\infty$ does not contain a plane and so is in fact a smooth minimal *surface* Σ_∞. Suppose $\mathcal{L}_\infty$ contained a plane P, and choose $R > \Delta_0$ so that $\partial B_R(0)$ meets each Σ_i transversely (such an R exists by Sard's theorem) and let Σ_i^0 be the component of $B_R(0) \cap \Sigma_i$ that contains 0. Notice that, as $\text{inj}_{\Sigma_i}(0) \leq \Delta_0$ and Σ_i has non-positive curvature, Σ_i^0 is not a disk and so $\chi(\Sigma_i^0) \leq 0$. The smooth convergence implies that for i sufficiently large there are domains $\Omega_i \subset P$ and smooth maps $u_i : \Omega_i \to \mathbb{R}$ so Σ_i^0 is the graph of u_i and the Σ_i^0 converge smoothly to Σ_i^∞, moreover the Ω_i exhaust $D_R = P \cap B_R$. Thus, we have that the area of Σ_i^0 is uniformly bounded as is its total curvature and the geodesic curvature of $\partial\Sigma_i^0$. Now by the Gauss-Bonnet theorem, $\int_{\Sigma_i^0} K + \int_{\partial\Sigma_i^0} k_g \leq 0$, whereas $\int_{D_R} K + \int_{\partial D_R} k_g = 2\pi$. However, the smooth convergence implies $\lim_{i\to\infty} \int_{\Sigma_i^0} K + \int_{\partial\Sigma_i^0} k_g = \int_{D_R} K + \int_{\partial D_R} k_g$, which is clearly impossible.

Thus, $\mathcal{L}_\infty$ does not contain a plane and hence no leaf of $\mathcal{L}$ is stable (by [56]). One may thus argue as in Appendix B of [12] to see that the Σ_i converge to some Σ_∞ with multiplicity 1. Roughly speaking, if the convergence was with a higher degree of multiplicity, one would be able to construct a positive Jacobi function on Σ_∞ which would force Σ_∞ to be stable (by [29]).

Let the Σ_i^0 continue to be as above. Then Σ_i^0 converges uniformly in C^∞ on compact sets and with multiplicity 1 to a surface Σ_∞^0 which is a component of $B_R(0) \cap \Sigma_\infty$. Notice that, by Proposition 7.2.1, Σ_i^0 has at most $e + g$ boundary components. If $\gamma_i = \partial\Sigma_i^0$ and $\gamma_\infty = \partial\Sigma_\infty^0$, then γ_i converge to γ_∞ smoothly and with multiplicity one. Then one immediately checks that $\lim_{i\to\infty} \int_{\Sigma_i^0} K = \int_{\Sigma_\infty^0} K$ and $\lim_{i\to\infty} \int_{\partial\Sigma_i^0} k_g = \int_{\partial\Sigma_\infty^0} k_g$ and so by the Gauss-Bonnet theorem Σ_∞^0 has non-positive Euler characteristic, i.e. is not a disk. Thus, the maximum principle implies that Σ_∞ is not simply connected. The convergence can only decrease the genus and increase number of ends by the indicated amount which gives the result. □

7.3 The Intrinsic and Extrinsic Normalization

We wish to apply Theorem 7.1.1 to sequences of surfaces in $\mathcal{E}(1, g, R_i)$. In particular, we hope to show that the resulting limit surfaces are in $\mathcal{E}(1, g', \infty)$ where $0 < g' \leq g$. The main tool we will use to restrict the topology of the limit surfaces is the no-mixing theorem of [12]. In order to apply the no-mixing theorem, we must first treat sequences that have stronger properties. Namely, we will first show that sequences which have both upper and lower bounds on the scale of the genus sub-sequentially converge to elements of $\mathcal{E}(1, g)$ and do so without loss of genus. When $g = 1$, such strong, two-sided, control follows when either the intrinsic or extrinsic normalization is imposed. Thus, for genus-one surfaces, Theorems 7.0.7 and 7.0.8 are immediate. When one does not have an upper bound on the outer scale of the genus. The no-mixing theorem implies that there is a scale, that is a fixed fraction of $r_+(\Sigma_i)$, on which each Σ_i still has connected boundary and has, as we are below $r_+(\Sigma_i)$, smaller genus then g. Thus, one can induct on the genus and obtain the result. Such an argument would prove both Theorems 7.0.7 and 7.0.8. However, the former is technically easier

to prove in this manner and with it a simple argument can be given to prove Theorem 7.0.8.

Let us first define the extrinsic scale of the genus precisely:

Definition 7.3.1. For $\Sigma \in \mathcal{E}(1, g, R)$ let

$$r_+(\Sigma) = \inf_{x \in B_R(0)} \inf \{r : B_r(x) \subset B_R(0) \text{ and } B_r(x) \cap \Sigma \text{ has a component of genus } g\}. \tag{7.2}$$

We call $r_+(\Sigma)$ the *outer extrinsic scale of the genus* of Σ. Furthermore, suppose for all $\epsilon > 0$, one of the components of $B_{r_+(\Sigma)+\epsilon}(x) \cap \Sigma$ has genus g; then we say the genus is *centered at* x.

Remark 7.3.2. Note that one trivially has that $r_+(\Sigma) < R$.

The outer scale of the genus measures how spread out all the handles are and the center of the genus should be thought of as a "center of mass" of the handles. We also need to measure the scale of individual handles and where, extrinsically, they are located. To that end define:

Definition 7.3.3. For $\Sigma \in \mathcal{E}(1, g, R)$ and $x \in B_R(0)$ Let

$$r_-(\Sigma, x) = \sup \{r : B_r(x) \subset B_R(0) \text{ and } B_r(x) \cap \Sigma \text{ has all components of genus zero}\} \tag{7.3}$$

If, for all r so $B_r(x) \subset B_R(0)$, every component of $B_r(x) \cap \Sigma$ is of genus zero set $r_-(\Sigma, x) = \infty$.

Definition 7.3.4. For $\Sigma \in \mathcal{E}(1, g, R)$ let

$$r_-(\Sigma) = \inf_{x \in B_R(0)} r_-(\Sigma, x). \tag{7.4}$$

We call $r_-(\Sigma)$ the *inner extrinsic scale of the genus* of Σ. Furthermore, suppose for all $\epsilon > 0$, one of the components of $B_{r_-(\Sigma)+\epsilon}(x) \cap \Sigma$ has positive genus; then we say that the genus is *concentrated at* x.

Remark 7.3.5. One easily checks that $r_+(\Sigma) \geq r_-(\Sigma)$ for $\Sigma \in \mathcal{E}(1, g, R)$, with equality holding if $g = 1$. When $g = 1$ we denote the common value by $r(\Sigma)$.

7.3.1 Two-sided bounds on the genus

We first need a simple topological lemma that is a localization of Lemma 6.4.1 and is proved using the maximum principle in an identical manner.

Lemma 7.3.6. *Let $\Sigma \in \mathcal{E}(1, g, R)$ and suppose the genus is centered at x. If $\bar{B}_r(y) \cap \bar{B}_{r_+(\Sigma)}(x) = \emptyset$ and $B_r(y) \subset B_R(0)$, then each component of $B_r(y) \cap \Sigma$ is a disk. Moreover, if $\bar{B}_{r_+(\Sigma)}(x) \subset B_r(y) \subset B_R(0)$, then one component of $B_r(y) \cap \Sigma$ has genus g and connected boundary and all other components are disks.*

We wish to use Theorem 7.1.1, but to do so we need to first check that a uniform extrinsic lower bound on the scale of the genus (i.e. on $r_-(\Sigma)$) gives a lower, intrinsic, bound on the injectivity radius. This is true, provided we have a uniform bound on $r_+(\Sigma)$, by the no-mixing theorem of [12]:

Lemma 7.3.7. *Fix $0 < \alpha \leq 1$ and $g \in \mathbb{Z}^+$. Then there exists $R_0 > 1$ and $1 > \delta_0 > 0$ depending only on α and g so: If $\Sigma \in \mathcal{E}(1, g, R)$ with $R \geq R_0$, $1 = r_-(\Sigma) \geq \alpha r_+(\Sigma)$, and the genus of Σ is centered at 0, then as long as $B_{\delta_0}(x) \subset B_R(0)$, every component of $B_{\delta_0}(x) \cap \Sigma$ is a disk.*

Proof. Suppose the lemma was not true. Then, one would have a sequence of surfaces $\Sigma_i \in \mathcal{E}(1, g, R_i)$ with $1 = r_-(\Sigma_i) \geq \alpha r_+(\Sigma_i)$, $R_i \to \infty$, and the genus of Σ_i centered at 0. Further, there would exist points x_i and a sequence $\delta_i \to 0$ so that one of the components of $B_{\delta_i}(x_i) \cap \Sigma_i$ was not a disk. Notice for fixed x and r, if $\bar{B}_r(x) \cap \bar{B}_{\alpha^{-1}}(0) = \emptyset$ with i large enough so $B_r(x) \subset B_{R_i}(0)$, then each component of $B_r(x) \cap \Sigma_i$ is a disk. Thus, we may assume $x_i \in B_{2\alpha^{-1}}(0)$. Because the injectivity radius of Σ_i at x_i goes to zero, we see that $\sup_{B_{2\alpha^{-1}}(0) \cap \Sigma_i} |A|^2 \to \infty$. Hence, by possible passing to a sub-sequence, the Σ_i convergence to a singular lamination $\mathcal{L}$.

Let us now determine $\mathcal{L}$ and see that this gives a contradiction. By possibly passing to a further sub-sequence, we may assume that $x_i \to x_\infty$. Pick i_0 large enough so that $|x_i - x_\infty| + \delta_i \leq 1/8$ for all $i \geq i_0$. Then for $i \geq i_0$, $B_{\delta_i}(x_i) \subset B_{1/2}(x_\infty)$ and thus $B_{1/2}(x_\infty) \cap \Sigma_i$ contains a non-disk component. As $r_-(\Sigma_i) > 1/2$, this component has genus zero. By the maximum principle the boundary of this component is not connected, and hence one checks that x_∞ is a point of $\mathcal{S}_{neck}$ of the lamination $\mathcal{L}$ (see Definition 3.2.5).

For any ball $B_r(x)$ with $\bar{B}_r(x) \cap \bar{B}_{\alpha^{-1}}(0) = \emptyset$ and i large enough so $B_r(x) \subset B_{R_i/2}(0)$, one has that all components of $B_r(x) \cap \Sigma_i$ are disks, and thus the maximum principle and the no-mixing theorem of [12] implies that the singular set $\mathcal{S}$ of $\mathcal{L}$ is contained in $B_{\alpha^{-1}}(0)$. As a consequence, one may rotate so that $\mathcal{L} \subset \{|x_3| \leq \alpha^{-1}\}$. Thus, for any $k \in \mathbb{N}$ there is an i_k so that for $i \geq i_k$, $B_k((0, 0, k + 2\alpha^{-1})) \cap \Sigma_i = \emptyset$ and $R_i > k^2$. Now set $\tilde{\Sigma}_k = \frac{1}{k}\Sigma_{i_k}$, so $\tilde{\Sigma}_k$ is a new sequence with the genus still centered at 0, $\partial\tilde{\Sigma}_k \cap B_k(0) = \emptyset$, $r_+(\tilde{\Sigma}_k) \leq \alpha^{-1}/k \to 0$, and $B_1((0, 0, 1 + 2\alpha^{-1}/k)) \cap \tilde{\Sigma}_l = \emptyset$ for $l \geq k$. Clearly the curvature in $B_{3\alpha^{-1}}(0)$ is still blowing up and so by possible passing to a sub-sequence we have convergence to a singular lamination $\tilde{\mathcal{L}}$. But $r_+(\tilde{\Sigma}_k) \to 0$ implies that $0 \in \mathcal{S}_{ulsc}$ while for $k > 3\alpha^{-1}$, $B_{1/4}((0, 0, 1)) \subset B_1((0, 0, 1 + 2\alpha^{-1}/k))$ and so for $k > 3\alpha^{-1}$, $B_{1/4}((0, 0, 1)) \cap \tilde{\Sigma}_k = \emptyset$ which contradicts the lamination result of [12] for ULSC sequences. □

We now show that the injectivity radius of Σ is uniformly bounded above by $\Delta_0 r_-(\Sigma)$, for $\Delta_0 > 0$ depending only on the ratio between the inner and outer extrinsic scales of the genus.

Lemma 7.3.8. *There exists R_0, Δ_0 with $R_0 \geq 5\Delta_0 > 10 > 0$, so: If $\Sigma \in \mathcal{E}(1, g, R)$, where $R > R_0$, and one of the components, Σ', of $\Sigma \cap B_{R/2}(0)$ satisfies $r_-(\Sigma', 0) \leq 1$ then the injectivity radius of some point of $\Sigma' \cap B_1(0)$ is bounded above by Δ_0.*

Proof. Pick $0 < \delta_1 \leq 1/2$ as in the weak chord-arc bounds of [24] (i.e. Proposition 3.2.3). We claim that we may choose $\Delta_0 = 2/\delta_1 \geq 3$ and $R_0 = 5\Delta_0$. To see this, suppose that Σ satisfies the hypotheses of the lemma, for some $R > R_0$ and Σ' was a component of $\Sigma \cap B_{R/2}$ so that $r_-(\Sigma', 0) \leq 1$, but the injectivity radius of each point of $\Sigma' \cap B_1$ is (strictly) bounded below by Δ_0.

Notice that, as $r_-(\Sigma', 0) \leq 1$, there is a point $x \in \Sigma' \cap B_1$ so that $\Sigma_{x,2}$ the component of $B_2(x) \cap \Sigma$ containing x has non-trivial genus. By assumption and choice of Δ_0, the intrinsic ball of radius Δ_0 in Σ centered at x is disjoint from the boundary and is topologically a disk. Then the weak chord-arc bounds of [24], i.e. Proposition 3.2.3, imply that the component of $B_2(x) \cap \Sigma$ containing x is contained in this disk, which by the maximum principle implies that this component is itself a disk. This contradiction proves the lemma. □

Corollary 7.3.9. *Fix $1 \geq \alpha > 0$ and let $\Sigma \in \mathcal{E}(1, g, R)$ and suppose that $1 = r_-(\Sigma) \geq \alpha r_+(\Sigma)$, $R \geq R_0\alpha^{-1}$, the genus is centered at 0, and R_0, Δ_0 are as above. Then there is a point $p_0 \in \Sigma \cap B_{\alpha^{-1}}$ with $\text{inj}_{\,\Sigma}(x_0) \leq \Delta_0\alpha^{-1}$.*

Proof. The center of the genus at 0 and $r_+(\Sigma) \leq \alpha^{-1}$ together imply that $r_-(\Sigma, 0) \leq \alpha^{-1}$. Thus, by rescaling, we may apply Lemma 7.3.8 to obtain a point $x_0 \in B_{\alpha^{-1}} \cap \Sigma$ so $\text{inj}_{\,\Sigma}(x_0) \leq \Delta_0\alpha^{-1}$. □

We may now prove a compactness result when we uniformly bound both the inner and outer scales of the genus.

Corollary 7.3.10. *Suppose $\Sigma_i \in \mathcal{E}(1, g, R_i)$ are such that $1 = r_-(\Sigma_i) \geq \alpha r_+(\Sigma_i)$, the genus of each Σ_i is centered at 0 and $R_i \to \infty$. Then a sub-sequence of the Σ_i converges uniformly in C^∞ on compact subsets of $\mathbb{R}^3$ and with multiplicity 1 to a surface $\Sigma_\infty \in \mathcal{E}(1, g, \infty)$ and $1 = r_-(\Sigma_\infty) \geq \alpha r_+(\Sigma_\infty)$.*

Proof. By Lemma 7.3.7, the injectivity radius of the Σ_i is uniformly bounded below by $\delta_0 > 0$. Moreover, by Corollary 7.3.9 there is a point p_i in the ball $B_{\alpha^{-1}}(0)$ so that $\text{inj}_{\,\Sigma_i}(p_i) \leq \Delta_0$. As a consequence, we may apply Theorem 7.1.1 and obtain a sub-sequence of the Σ_i that converges uniformly in C^∞ on compact subsets of $\mathbb{R}^3$ to some complete, embedded (by the maximum principle) non-simply connected minimal surface Σ_∞. Moreover, the convergence is with multiplicity one.

Choose $R > 2\alpha^{-1}$ so that $\partial B_R(0)$ meets each Σ_i transversely (such an R exists by Sard's theorem) and let Σ_i^0 be the component of $B_R(0) \cap \Sigma_i$ that contains the genus. Then, Σ_i^0 converges uniformly in C^∞ on compact sets and with multiplicity 1 to a surface Σ_∞^0 which is a component of $B_R(0) \cap \Sigma_\infty$. If $\gamma_i = \partial\Sigma_i^0$ and $\gamma_\infty = \partial\Sigma_\infty^0$, then γ_i converge to γ_∞ smoothly and with multiplicity one. Then, one immediately checks that $\lim_{i\to\infty} \int_{\Sigma_i^0} K = \int_{\Sigma_\infty^0} K$ and $\lim_{i\to\infty} \int_{\Sigma_i^0} k_g = \int_{\Sigma_\infty^0} k_g$ and so by the Gauss-Bonnet theorem Σ_∞^0 has genus g. On the other hand, any other components of $B_R(0) \cap \Sigma_i$ are necessarily disks and so one concludes by a similar argument that the same is true for any other component of $B_R(0) \cap \Sigma_\infty$. Similarly, for any ball disjoint from $B_R(0)$ every component of the intersection of the ball with Σ_i is a disk and hence the same is true for Σ_∞ and so $r_+(\Sigma_\infty) \leq \alpha^{-1}$. Finally, note that $\partial\Sigma_i^0$ is connected by

Lemma 7.3.6 and so the same is true of $\partial\Sigma_i^0$. As a consequence, we conclude that Σ_∞ is in $\mathcal{E}(1, g, \infty)$. Notice that the above argument gives $r_-(\Sigma_\infty) < R$ for a dense set of $R > 1$ and hence $r_-(\Sigma_\infty) \leq 1$. On the other hand as $B_{1-\delta}(x) \cap \Sigma_i$ contains only components of genus zero, this is also true of Σ_∞ and so $r_-(\Sigma_\infty) > 1 - \delta$. Letting $\delta \to 0$ gives the final conclusion. □

7.3.2 Intrinsic normalization

The weak-chord arc bounds of [24] imply that a uniform lower bound on the injectivity radius of Σ gives a uniform lower bound on the scale of the genus of Σ, i.e. on $r_-(\Sigma)$. Thus, to prove Theorem 7.0.7 we must understand what happens with the outer scale.

For genus-one surfaces, control on the inner scale of the genus automatically implies control on the outer scale (as they are equal), moreover, an easy argument relates this scale to the injectivity radius at 0. In particular, Theorem 7.0.7 follows immediately from Corollary 7.3.10 for genus-one surfaces. On the other hand, when the genus is ≥ 2, the possibility remains that the outer scale is unbounded and so Corollary 7.3.10 cannot be immediately applied. However, in this case, the lamination theory of Colding and Minicozzi [12] implies that by restricting to a scale that is a fixed fraction of the outer scale, there exists a connected component of the surface with connected boundary, smaller genus, and suitable control on the outer scale of the surface relative to the new scale of the genus. That is, one may induct on the genus. This is precisely how we will prove Theorem 7.0.7:

Theorem 7.3.11. *Suppose $\Sigma_i \in \mathcal{E}(1, g, R_i)$ ($g \geq 1$) with $0 \in \Sigma_i$, $\text{inj}_{\Sigma_i} \geq 1$, $\text{inj}_{\Sigma_i}(0) \leq \Delta_0$ and $R_i/r_+(\Sigma_i) \to \infty$. Then a sub-sequence of the Σ_i converges uniformly in C^∞ on compact subsets of $\mathbb{R}^3$ with multiplicity 1 to a surface $\Sigma_\infty \in \cup_{l=1}^g \mathcal{E}(1, l)$.*

Proof. First note that the lower bound on the injectivity radius and the weak chord-arc bounds of [24] (i.e. Proposition 3.2.3) imply that $r_+(\Sigma_i) \geq r_-(\Sigma_i) > \delta_0 > 0$. Thus, $R_i \to \infty$. If there is a sub-sequence of the Σ_i so $r_+(\Sigma_i) \leq C$, then Lemma 7.3.6 and the upper bound on the injectivity radius at 0 together imply that, x_i, the centers of the genus of the Σ_i, lie in the ball $B_{2C}(0)$. In this case, the theorem follows immediately from Corollary 7.3.10. Thus, we may assume that $\lim_{i\to\infty} r_+(\Sigma_i) = \infty$.

We will handle this by induction on the genus. When $g = 1$ we consider the sequence of rescalings of the Σ_i, $\tilde{\Sigma}_i = r(\Sigma)^{-1}\Sigma_i$. Notice that, $r(\tilde{\Sigma}_i) = 1$, but the injectivity radius at 0 of this sequence goes to zero. These two facts and Lemma 7.3.6 imply that the centers of the genus, $\tilde{x}_i$, lie in $B_2(0)$. Thus, Corollary 7.0.8 implies the sequence contains a convergent sub-sequence which contradicts the injectivity radius going to 0 at infinity. Thus, $r(\Sigma_i) \leq C$ is uniformly bounded which proves the theorem when $g = 1$.

For any $g > 1$, assume the theorem holds for all $1 \leq g' < g$. We claim this implies the result is also true for g, and hence the theorem is true by induction. To that end let $\lambda_i = r_+(\Sigma_i)$ and set $\tilde{\Sigma}_i = \lambda_i^{-1}\Sigma_i$. Then, the $\tilde{\Sigma}_i$ have injectivity radius at 0 going to 0 and $r_+(\tilde{\Sigma}_i) = 1$ and so, by Lemma 7.3.6, the centers of the genus, $\tilde{x}_i$, lie in $B_3(0)$. Because, $\text{inj}_{\tilde{\Sigma}_i}(0) \to 0$, the curvature of the sequence blows-up at 0. Thus, up to passing to a sub-sequence, $\tilde{\Sigma}_i$ converges to a lamination $\tilde{\mathcal{L}}$ with singular set $\mathcal{S}$.

The fact that the centers of the genus of $\tilde{\Sigma}_i$ are near 0, $r_+(\tilde{\Sigma}_i) = 1$ and the no-mixing theorem of [12] together imply that, up to passing to a further sub-sequence, $0 \in \mathcal{S}_{ulsc}$. For details on why this is so, see the proof Lemma 7.3.7.

Thus, by definition (see 3.2.4), there is a radius $0 < r < 1$ and radii $r_i \to 0$ so that $B_r(0) \cap \tilde{\Sigma}_i$ has the same genus, $\tilde{g}_i$, as $B_{r_i}(0) \cap \tilde{\Sigma}_i$ and the boundary of each component of $B_{r_i}(0) \cap \tilde{\Sigma}_i$ is connected. We claim that there exists $r' \leq r$ so that, after possibly passing to a sub-sequence, each component of $B_{r'}(y_\infty) \cap \tilde{\Sigma}_i$ also has connected boundary. Indeed, if this was not the case then one could find $\tilde{r}_i \in (r_i, r)$ with $\tilde{r}_i \to 0$ and some component of $B_{\tilde{r}_i}(y_\infty) \cap \tilde{\Sigma}_i$ having disconnected boundary. But notice the genus of $B_{\tilde{r}_i}(y_\infty) \cap \tilde{\Sigma}_i$ is equal to the genus of $B_r(y_\infty) \cap \tilde{\Sigma}_i$, but, by definition, this would imply $y_\infty \in \mathcal{S}_{neck}$, contradicting the no-mixing theorem.

The facts that $\text{inj}_{\tilde{\Sigma}_i}(0) \to 0$, $r_i \to 0$ and $r_+(\tilde{\Sigma}_i) = 1$ together imply $1 \leq \tilde{g}_i < g$. Let $\tilde{\Sigma}'_i$ be the component of $B_{r'}(0) \cap \tilde{\Sigma}_i$ that contains 0 and let $\Sigma'_i = \lambda_i \tilde{\Sigma}'_i$. Then $\Sigma'_i \in \mathcal{E}(1, g'_i, \lambda_i r')$, where $1 \leq g'_i \leq \tilde{g}_i < g$. Notice that, $r_+(\Sigma'_i) \leq r_i \lambda_i$ and so

$$\frac{\lambda_i r'}{r_+(\Sigma'_i)} \geq \frac{r'}{r_i} \to \infty. \tag{7.5}$$

In addition, by passing to sub-sequence, there is a g', so $1 \leq g' < g$ and $\Sigma'_i \in \mathcal{E}(1, g', \lambda_i r')$. Thus, Σ'_i satisfies the conditions of the inductive hypothesis and so contains a further sub-sequence that converges smoothly and with multiplicity one to a surface $\Sigma'_\infty \in \mathcal{E}(1, g'')$ where $1 \leq g'' \leq g'$. Notice that Σ'_∞ is properly embedded and the Σ'_i converge to Σ'_∞ with multiplicity 1. Moreover, there can be no complete properly embedded minimal surface in $\mathcal{R}^3 \backslash \Sigma_\infty$. Thus, for any fixed compact subset of $\mathbb{R}^3$, K, and for i sufficiently large, depending on K, $\Sigma_i \cap K = \Sigma'_i \cap K$, and so Σ_i converge to Σ'_∞, which proves the theorem. □

7.3.3 Extrinsic normalization

Having proved Theorem 7.0.7, we now use it to prove Theorem 7.0.8. In order to do so, we need to show that a uniform lower bound on the scale of the genus (i.e. on r_-) gives a lower bound on the injectivity radius. Recall, in Lemma 7.3.7 this was proved, using the no-mixing theorem, assuming also an upper bound on the scale of the genus. Theorem 7.0.7 allows us to remove this second condition. That is:

Lemma 7.3.12. *Fix $g \in \mathbb{Z}^+$, then there exists $\Omega = \Omega > 8$ and $\alpha_0 = \alpha_0 > 0$, depending on g, so: For $R > 1$ if $\Sigma \in \mathcal{E}(1, g, R)$, $r_-(\Sigma) = 1$ and $R \geq \Omega r_+(\Sigma)$ then for all $p \in B_{R/2} \cap \Sigma$, $\text{inj}_\Sigma(p) \geq \alpha_0$.*

Proof. Suppose the lemma was not true and that one had a sequence of $\Omega_i \to \infty$ and $\Sigma_i \in \mathcal{E}(1, g, R_i)$ so that $r_-(\Sigma)_i = 1$ and $R_i \geq \Omega_i r_+(\Sigma)$, but $\min_{\bar{B}_{R_i/2} \cap \Sigma_i} \text{inj}_{\Sigma_i} \to 0$ (recall, $\text{inj}_\Sigma(p)$ is a continuous function in p). Notice that, as $r_+(\Sigma) \geq 1$, $R_i \to \infty$. Let p_i be a point of $\Sigma_i \cap B_{R_i/2}$ so $\lambda_i = \text{inj}_{\Sigma_i}(p_i) = \min_{\bar{B}_{R_i/2} \cap \Sigma_i} \text{inj}_{\Sigma_i}$. Proposition 7.3.6, implies that $|p_i| \leq 2r_+(\Sigma_i) \leq 2\frac{R_i}{\Omega_i}$. Notice that $B_{R_i/4}(p_i) \subset B_{R_i/2}(0)$, because $\Omega_i > 8$. Also, by assumption $r_-(\Sigma_i, p_i) \geq 1$.

Now let $\Sigma_i' = \lambda_i^{-1}((\Sigma_i)_{p_i,R_i/4} - p_i)$ (recall, $\Sigma_{x,R}$ is the component of $B_R(x) \cap \Sigma$ containing x). By Proposition 7.3.6, $\Sigma_i' \in \mathcal{E}(1, g_i', \lambda_i^{-1}R_i/4)$ where $1 \leq g_i' \leq g$ and $\Omega_i r_+(\Sigma_i') \leq {\lambda_i}^{-1}R_i$. Moreover, the injectivity radius of Σ_i' is uniformly bounded below by 1 and $\text{inj}_{\Sigma_i'}(0) = 1$. Thus, we may apply Theorem 7.0.7 to see that a sub-sequence of the Σ_i' converge to an element $\Sigma_\infty' \in \mathcal{E}(1, g')$ where $1 \leq g' \leq g$. Notice that $g' \geq 1$ and so $r_-(\Sigma_\infty', 0) = C < \infty$. But this implies that $r_-(\Sigma_i', 0) \leq 2C$ for sufficiently large i. But this, in turn, implies that $r_-(\Sigma_i, 0) \leq 2C\lambda_i < 1$, for large enough i, which is a contradiction and proves the lemma. □

We can now easily prove Theorem 7.0.8:

Theorem 7.3.13. *Suppose $\Sigma_i \in \mathcal{E}(1, g, R_i)$ ($g \geq 1$) with $r_-(\Sigma_i) = 1$, $r_-(\Sigma_i, 0) \leq C$, and $R_i/r_+(\Sigma_i) \to \infty$. Then, a sub-sequence of the Σ_i converges uniformly in C^∞ on compact subsets of $\mathbb{R}^3$ with multiplicity 1 to a surface $\Sigma_\infty \in \cup_{l=1}^{g}\mathcal{E}(1, l, \infty)$ with $r_-(\Sigma_\infty) \leq C$.*

Proof. By replacing Σ_i by the component of $\Sigma_i \cap B_{R_i/\Omega}$ that contains the genus, Lemma 7.3.12 tells us that the injectivity radius of Σ_i is uniformly bounded below by $\alpha_0 > 0$. On the other hand, because $r_-(\Sigma_i, 0) \leq C$, a rescaling of Lemma 7.3.8 implies that $\text{inj}_{\Sigma_i}(p_i) \leq \Delta_0 C$, for some $p_i \in B_1 \cap \Sigma_i$, as long as i is sufficiently large. Thus, the Σ_i satisfy the conditions of Theorem 7.0.7 which allows us extract a convergent sub-sequence. □

7.4 Applications

The compactness results developed in the previous section are particularly strong for sequences of genus-one surfaces, as there is no "loss" of genus. In particular, they proved more information about the geometric structure of elements of $\mathcal{E}(1, 1, R)$. We present two such results in this section.

7.4.1 Compactness of $\mathcal{E}(1, 1)$

Throughout this section, we consider only complete surfaces. Recall, in Chapter 6, we showed that any $\Sigma \in \mathcal{E}(1)$ is conformally a once punctured compact Riemann surface and, if it is not a plane, is asymptotic (in a Hausdorff sense) to some helicoid. When the genus is positive there are at least two interesting scales, the scale of the asymptotic helicoid and the scale of the genus. In principle, one might expect a relationship between these two scales. This is the case for genus one, however, due to the possibility that one may "lose" genus, as noted in Theorem 7.0.8, we cannot (as yet) establish such a connection for genus 2 or greater.

Let us now focus on the space $\mathcal{E}(1, 1)$, i.e. genus-one helicoids. We show that, for any $\Sigma \in \mathcal{E}(1, 1)$, there is an upper and lower bound on the ratio between the scale of the genus and the scale of the asymptotic helicoid. As a consequence, we deduce that any sequence of elements of $\mathcal{E}(1, 1)$ that are asymptotic to the same helicoid H has a sub-sequence that converges smoothly on compact subsets to an element of $\mathcal{E}(1, 1)$ that is also asymptotic to H (or to H itself).

Theorem 7.4.1. *Let $\Sigma_i \in \mathcal{E}(1,1)$ and suppose that all the Σ_i are asymptotic to H, a fixed helicoid. Then, a sub-sequence of the Σ_i converge uniformly in C^∞ on compact subsets of $\mathbb{R}^3$ to $\Sigma_\infty \in \mathcal{E}(1,1) \cup \{H\}$ with Σ_∞ asymptotic to (or equaling) H.*

Remark 7.4.2. Translations along the axis show H may occur as a limit.

The theorem will follow from evaluating certain path integrals of holomorphic Weierstrass data. To that end, we first establish a uniform R such that all vertical normals of each Σ_i (after a rotation) occur in $B_R(0)$. We then find annular ends Γ_i, conformally mapped to the same domain in $\mathbb{C}$ by $z_i = (x_3)_i + \sqrt{-1}(x_3^*)_i$ and with Weierstrass data as described Corollary 6.0.8. Finally, we use calculus of residues on $\partial\Gamma_i$ to establish uniform control on the center and radius of the genus for a sub-sequence of Σ_i.

Note that Theorem 6.1.1 implies that for $\Sigma \in \mathcal{E}(1,1)$, there are two points where the Gauss map points parallel to the axis of the asymptotic helicoid. As mentioned, we first need to gain uniform control on the position of these points.

Lemma 7.4.3. *Suppose $\Sigma \in \mathcal{E}(1,1)$, the genus of Σ is centered at 0, $r(\Sigma) = 1$, and that g, the usual stereographic projection of the Gauss map of Σ, has only a single pole and single zero. Then there is an $R \geq 1$ independent of Σ so that the pole and zero of g lie in $B_R(0) \cap \Sigma$.*

Remark 7.4.4. Theorem 6.1.1 implies that, after translating, rescaling and rotating any $\Sigma \in \mathcal{E}(1,1)$ appropriately, the conditions of the lemma apply.

Proof. Suppose this was not the case. That is, one has a sequence $\Sigma_i \in \mathcal{E}(1,1)$ so that the genus of each Σ_i is centered at 0, $r(\Sigma_i) = 1$, and each g_i has a single pole and single zero, at least one of which does not lie in $B_i(0)$. By rotating Σ_i, we may assume the pole does not lie in $B_i(0)$. By Corollary 7.0.8 a sub-sequence of the Σ_i converge uniformly in C^∞ on compact subsets of $\mathbb{R}^3$, with multiplicity 1, to $\Sigma_\infty \in \mathcal{E}(1,1)$ where $r(\Sigma_\infty) = 1$.

We note that Theorem 6.1.1 implies, by our normalization of the Σ_i, that for $i < \infty$, $\frac{dg_i}{g_i}$ is meromorphic with a double pole at ∞. Moreover, g_∞ has at least one zero. We claim it has only one zero and one pole and consequently, $\frac{dg_\infty}{g_\infty}$ is meromorphic with a double pole at ∞.

Suppose g_∞ has more than one zero and call two such zeros $q_1, q_2 \in \Sigma_\infty$. Denote by σ_∞^j a closed, embedded curve in the component of $B_{\delta_0/2}(q_j) \cap \Sigma_\infty$ that contains q_j, chosen so that σ_∞^j surrounds q_j but neither surrounds nor contains any other pole or zero of g_∞. Additionally, we choose the two σ_∞^j to be disjoint. Thus, $\int_{\sigma_\infty^j} \frac{dg_\infty}{g_\infty} = 2\pi\sqrt{-1}$.

By the convergence, there are smooth, embedded, closed curves σ_i^j $(j = 1, 2)$ in Σ_i so that σ_i^j converges smoothly to σ_∞^j. Let $D_i^j \subset \Sigma_i$ denote a disk such that $\partial D_i^j = \sigma_i^j$. For large enough i, $D_i^1 \cap D_i^2 = \emptyset$. Because there is at most one zero of g_i in Σ_i, for each i either $\int_{\sigma_i^1} \frac{dg_i}{g_i} = 0$ or the same is true for σ_i^2 (for i sufficiently large there can be no pole by assumption, though the claim still follows without this hypothesis). Letting i go to ∞ gives a contradiction; so g_∞ has only one zero. Similarly, g_∞ has only one pole.

To conclude the proof, note there exists some R_1 such that the pole, p_∞, of g_∞ is in $B_{R_1} \cap \Sigma_\infty$. Let $\sigma_\infty \subset \Sigma_\infty$ be a smooth, embedded, closed curve in $B_{\delta_0/2}(p_\infty)$ that surrounds p_∞ and neither contains nor surrounds the zero of g_∞. Thus, $\int_{\sigma_\infty} \frac{dg_\infty}{g_\infty} = -2\pi\sqrt{-1}$. Then by our convergence result, there are smooth, embedded, closed curves $\sigma_i \subset \Sigma_i \cap B_{3\delta_0/4}(p_\infty)$, with σ_i converging to σ_∞. Note σ_i is necessarily null-homotopic and by perturbing, if necessary, we may assume g_i has no zero on σ_i. For i large enough so $\sigma_\infty \subset B_{i/2}(0)$ we compute $\frac{1}{2\pi\sqrt{-1}} \int_{\sigma_i} \frac{dg_i}{g_i} \geq 0$ (as σ_i may contain the zero of g_i). Letting i go to infinity and using the smooth convergence, one obtains a contradiction. □

Before proving the main compactness result, Theorem 7.0.6, we establish the necessary uniform control on the center and radius of the genus for surfaces in $\mathcal{E}(1,1)$ that are asymptotic to a fixed helicoid H. Throughout the following proof, we make repeated use of results from Section 6.3.

Lemma 7.4.5. *Let $\Sigma_i \in \mathcal{E}(1,1)$ and suppose that all the Σ_i are asymptotic to the same helicoid, H, which has axis the x_3-axis. Then, there exist $C_1, C_2 > 0$ and a sub-sequence (also called Σ_i) such that $1/C_1 \leq r(\Sigma_i) \leq C_1$ and, after a rotation, $|x_1(p_i)| + |x_2(p_i)| \leq C_2$, where p_i is the center of the genus of each Σ_i.*

Proof. Translate each Σ_i by $-p_i$ so that the genus of each of the Σ_i is centered at 0. Then rescale each Σ_i by α_i so that after the rescaling $r(\Sigma_i) = 1$. Thus, each rescaled and translated surface Σ_i is asymptotic to the helicoid $H_i = \alpha_i(H - p_i)$.

By Corollary 7.0.8, passing to a sub-sequence, Σ_i converges uniformly on compact sets to some Σ_∞ with multiplicity one. By Corollary 6.0.9 we know that Σ_∞ is asymptotic to some helicoid H'. Now since each Σ_i is asymptotic to H_i, which has an axis parallel to H, after possible rotating so H is a vertical helicoid, the stereographic projection g_i of the Gauss map of Σ_i has exactly one pole and one zero. Thus, as in the proof of Lemma 7.4.3, we can conclude the same for Σ_∞.

Now pick R big enough so that both the zero and pole of g_∞ lie on the component of $B_R(0) \cap \Sigma_\infty$ containing the genus and so $\partial B_{2R}(0)$ meets each Σ_i, $1 \leq i \leq \infty$, transversely. By our convergence result and Lemma 7.4.3 (and in particular arguments as in the proof of that lemma), there exists an i_0 such that, for $i_0 \leq i \leq \infty$, the zero and pole of g_i lie in the component Σ_i^0 of $B_{2R}(0) \cap \Sigma_i$ containing the genus. Thus, for $i_0 \leq i \leq \infty$, $\Gamma_i = \Sigma_i \backslash \bar{\Sigma}_i^0$ is topologically an annulus and moreover g_i has no poles or zeros in Γ_i. Hence, by the arguments of Section 6.3, $z_i = (x_3)_i + \sqrt{-1}(x_3)_i^* : \Gamma_i \to \mathbb{C}$ and $f_i = \log g_i : \Gamma_i \to \mathbb{C}$ are well-defined. (Here $(x_3)_i$ is x_3 restricted to Σ_i and $(x_3)_i^*$ is the harmonic conjugate of $(x_3)_i$.) Note that, by Chapter 6, $f_i(p) = \sqrt{-1}\lambda_i z_i(p) + F_i(p)$ where λ_i determines the scale of the helicoid H_i and $F_i(p)$ is holomorphic on Γ_i and indeed extends holomorphically to ∞ with a 0 there.

By suitably translating $(x_3)_i^*$, $z_\infty(\Gamma_\infty) \supset \left\{z \in \mathbb{C} : |z| > \frac{1}{2}C\right\}$ for some $C > 0$, and hence by increasing i_0, if needed, for $i_0 \leq i \leq \infty$,

$$z_i(\Gamma_i) \supset \{z \in \mathbb{C} : |z| > C\} = A_C. \tag{7.6}$$

By precomposing with z_i^{-1}, we may think of f_i as a holomorphic function on A_C. If

u is the standard coordinate of $\mathbb{C}$ restricted to A_C, then for $i_0 \leq i \leq \infty$, $f_i(u) = \sqrt{-1}\lambda_i u + F_i(u)$ where F_i is a holomorphic function which extends holomorphically (and with a zero) to ∞.

Clearly, there is an $R' > 2R$ so that $\{p \in \Gamma_\infty : |z_\infty(p)| \leq 2C\} \subset B_{R'}(0)$ thus by the convergence (and increasing i_0) for $i_0 \leq i \leq \infty$, $\{p \in \Gamma_i : |z_i(p)| \leq 2C\} \subset B_{2R'}(0)$. As a consequence, the uniform convergence of Σ_i to Σ_∞ implies that for $\gamma = \left\{u : |u| = \frac{3}{2}C\right\} \subset A_C$, $f_i \to f_\infty$ in $C^\infty(\gamma)$. On the other hand, the calculus of residues implies that for $i_0 \leq i \leq \infty$,

$$\int_\gamma f_i(u)\frac{du}{u^2} = -2\pi\lambda_i \tag{7.7}$$

and hence we see immediately that $\lambda_i \to \lambda_\infty > 0$. Since the initial helicoid H had some λ_H associated with its Weierstrass data, this gives an upper and lower bound on the rescaling of each initial Σ_i, thus producing the necessary C_1.

Since each F_i is holomorphic on A_C with a holomorphic extension to ∞ (and a zero there), we can expand in a Laurent series, i.e. for every $u \in A_C$ one has

$$F_i(u) = \sum_{j=1}^{\infty} \frac{a_{i,j}}{u^j} \tag{7.8}$$

where this is a convergent sum. Thus, for $i_0 \leq i \leq \infty$

$$\int_\gamma f_i(u)u^{j-1}du = 2\pi\sqrt{-1}a_{i,j} \tag{7.9}$$

and hence $\lim_{i\to\infty} a_{i,j} = a_{\infty,j}$. It follows that $F_i \to F_\infty$ in $C^\infty(\bar{A}_{2C})$, where $\bar{A}_{2C} = \{u : 2C \leq |u| \leq \infty\}$.

We now show the Weierstrass representation then implies that H_i converge to H_∞ and hence that $x_1(p_i) \to x_1(p_\infty)$ and $x_2(p_i) \to x_2(p_\infty)$. This will produce the necessary bound, C_2, on the distance between the center of the genus and the axis of the initial helicoid H. To see this, note that the convergence $F_i \to F_\infty$ implies there is a uniform C_0 so that for $u > 2C$ and $i_0 \leq i \leq \infty$, one can write $F_i(u) = \frac{a_{i,1}}{u} + \tilde{F}_i(u)$, where $|\tilde{F}_i(u)| \leq \frac{C_0}{u^2}$ and $|a_{i,1}| \leq C_0$. Recall the Weierstrass representation gives that

$$dx_1 - \sqrt{-1}dx_2 = g^{-1}dh - \bar{g}d\bar{h}, \tag{7.10}$$

where $dh = dx_3 + \sqrt{-1}dx_3^*$ is the height differential. Integrating this form along $\left\{t + (\sqrt{-1})0 : t \in [3C, t_1]\right\} \subset A_C$, we see

$$((x_1)_i(t_1) - (x_1)_i(3C)) - \sqrt{-1}((x_2)_i(t_1) - (x_2)_i(3C)) = \int_{3C}^{t_1} H_i(t)dt \tag{7.11}$$

where $H_i(t) = e^{-\sqrt{-1}(\lambda_i t + \operatorname{Im} F_i(t))}(e^{-\operatorname{Re} F_i(t)} - e^{\operatorname{Re} F_i(t)})$. For C sufficiently large, $|F_i(t)| \leq$

1/2 and so expanding in a power series,

$$H_i(t) = -2e^{-\sqrt{-1}\lambda_i t}\frac{\operatorname{Re} a_{i,1}}{t} + G_i(t) \tag{7.12}$$

where here $|G_i(t)| \leq \frac{10C_0}{t^2}$.

The first term is a convergent (as $t_1 \to \infty$) oscillating integral while the integral of $G_i(t)$ is absolutely convergent. Thus, there exists a C_2 depending only on C_0 (and in particular independent of t_1, i) so, for $i_0 \leq i \leq \infty$, on each Σ_i,

$$|(x_1)_i(t_1) - (x_1)_i(3C)| + |(x_2)_i(t_1) - (x_2)_i(3C)| \leq C_2. \tag{7.13}$$

Recall the translated surfaces Σ_i have genus centered at zero. Since one finds the axis by letting $t_1 \to \infty$, the above bound shows each translated surface has axis a uniform distance from the origin. Thus, the original center for each genus, p_i, satisfies the desired uniform bound. □

The previous lemma tells us that for any sequence of surfaces in $\mathcal{E}(1,1)$, asymptotic to a fixed helicoid, there is a sub-sequence with the scale of the genus uniformly controlled and the center of the genus lying inside of a cylinder. With this information, we can now show Theorem 7.0.6.

Proof. By the previous lemma, we know that there exists an $R > 0$ and a sub-sequence Σ_i such that $r(\Sigma_i) \to r_\infty > 0$ and the genus of these Σ_i is centered in a cylinder of radius R. With this sort of uniform control on the genus, one can apply Theorem 7.0.8 to show that either the center of the genus goes to ∞, or $\Sigma_i \to \Sigma_\infty \in \mathcal{E}(1,1)$, which is asymptotic to some helicoid. If the center goes to ∞, the above lemma shows that it must do so inside of a cylinder around the axis, and hence $\Sigma_i \to H$.

By the same techniques of the previous lemma, if the genus does not go to ∞ then, given that $f_i = \sqrt{-1}\lambda_H u + F_i(u)$, we see that $f_\infty = \sqrt{-1}\lambda_H u + F_\infty(u)$. Thus, in this case, Σ_∞ is in fact asymptotic to the original helicoid H. □

7.4.2 Geometric Structure of $\mathcal{E}(1,1,R)$

An immediate local result of Theorem 7.0.6 is the following theorem. It should be compared with the structural results of Chapter 5.

Theorem 7.4.6. *Given $\epsilon > 0$ and $R \geq 1$ there exists an $R' = R'(\epsilon, R) \geq R$ so that: if $\Sigma \in \mathcal{E}(1,1,R')$ with $r(\Sigma) = 1$ and the genus of Σ is centered at 0, then the component of $B_R(0) \cap \Sigma$ containing the genus is bi-Lipschitz with a subset of an element of $\mathcal{E}(1,1)$ and the Lipschitz constant is in $(1-\epsilon, 1+\epsilon)$.*

Proof. We proceed by contradiction and assume no such R' exists. Thus, we obtain a sequence of $\Sigma_i \in \mathcal{E}(1,1,R_i)$ with $R_i \to \infty$, $r(\Sigma_i) = 1$, and the genus of each Σ_i centered at 0 but Σ_i^0, the component of $B_R(0) \cap \Sigma_i$ containing the genus, is not bi-Lipschitz with a subset of any element of $\mathcal{E}(1,1)$. By Corollary 7.0.8, a sub-sequence of the Σ_i converges uniformly in C^∞ on compact subsets of $\mathbb{R}^3$ to $\Sigma_\infty \in \mathcal{E}(1,1)$,

with $r(\Sigma_\infty) = 1$, with multiplicity 1. In particular, Σ_i^0, the component of $\Sigma_i \cap B_R(0)$ containing the genus, converges to Σ_∞^0, similarly defined. Find C so that $\max |A_{\Sigma_\infty^0}| \leq C$.

Choose R' large enough to ensure minimizing geodesics between points in Σ_∞^0 lie in $\Sigma_\infty \cap B_{R'/2}$ (using the properness result of [24]). By the smooth convergence on compact sets, there exists i_0 large such that for all $i \geq i_0$, minimizing geodesics between points in Σ_i^0 lie in $\Sigma_i \cap B_{R'}$. For any ϵ, and increasing i if necessary, we find a smooth ν_i defined on a subset of Σ_∞ so that $C|\nu_i| + |\nabla_{\Sigma_\infty} \nu_i| < \epsilon$ and the graph of ν_i is the component of $\Sigma_i \cap B_{R'}$ containing the genus. Then Lemma 5.1.2 gives the desired contradiction. $\square$

Chapter 8

Conclusion

We have completely understood the conformal and geometric asymptotics of the ends of elements of $\mathcal{E}(1)$. In particular, we have classified the conformal type of surfaces in $\mathcal{E}(1)$ and completely classified the surfaces in $\mathcal{E}(1,0)$. Nevertheless, many interesting questions remain open. One important task is to verify, for $g > 1$, that the space $\mathcal{E}(1,g)$ is actually non-trivial. That is, to rigorously prove the existence of genus-two (and higher) helicoids. Computer graphics suggest that there is an embedded genus-two helicoid but at present there is no rigorous proof. It is possible that the compactness theory developed in Chapter 7 might provide some insight in this direction. Another important question regards the finer geometric structure of elements of $\mathcal{E}(1)$. The most ambitious conjecture in this direction is the following due to Weber, Hoffman and Wolf (for genus one) [61] and Meeks and Rosenberg (for higher genus):

Conjecture 8.0.7. *For each $g \geq 1$ there exists a unique (after normalizing) element of $\mathcal{E}(1,g)$*

This result seems a bit optimistic and there is not much intuition as to why such a strong result should be true. A less ambitious conjecture is:

Conjecture 8.0.8. *For each $g \geq 1$ there are at most a finite number (after normalizing) of elements of $\mathcal{E}(1,g)$*

The Weierstrass representation, Theorem 6.1.1 and the compactness theory of Chapter 7 provide some evidence that this conjecture is at least reasonable. Namely, Theorem 6.1.1 and standard facts about meromorphic one-forms on compact surfaces imply that $\frac{dg}{g}$ and dh are elements in a finite-dimensional vector space (with dimension bounded in terms of the genus). In other words, they are determined up to a finite number of parameters. On the other hand, for the Weierstrass representation to be well-defined, g and dh must satisfy a certain number (depending also on the genus) of (non-linear) constraints (i.e. the period conditions, see (2.3)). In [7], Bobenko discusses the construction of immersed genus-g helicoids (see Remark 8.0.10) and notes that in general this is an over-determined problem. In other words, there are more non-linear equations coming from the period conditions than there are parameters. This leads one to believe that the set of such helicoids is, at best, discrete. For $\mathcal{E}(1,1)$

this immediately implies by 7.0.6 that one has a finite number of them, whereas for higher genus one would need a suitable compactness theory.

There are some weaker results that would still be interesting. In [7], Bobenko also notes that if the underlying once-punctured Riemann surface admits a conformal involution compatible with the Weierstrass data, then the situation is markedly simpler. Indeed, the number of unknown parameters and number of constraints coming from the period conditions are not only reduced (which one expects) but actually become equal. Thus, the problem becomes (at least in principle) well-posed. As the involution induces (due to the compatibility condition and Weierstrass representation) a symmetry on the surface (rotation around a coordinate axis by 180°), this leads him to the following conjecture:

Conjecture 8.0.9. *(Bobenko) Let Σ be an immersed genus-g helicoid, then Σ is symmetric with respect to a* 180° *rotation around one of the coordinate axes.*

Remark 8.0.10. Here an immersed genus-g helicoid is a minimally immersed once punctured compact Riemann surface whose Weierstrass data at the puncture satisfies the same conditions as in Theorem 6.1.1.

One would like to prove this for $\mathcal{E}(1)$ (i.e. embedded genus g helicoids) as it would provide a major restriction on the possible conformal structures of elements of genus greater than 1.

Bibliography

[1] J. Bernstein and C. Breiner. Compactness properties of the space of genus-g helicoids. *In preparation.*

[2] J. Bernstein and C. Breiner. Conformal structure of minimal surfaces with finite topology. *To Appear Commentarii Mathematici Helvetici.* `http://arxiv.org/abs/0810.4478`.

[3] J. Bernstein and C. Breiner. Helicoid-like minimal disks and uniqueness. *Preprint.* `http://arxiv.org/abs/0802.1497`.

[4] J. Bernstein and C. Breiner. Distortions of the helicoid. *Geometriae Dedicata*, 137(1):143–147, 2008.

[5] S. Bernstein. Über ein geometrisches Theorem und seine Anwendung auf die partiellen Differentialgleichungen vom ellipschen Typos. *Math. Zeit.*, 26:551–558, 1927.

[6] L. Bers. Isolated singularities of minimal surfaces. *Ann. of Math. (2)*, 53:364–386, 1951.

[7] A. I. Bobenko. Helicoids with handles and Baker-Akhiezer spinors. *Math. Zeit.*, 229(1):9–29, 1998.

[8] E. Calabi. *Proceedings of the United States-Japan Seminar in Differential Geometry*, chapter Problems in differential geometry. Nippon Hyoronsha Co., 1965.

[9] M. Calle and D. Lee. Non-proper helicoid-like limits of closed minimal surfaces in 3-manifolds. *Mathematische Zeitschrift*, pages 1–12.

[10] M. Do Carmo. *Riemannian Geometry.* Birkhäuser, 1992.

[11] H. I. Choi and R. Schoen. The space of minimal embeddings of a surface into a three-dimensional manifold of positive Ricci curvature. *Inventiones Mathematicae*, 81(3):387–394, 1985.

[12] T. H. Colding and W. P. Minicozzi II. The Space of Embedded Minimal Surfaces of Fixed Genus in a 3-manifold V; Fixed Genus. *Preprint.* `http://arxiv.org/abs/math/0509647`.

[13] T. H. Colding and W. P. Minicozzi II. *Minimal Surfaces, Courant Lecture Notes in Math., 4*. New York University, Courant Institute of Math. Sciences, New York, 1999.

[14] T. H. Colding and W. P. Minicozzi II. Minimal annuli with and without slits. *Jour. of Symplectic Geometry*, 1(1):47–62, 2002.

[15] T. H. Colding and W. P. Minicozzi II. Multivalued minimal graphs and properness of disks. *Int. Math. Res. Not.*, (21):1111–1127, 2002.

[16] T. H. Colding and W. P. Minicozzi II. On the structure of embedded minimal annuli. *International Mathematics Research Notices*, 2002(29):1539, 2002.

[17] T. H. Colding and W. P. Minicozzi II. Embedded minimal disks: Proper versus nonproper - global versus local. *Trans. of the AMS*, 356:283–289, 2004.

[18] T. H. Colding and W. P. Minicozzi II. An excursion into geometric analysis. *Surv. in Diff. Geom.*, IX:83–146, 2004.

[19] T. H. Colding and W. P. Minicozzi II. The space of embedded minimal surfaces of fixed genus in a 3-manifold I; Estimates off the axis for disks. *Ann. of Math. (2)*, 160(1):27–68, 2004.

[20] T. H. Colding and W. P. Minicozzi II. The space of embedded minimal surfaces of fixed genus in a 3-manifold II; Multi-valued graphs in disks. *Ann. of Math. (2)*, 160(1):69–92, 2004.

[21] T. H. Colding and W. P. Minicozzi II. The space of embedded minimal surfaces of fixed genus in a 3-manifold III; Planar domains. *Ann. of Math. (2)*, 160(2):523–572, 2004.

[22] T. H. Colding and W. P. Minicozzi II. The space of embedded minimal surfaces of fixed genus in a 3-manifold IV; Locally simply connected. *Ann. of Math. (2)*, 160(2):573–615, 2004.

[23] T. H. Colding and W. P. Minicozzi II. Shapes of embedded minimal surfaces. *PNAS*, 103(30):11106–11111, 2006.

[24] T. H. Colding and W. P. Minicozzi II. The Calabi-Yau conjectures for embedded surfaces. *Ann. of Math.*, 167(1):211–243, 2008.

[25] P. Collin. Topologie et courboure des surfaces minimales proprement plongees de $\mathbb{R}^3$. *Ann. of Math.*, 145:1–31, 1997.

[26] P. Collin, R. Kusner, W. H. Meeks III, and H. Rosenberg. The topology, geometry and conformal structure of properly embedded minimal surfaces. *J. Differential Geom.*, 67(2):377–393, 2004.

[27] C. Costa. Example of a complete minimal immersion in $\mathbb{R}^3$ with three embedded ends. *Bol. Soc. Bra. Mat.*, 15:47–54, 1984.

[28] B. Dean. Embedded minimal disks with prescribed curvature blowup. *Proceedings of the American Mathematical Society*, 134(4):1197–1204, 2006.

[29] D. Fischer-Colbrie and R. Schoen. The structure of complete stable minimal surfaces in 3-manifolds of nonnegative scalar curvature. *Comm. Pure Appl. Math.*, 33:199–211, 1980.

[30] D. Gilbarg and N. S. Trudinger. *Elliptic Partial Differential Equations of Second Order*. Springer-Verlag, 1998.

[31] L. Hauswirth, J. Perez, and P. Romon. Embedded minimal ends of finite type. *Trans. AMS*, 353(4):1335–1370, 2001.

[32] D. Hoffman and W. H. Meeks III. A complete embedded minimal surface in $\mathbb{R}^3$ with genus one and three ends. *J. Differential Geom.*, 21(1):109–127, 1985.

[33] D. Hoffman and W. H. Meeks III. The asymptotic behavior of properly embedded minimal surfaces of finite topology. *J. Amer. Math. Soc.*, 2(4):667–682, 1989.

[34] D. Hoffman and W. H. Meeks III. Embedded minimal surfaces of finite topology. *Annals of Mathematics*, pages 1–34, 1990.

[35] D. Hoffman and W. H. Meeks III. The strong halfspace theorem for minimal surfaces. *Inventiones Mathematicae*, 101(1):373–377, 1990.

[36] D. Hoffman, H. Karcher, and F. Wei. *Global Analysis in Modern Mathematics*, chapter The Genus One Helicoid and the Minimal Surfaces that Led to its Discovery. Publish or Perish, 1993.

[37] D. Hoffman and J. McCuan. Embedded minimal ends asymptotic to the Helicoid. *Communications in Analysis and Geometry*, 11(4):721–736, 2003.

[38] D. Hoffman and F. Wei. Deforming the singly periodic genus-one helicoid. *Experimental Mathematics*, 11(2):207–218, 2002.

[39] D. Hoffman and B. White. The geometry of genus-one helicoids. *Comm. Math. Helv.* To Appear.

[40] D. Hoffman and B. White. Genus-one helicoids from a variational point of view. *Comm. Math. Helv.*, 83(4):767–813, 2008.

[41] A. Huber. On subharmonic functions and differential geometry in the large. *Commentarii Mathematici Helvetici*, 32(1):13–72, 1958.

[42] W. H. Meeks III, J. Perez, and A. Ros. Embedded minimal surfaces: removable singularities, local pictures and parking garage structures, the dynamics of dilation invariant collections and the characterization of examples of quadratic curvature decay. *Preprint*.

[43] W. H. Meeks III, J. Perez, and A. Ros. The Geometry of Minimal Surfaces of Finite Genus III; Bounds on the Topology and Index of Classical Minimal Surfaces. *Preprint*.

[44] W. H. Meeks III, J. Perez, and A. Ros. Uniqueness of the Riemann Minimal Example. *Inventiones Mathematicae*, 131:107–132, 1998.

[45] W. H. Meeks III and H. Rosenberg. The uniqueness of the helicoid. *Ann. of Math. (2)*, 161(2):727–758, 2005.

[46] W. H. Meeks III and S. T. Yau. The classical Plateau problem and the topology of three-dimensional manifolds. The embedding of the solution given by Douglas-Morrey and an analytic proof of Dehn's lemma. *Topology*, 21(4):409–442, 1982.

[47] W. H. Meeks III and S. T. Yau. The existence of embedded minimal surfaces and the problem of uniqueness. *Mathematische Zeitschrift*, 179(2):151–168, 1982.

[48] W.H. Meeks III and H. Rosenberg. The geometry and conformal structure of properly embedded minimal surfaces of finite topology in $\mathbb{R}^3$. *Invent. Math*, 114(3):625–639, 1993.

[49] S. Khan. A Minimal Lamination of the Unit Ball with Singularities along a Line Segment. *Preprint.* `http://arxiv.org/abs/0902.3641`.

[50] F. López and A. Ros. On embedded complete minimal surfaces of genus zero. *J. Differential Geom.*, 33(1):293–300, 1991.

[51] W. H. Meeks and M. Weber. Bending the helicoid. *Mathematische Annalen*, 339(4):783–798, 2007.

[52] N. Nadirashvili. Hadamard's and Calabi-Yau's conjectures on negatively curved and minimal surfaces. *Invent. Math.*, 126:457?465, 1996.

[53] R. Osserman. Global properties of minimal surfaces in E^3 and E^n. *Annals of Mathematics*, pages 340–364, 1964.

[54] R. Osserman. *A survey of minimal surfaces*. Dover Publications, 1986.

[55] T. Rado. On the problem of Plateau. *Ergebnisse der Math. und ihrer Grenzgebiete*, 2, 1953.

[56] R. Schoen. *Seminar on Minimal Submanifolds*, volume 103 of *Ann. of Math. Studies*, chapter Estimates for stable minimal surfaces in three-dimensional manifolds, pages 111–126. Princeton University Press, Princeton, N.J., 1983.

[57] R. Schoen. Uniqueness, symmetry, and embeddedness of minimal surfaces. *J. Differential Geom.*, 18:791–809, 1983.

[58] R. Schoen and L. Simon. *Seminar on minimal submanifolds, Ann. of Math. Studies*, chapter Regularity of simply connected surfaces with quasiconformal Gauss map. Princeton University Press, 1983.

[59] M. Weber, D. Hoffman, and M. Wolf. The genus-one helicoid as a limit of screw-motion invariant helicoids with handles. *Clay Math. Proc., Global Theory of Minimal Surfaces*, 2:243–258, 2001.

[60] M. Weber, D. Hoffman, and M. Wolf. An embedded genus-one helicoid. *PNAS*, 102(46):16566–16568, 2005.

[61] M. Weber, D. Hoffman, and M. Wolf. An embedded genus-one helicoid. *Annals of Math.*, 169(2):347–448, 2009.